Remote Sensing of Tamarisk (*Tamarix* spp.*)* Defoliation by the Tamarisk Leaf Beetle (*Diorhabda carinulata*) Along the Colorado River in Arizona

By Ashton Bedford

A Thesis Submitted in Partial Fulfillment

of the Requirements for the Degree of

Master of Science

in Applied Geospatial Sciences

Northern Arizona University

May 2016

Approved:

Erik Schiefer, Ph.D., Chair

Barbara Ralston, Ph.D.

Temuulen Sankey, Ph.D.

Joel Sankey, Ph.D.

Amanda Stan, Ph.D

ABSTRACT

REMOTE SENSING OF TAMARISK (*TAMARIX* SPP.*)* DEFOLIATION BY THE TAMARISK LEAF BEETLE (*DIORHABDA CARINULATA*) ALONG THE COLORADO RIVER IN ARIZONA

ASHTON BEDFORD

The primary objective of this study was to compare the canopy cover of tamarisk (*Tamarix species*) stands with Tamarisk beetle (*Diorhabda carinulata*) presence and absence in the Grand Canyon over a four year period from May 2009 to May 2013. I used high spatial resolution data of 0.2 m available from the United States Geologic Survey (USGS). The imagery spans the Colorado River from Glen Canyon Dam to Lake Mead, and includes portions of Glen Canyon National Recreation Area and Grand Canyon National Park. The tamarisk beetle was first reported in this segment of the Colorado River in 2009, and therefore the May 2009 dataset characterizes tamarisk vegetation prior to beetle arrival, while the 2013 imagery characterizes tamarisk vegetation after the tamarisk beetle arrival. This comparison of pre- and post-beetle vegetation was performed using the Normalized Difference Vegetation Index (NDVI) and the Enhanced Vegetation Index (EVI) assessment. An estimate of Leaf Area Index (LAI) was also assessed. A secondary objective was to determine whether significant relationships exist between sunlight exposure, tamarisk canopy cover, and beetle observations. The rationale for the secondary objective analysis is due to the Critical Day Length requirements for the beetles before they enter dormancy as a signaling mechanism to overwinter in the ground of tamarisk stands. The tamarisk classification accuracy varied depending on associated vegetation within each study reach. Change detection analysis was still able to identify areas of tamarisk NDVI/EVI decline. Multivariate models predicting percent tamarisk decline in the study areas were unable to produce models with a high model fit. Multivariate models did show that certain environmental variables including initial tamarisk area, viewshed and amount of sunlight were significant across most reaches.

Table of Contents

Contents

List of Tables

List of Figures

Chapter 1 - Introduction

Tamarix species, commonly known as tamarisks or saltcedar, are one of the primary woody species along the Colorado River in Arizona. Although exotic, this species provides important cultural and ecosystem services along the Colorado River including providing habitat for the endangered southwestern willow flycatcher (*Empidonax traillii extimus*), as well as recreational benefits such as shelter (Hultine et al. 2010, Malakoff, D. 1999 and Sogge et al. 2008). The tamarisk beetle *Diorhabda carinulata*, unintentionally arrived in Arizona in 2009 after being introduced in the United States of America (USA) in 2001 as a biological agent to control tamarisk populations (Deloach et al. 2004). This beetle feeds on tamarisk leaves and may therefore result in significant mortality of tamarisks; leading to potentially intended and unintended consequences along the Colorado River in Glen and Grand Canyons including change in plant community quality, and structure, recreational benefits, and carbons nutrient cycling (Hultine et al. 2010). The analysis of remotely sensed data can be efficient for identifying tamarisk decline caused by tamarisk beetles across large areas of Glen and Grand Canyon that are difficult to survey using traditional ground surveys. Identifying areas of tamarisk decline across large areas in Glen and Grand Canyons will allow researchers and managers to better monitor the effects of tamarisk decline and develop solutions to address these impacts, if necessary. Using remotely-sensed tamarisk decline data along with a dataset of beetle observation survey data could allow a more complete understanding of how beetle population numbers relate to tamarisk decline. Moreover, developing a better understanding of environmental variables that could

influence tamarisk beetle site selection could help to predict where tamarisk decline is likely to happen in the future. Use of a sun model dataset, specifically, combined with environmental variables generated in this study may identify some environmental preferences for tamarisk beetles along the Colorado River in Glen and Grand Canyons.

Tamarisks were introduced to North America to serve as erosion control along rivers and as an ornamental in the mid-1800s (Brock 1994). Tamarisks form homogenous stands along rivers and historic flood plains (Brock 1994), can grow quickly and promote saline soils that native vegetation cannot tolerate (Shafroth et al. 1995). The tamarisk draws up water and salts from deep in the water table, stores the salts in its leaves, and drops its leaves in the fall, resulting in alkaline soil (Shafroth et al. 1995). Tamarisks have expanded rapidly throughout arid regions of the United States since the 1950s, and river regulation created from dam construction has aided the species' expansion (Stromberg et al. 2007).

Tamarisk control through traditional chemical, mechanical, and burn treatment methods has proven costly and ineffective (Hultine 2010). Extensive research, focused on biological control options, led to the study and release of tamarisk beetle (*Diorhabda carinulata*) (Bean 2012). The beetle was released into Colorado, Utah, Wyoming, Nevada, California, and Texas in May 2001 (Snyder et al. 2010). Previously there were three species of this beetle (*Diorhabda elongata*, *Diorhabda deserticola*, and, *Diorhabda carinulata*), but now have been combined into the single species of *Diorhabda carinulata* (Bean 2012). The beetles released into Colorado and Utah have now traveled into Arizona (Johnson et al. 2012). The tamarisk beetle preys on tamarisks by defoliating the

leaves of the plant (Snyder et al. 2010). This feeding cycle can occur multiple times per year (Snyder et al. 2010), and each defoliation cycle can progressively weaken the plant (Snyder et al. 2010). These defoliation events can be detected with remotely sensed data (Fletcher 2013) and the loss of leaf area is noticeable in the visible color and near-infrared portions of the electromagnetic spectrum (Dennison et al. 2009).

The tamarisk beetle‘s southern range is expanding beyond the geographic boundaries that researchers initially thought possible (Bean et al. 2012). The beetle was initially believed to be unable to survive south of 38 degrees north latitude (Bean et al. 2012), due to a dormancy cycle known as diapause. In diapause, the beetle enters dormancy after day length decreases past a certain number of hours (Bean et al. 2007). Five years after the initial beetle release in 2001, Bean et al. (2012) documented that the beetles were entering diapause later into the year, particularly more southern-reaching populations. Deloach et al. (2004) also noted that there are populations of beetle found in their native habitats in China, Tunisia, Turkmenistan, and Greece in Crete that require as little as 10 hours of sunlight to maintain populations. Therefore it is likely that the Colorado River from Glen Canyon Dam through the western boundary of Grand Canyon National Park could have enough daylight to allow tamarisk beetle establishment. The first observation of the tamarisk beetle in Arizona in 2009 was 12 miles downstream of Lees Ferry along the Colorado River (Minard 2011).

Hultine et al. (2010) suggest various ecological and societal consequences from rapid decline and defoliation of tamarisks from beetle activity, including changes related to carbon and nutrient cycling, plant community composition, change in vegetation

structure, and recreational impacts (Hultine et al. 2010). Several factors may negatively impact native vegetation after tamarisk decline. Native vegetation may have trouble establishing naturally after tamarisks are removed (Bay and Sher 2008, and Shafroth et al. 2008). Changes to the flood regime of a riparian system decrease the ability of native riparian vegetation to establish (Fenner et al. 1985), but upland native vegetation with less water demands may be able to occupy areas that were previously dominated by tamarisks. Dams limit natural winter and spring flooding events from taking place (Fenner et al. 1985), which are important for native species germination such as cottonwoods and willows (Stromberg 1998), while unregulated winter floods scour away established vegetation, transport sediment and saturate soil to promote seedling establishment and growth (Stromberg 1998). Native riparian vegetation downstream of Glen Canyon Dam will likely have difficulty establishing in weakened or dead tamarisk stands.

Remote sensing data allows for analysis of tamarisk defoliation over large geographic extent (Dennison et al. 2009). Dennison et al. (2009) describe the importance of remote sensing data that has high temporal and spatial resolution. High temporal resolution allows the capture of each defoliation event brought on by the tamarisk beetles (Dennison et al. 2009), whereas high spatial resolution more accurately captures smaller tamarisk stands or individual plants (Dennison et al. 2009). Fletcher (2013) recommends additional research testing the application of high-resolution imagery for measuring tamarisk beetle effects as a biological control. High spatial resolution data allow for more accurate spatial and change detection analysis, by allowing for identification of

individual tamarisks (Meng et al. 2012). Observation of individual tamarisks would also allow more precise readings than can be achieved with coarser spatial resolutions. This thesis research benefits from airborne imagery with very high spatial resolution but low temporal resolution.

Identifying defoliated tamarisk stands provides vital information to land managers, as the defoliated tamarisk stands can lead to a variety of management issues (Hultine et al. 2010). If the tamarisk beetle is identified as the cause, this information will help to measure the spread and impact of the beetle. Identifying areas of tamarisk defoliation also enables managers to develop an action plan to more closely monitor and address the effects of tamarisk defoliation.

The primary objective of this thesis was to implement a supervised classification using remote sensed overflight imagery at high spatial resolution provided by the United States Geologic Survey (USGS) of tamarisks along three reaches of the Colorado River and complete change detection analyses of the classified pixels between 2009 and 2013. Separate change detection analyses was carried out based on the Normalized Difference Vegetation Index (NDVI) and Enhanced Vegetation Index (EVI) values from 2009 to 2013. Change detection results were analyzed by dividing each study reach into .16 km segments (Sankey et al., 2015) to more accurately identify where tamarisk decline was located and to better quantify the levels of decline. These change detection values were also compared using buffers created from presence or absence of beetle surveys that were carried out between 2010 and 2012 to compare levels of decline between the two categories. Simple and multiple linear regression models were completed to identify the

possible relationship between environmental variables including sunlight variables on the percent of tamarisks decline. The same variables were also used to identify the relationship to beetle observations within the study reaches.

I hypothesize the tamarisk classification, coupled with the fairly strict change detection ratio will focus identification on areas of notable tamarisk defoliation. Furthermore, the change detection ratio will limit the amount of incorrectly classified non-tamarisk vegetation species to be included in the change detection result because of the higher threshold that is set, thereby creating a more accurate image of tamarisk defoliation. In addition, I will observe a correlation between increased tamarisk defoliation and areas of observed tamarisk beetles, when compared to the study reaches as a whole. Finally, I think a positive relationship between the amount of daylight in a river segment and the amount of tamarisk defoliation in that river segment will be observed, because longer day lengths would provide more time for beetle activity before entering diapause.

Chapter 2 – Literature Review

Lewis et al. 2003 observed that tamarisk beetle performance varies between different species of tamarisks. The performance of beetle and larvae was measure between old and young leaves of *Tamarix ramosissima*, and *Tamarix parviflora*, but foliage in general of *Tamarix canariensis*, and *Tamarix aphylla*. This performance was measured by the number of eggs produced by each female based on the species of tamarisk the beetle and larvae was feeding on, and the number of larvae that completed all life cycles to become breeding adults. Lewis et al. (2003) found that all these species of tamarisk allowed for potentially stable populations of beetles. Lewis et al. 2003 found that tamarisk beetle performance was best when raised on young *Tamarix ramosissima* foliage. Tamarisks in Glen and Grand Canyons are a hybrid swarm of these species. This means it is likely there may be a preference for beetles to target certain stands of tamarisks based on their resemblance to *Tamarix ramosissima* as well as targeting younger foliage of tamarisks in general.

Archambault et al. (2009) developed a daylight model to analyze if there was a linear relationship to beetle observations and sunlight where beetles were observed based on the assumption of Critical Day Length (CDL) requirements that prepare beetles for entering diapause. The model was based on the total day lengths from the growing season of tamarisks in their study area of Dinosaur National Monument. Their findings showed that total daylight was not a significant factor where beetles were observed, and linear regression model R^2 values were near zero. This information led the researchers to

conclude that total hours of daylight in a location are not a critical driver of beetle establishment.

Various remote sensing data have been used to monitor the effects of *Diorhabda carinulata* on tamarisks including visible spectrum color photographs (Fletcher, 2013; Carruthers et al. 2006), Landsat TM (Meng et al. 2012, Archambault et al. 2009), CASI II (Carruthers et al. 2006), Advanced Spaceborne Thermal Emission and Reflection Radiometer (ASTER) (Dennison et al. 2009), and Moderate Resolution Imaging Spectroradiometer (MODIS) (Dennison et al. 2009). The different sensors all capture the same type of information in the visible color spectrum and the near-infrared spectrum. However, they have tradeoffs in spatial and temporal resolution allowing different analyses of *Diorhabda carinulata* effects on Tamarisk stands (Table 1).

Temporal resolution is an important factor in analyzing impacts of the tamarisk beetle. Imagery with high temporal resolution can capture each defoliation event brought on by tamarisk beetles, this type of information could be used to track the migration of tamarisk beetles within one season by monitoring the spread of beetles by the defoliation events of tamarisks (Table 1). To maintain accurate analysis over time, images from separate years should be from as similar a date as possible, or should capture the same phenological state. MODIS data has a high temporal resolution with daily imagery in very coarse spatial resolution of 250 meters (Dennison et al. 2009), while Landsat imagery has a 16-day revisit cycle and a spatial resolution of 30 meters for most bands (Lillesand et al. 2008: 400). Aerial imagery from overflights have the advantage of targeted dates as long as flight safety standards are met. The 2009 and 2013 imagery in

this study were both acquired in May providing an ideal opportunity to detect changes in tamarisk over the four years.

Aerial photographs capturing blue, green, and red reflectance values have been tested to monitor tamarisk beetle effects (Carruthers et al. 2006). Carruthers et al. (2006) used orthorectified scanned aerial photographs with a spatial resolution of 0.3 m to carry out a supervised (automated) classification of tamarisks in California. The pictures were taken during a time when tamarisks and agricultural trees were blooming. Both vegetation types had similar purple blooms which led to classification problems. Additional steps were then needed to identify tamarisk stands (Carruthers et al. 2006). Fletcher (2013) used aerial photographs to qualitatively monitor and identify tamarisk defoliation in Texas using two sets of photos from July 8 2011 and September 8 2011. The photos were georeferenced during photo capture and visually inspected and compared against each other. A geodatabase was created marking areas with tamarisk defoliation occurring between the July 8 and September 8 photos.

Table 1: Table comparing the resolutions and revisit lengths for remote sensing data used in mapping tamarisk defoliation.

Remote Sensing Data Type	Spatial Resolution For Visible and NIR	Temporal Resolution
Overflight Imagery	>1m	Variable
Landsat	30 m	16 day
ASTER	15 m	16 day
MODIS	250 m	1-2 days

Vegetation indices are a well-established method for analysis of remotely sensed data (Glenn et al. 2008). Vegetation indices such as the NDVI (Equation 1) (Rouse et al. 1974) and EVI (Equation 2) correlate with vegetation traits such as productivity, condition, foliage, and cover by providing standard values that indicate the "greenness" of a pixel (Glenn et al. 2008, Pettorelli et al. 2005). NDVI and EVI are also correlated with the level of fraction of absorbed photosynthetic active radiation (fAPAR) intercepted by the canopy which relates to vegetative processes such as photosynthesis, phenology, primary productivity, net carbon fixation, gross primary productivity, and plant transpiration (Glenn et al. 2008). The values of these traits and processes stem from the amount of green leaves in the vegetation.

Near-infrared (NIR) band wavelength corresponds to the 0.7-1.3 μm portion of the spectrum, while the red and blue band wavelengths are 0.6-0.7 μm and 0.4-0.5 μm, respectively. Equations 1 and 2 operate on the basis that NIR wavelengths are highly reflected by plant cell walls and red wavelengths are absorbed by chlorophyll pigments (Glenn et al. 2008). Both of these vegetation indices provide standardized range of values between -1 and 1. Water absorbs NIR wavelengths and results in negative values, soils have low positive values, while dense vegetation has high positive values since vegetation mostly reflects NIR wavelengths. These standardized ratios allow simple comparisons between different dates (Glenn et al. 2008).

The EVI Equation (Equation 2) must be calculated using reflectance values, instead of radiance, as it was developed for use with MODIS imagery in reflectance values. The EVI uses the blue band, along with coefficients to limit the effect of aerosols

in the image which affect the value of the red band. The coefficients represent the following values: 2.5 is for the gain factor, 1 addresses canopy values, 6 and 7.5 are coefficients which account for aerosols in the image that affect the red band.

Equation 1: Normalized Difference Vegetation Index Equation

$$NDVI = (NIR - RED) / (NIR + RED)$$

Equation 2: Enhanced Vegetation Index Equation

$$EVI = 2.5 \times (NIR - RED) / (NIR + 6 \times RED - 7.5 \times BLUE + 1)$$

Ralston et al. (2008) carried out a supervised classification based on 15 vegetation classes and 3 non-vegetation classes from Glen Canyon Dam to Lake Mead based on USGS overflight data gathered in 2002. A 15 band layer was created for use in this classification. The dataset consisted of the original blue, green, red and NIR bands, 6 ratio bands based on the original 4 band image, 4 texture bands and 1 vegetation density band. Multiple types of accuracy assessments were carried out including fuzzy logic accuracy assessments. Setting the fuzzy logic setting to requiring an exact match used a total of 93 points between 6 vegetation classes consisting of 1) *Baccharis emoryi* and *Salix exigua*, 2) *Prosopis glandulosa*, *Acacia greggii* and *Baccharis sarothroides*, 3) *Tamarix ramosissima* and *Aster spinosa*, 4) *Pluchea sericea*, 5) sparse shrubs, and 6) wetland herbaceous species consisting of *Phragmites*/*Scirpus*, *Typha domingensis* and *Carex aquatilis*. Within this assessment, the overall accuracy was 49%, with the tamarisk class having a producer's and user's accuracy of 53% and 58% respectively. Producer's

accuracy reflects the omission error, or percent of validation pixels correctly classified for a particular class, while user's accuracy reflects commission error, or the probability that a pixel belonging to a certain class actually belongs to that class on the ground (Lillesand et al. 2008: 586). The *Pluchea sericea* class accounted for most of the commission errors decreasing user's accuracy. In other words, *Pluchea sericea* was most often misclassified as tamarisks. Classes 1 and 2 accounted for the majority of the omission error, meaning that vegetation belonging to classes 1 and 2 were classified as tamarisks incorrectly lowering the tamarisk producer's accuracy to 41%.

Change Detection of Tamarisks

Multiple studies have used the red and NIR band with remote data to calculate the change in NDVI of tamarisks as a result of tamarisk beetles using Landsat TM (Archambault et al. 2009), ASTER (Dennison et al. 2009), MODIS (Nagler et al. 2014, and Dennison et al. 2009) and CASI II imagery (Carruthers et al. 2006). An EVI can also be estimated if a blue band is available (Dennison et al. 2009, and Archambault et al. 2009). These vegetation indices allow for quantitative analysis of the change in leaf area (Dennison et al. 2009), where decreasing leaf area correlates to a lower vegetation index value (Dennison et al. 2009). Nagler et al. (2014) was able to use MODIS imagery on large tamarisk stands to observe seasonal defoliation events brought on by tamarisk beetles. The defoliation events in mid-June resulted in similar NDVI values of around .25 in January (winter) when no leaves would be present. Using 15 m resolution ASTER imagery, Dennison et al. (2009) manually drew polygons around tamarisk stands and then identified a decrease in NDVI values in dense tamarisk stands due to *Diorhabda*

carinulata over two years. They found that 15% of all pixels had declined more than 0.1 in their NDVI values.

A primary factor influencing tamarisk change detection is pixel size. Fletcher (2013) used a digital camera to track beetle defoliation. This magnified camera was able to obtain a pixel resolution of 0.5 meters (Fletcher 2013). However, vegetation index was not estimated in the Fletcher study because the images were standard Red-Green-Blue (RGB) photographs, and did not have a near-infrared band. The coarse resolution of satellite data from Landsat TM (Archambault et al. 2009), ASTER (Dennison et al. 2009), and MODIS (Dennison et al. 2009) can limit the effective area for analysis to only large, dense stands of tamarisk. Landsat TM visible and near-infrared bands have a spatial resolution of 30 meters (Lillesand et al. 2008: 400). ASTER imagery has a spatial resolution of 15 meters for the visible and near-infrared bands (Dennison et al. 2009), while MODIS data has a spatial resolution of 250 meters for the near-infrared bands (Dennison et al. 2009). However, many tamarisk trees and stands can be smaller than these pixel sizes and appreciable change in such trees and stands can go undetected.

Nagler et al. (2014) demonstrated that MODIS data can be effective in tracking tamarisk defoliation events. In their study, MODIS pixels coincident with ground survey plots were used to calculate NDVI and EVI (Nagler et al. 2014). EVI values were then used to estimate Leaf Area Index (LAI) values using the following Equation:

Equation 3: Leaf Are Index Equation for tamarisks

LAI = 8.74EVI–0.68 (Nagler et al. 2014).

The high temporal resolution of the MODIS data in this study allowed exact identification of peak defoliation events. This temporal resolution enabled the observation that study sites further downriver were entering peak defoliation later into the year (Nagler et al. 2014), which indicated that beetles were migrating during the growing season to areas previously without beetles (Nagler et al. 2014). Nagler et al. (2014) note that MODIS should not be used as a standalone method for analyzing beetle effects, but can also be an important compliment to ground-monitored sites, or high resolution imagery (Nagler et al. 2014).

Meng et al. (2012) used Landsat 5TM imagery for a change detection study of tamarisk defoliation located in eastern Utah and western Colorado from 2006 through 2010. Images captured during late August and early September of each year were used each year to track changes. Two algorithms to detect tamarisk defoliation were tested separately within the same study area. These algorithms were Disturbance Index (DI), and Random Forest (RF). This study did not track change in NDVI values. Ground-measured beetle points were used with 100 m buffers to assess the accuracy of each algorithm and to identify which 100 m buffer points showed evidence of beetle activity (Meng et al. 2012). If a 100 m buffer point had any pixel showing a change threshold value for DI or RF, then that point was marked as having beetle activity (Ground collected beetle points were used with 100 m buffers to assess the accuracy of each algorithm and to identify which 100 m buffer points showed evidence of beetle activity (Meng et al. 2012).

The DI value is calculated by DI = Brightness – (Greenness + Wetness) (Healey et al. 2005). Tasseled Cap transformations first convert the 6 Landsat TM reflectance bands to the three values of Brightness, Greenness and Wetness (Healey et al. 2005). High DI values correspond to areas showing disturbance, since there is a lack of vegetation to display Greenness and Wetness values, and greater ground surfaces which generally have higher Brightness values (Healey et al. 2005). Change thresholds can then be established for a study area to identify disturbance for an area. The RF algorithm used 42 different variables including texture, and Tasseled Cap transformation values (Meng et al. 2012). Training pixels of defoliated and non-defoliated tamarisks were then manually identified from the 2006-2007 images, and used for all subsequent images as well (Meng et al. 2012). The RF decision tree helps to limit the chance of over fitting that often occurs with supervised classification (Meng et al. 2012).

Accuracy assessments for both of these algorithms focused on comparing whether tamarisk pixels were correctly classified as defoliated or non-defoliated pixels (Meng et al. 2012). The DI method overall accuracy varied between study years, ranging from 72.72% to 88.20% (Meng et al. 2012). The accuracy increased as the ratio of defoliated pixels increased. The RF method had an overall accuracy ranging from 80.57% to 86.49% (Meng et al. 2012). Producer's and User's accuracy for foliated tamarisks using the DI method ranged from 95.67%-100% and 68.5%-77.37% respectively. Producer's and User's accuracy for foliated tamarisks using the RF method ranged from 95.75%-100% and 72.29%-79.1% respectively. For this thesis, comparing the producer's and user's accuracy of identification of non-defoliated tamarisk pixels will be most helpful,

because I first classified non-defoliated tamarisk pixels in 2009, and determined the change of those classified pixels between 2009 and 2013.

Chapter 3 – Available Data and Methods

Study Area

This study focuses on three reaches along an approximately 300 km stretch of the Colorado River in Arizona (Figure 1). The Colorado River changes in elevation from around 955 meters at the base of Glen Canyon Dam to around 354 meters at Lake Mead. The temperature along the Colorado River varies greatly by season (Figure 2). Summer temperatures range from 22 °C to 41 °C while winter temperatures range from 2 °C to 13 °C (National Park Service, 2015). The average annual precipitation along the Colorado River is 21.6 cm (8.51 inches), but can be as little as 15 cm near Lees Ferry (National Park Service, 2015). Precipitation occurs primarily during the winter and the summer monsoon season (Figure 3).

The three reaches along the Colorado River included in this study are Glen Canyon, Kanab Creek and National Canyon. Site orientation for this study is based on the Grand Canyon Monitoring and Research Center (GCMRC) river units. Lees Ferry, the beginning of the Grand Canyon National Park Service boundary, is the starting point for the GCMRC river units. The river distance and areas above Lees Ferry, therefore, has negative values in the GCMRC river units. The first reach included in this study extends from Glen Canyon Dam, 25.4 km (15.8 miles) to 5.8 km (3.6 miles) downstream from Lees Ferry, a total of 31.5 km (19.6 miles). The Kanab reach extends from 216.6 km – 250.6 km downstream of Lees Ferry (river mile 134.6 – 155.7), a total of 33.5 km (20.8 miles). The Kanab creek confluence is located at 231.7 km (river mile 144). The third reach, National, extends from 255.2 km – 290.5 km downstream from Lees Ferry (river

mile 158.6 – 180.5), a total of 35.7 km (22.2 miles). National Canyon confluence is located at 268.8 km (167 mile).

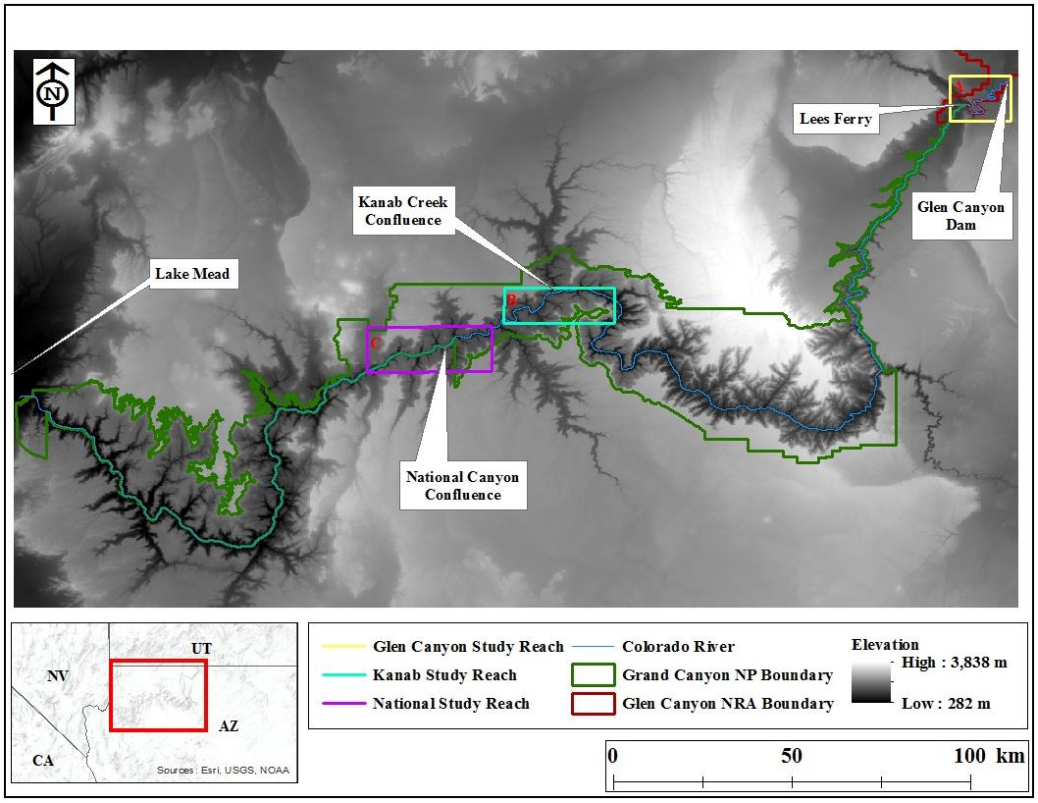

Figure 1: Map of Study Areas A) Glen Canyon, B) Kanab, and C) National study reaches respectively.

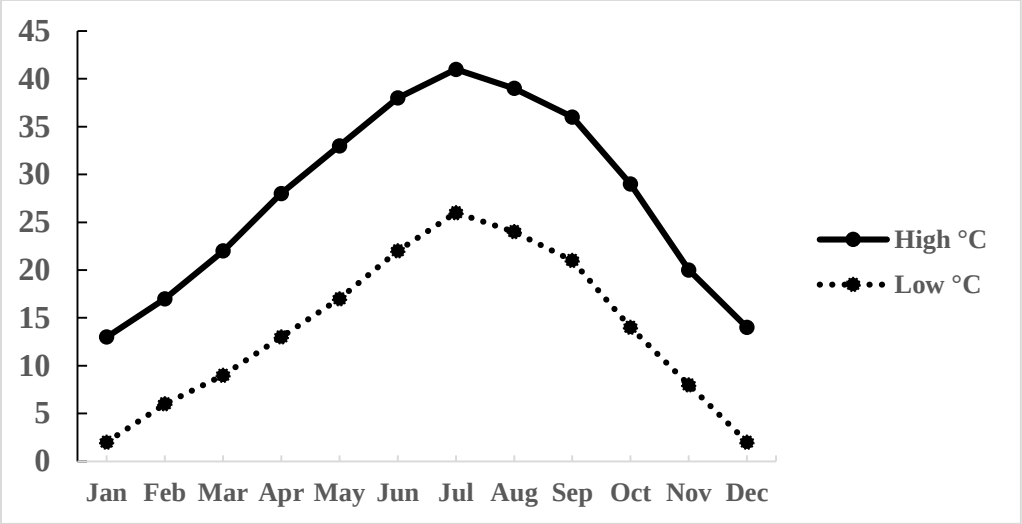

Figure 2: Average temperature in inner canyon at Phantom (National Park Service, 2015).

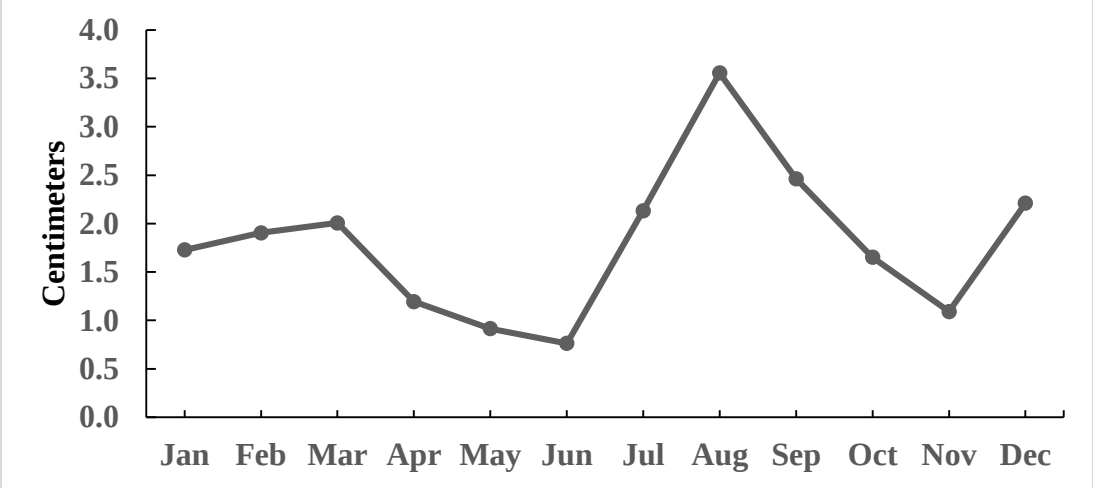

Figure 3: Average precipitation in inner canyon at Phantom Ranch by month (National Park Service, 2015).

Remote Sensing Data

The remote sensing data, provided by the Unites States Geologic Survey (USGS), consists of orthorectified aerial imagery with 0.2 m spatial resolution and four spectral bands: blue (0.460 µm), green (0.560 µm), red (0.635 µm), and NIR (0.860 µm). The imagery was acquired in late May around Memorial Day for both 2009 and 2013 from a fixed-wing aircraft (Davis 2012). Late May is a desirable date for this study: vegetation is in full leaf development for the season, and the beetles will have likely emerged from the ground litter by late April or early May, possibly limiting the impacts to tamarisk leaf mass for the current year (Lewis et al. 2003). This time of year also serves as a good representation of initial health of tamarisks entering the growing season. The 2009 data is considered a "pre-beetle" image, while the 2013 data serves as a "post-beetle" image.

Field Collection of Tamarisk Training and Validation Data

Multiple field trips were completed to collect vegetation classification training data (Table 2). Large scale field maps were created for each visited site using the 2009 USGS multispectral data for collection of training and validation points. Maps were printed in a RGB color scheme, and used to visually identify tamarisk stands, as well as any other vegetation type that occurred in the same extent as tamarisks. The high spatial resolution of these maps allowed for good site orientation and identification of various vegetation species and avoided the need for low accuracy GPS units.

Table 2: Table identifying locations for collection of tamarisk training and validation points for Glen Canyon reach, as well as collection of training points for Kanab and National reach.

Study Reach	River km	Site Name	Date Visited
Glen Canyon	-17.7	Ferry Swale	11/25/2014
Glen Canyon	-15.8 to -13.7	Horseshoe Bend	12/5/2014-12/7/2014
Glen Canyon	1.9	Paria Beach	1/8/2015-1/9/2015
Kanab	224.7	Fishtail Camp	10/6/2014
National	277.8		10/8/2014

Care was given to only identify pure tamarisk pixels with green leaves absent of any other vegetation type. Tamarisk pixels were only selected if there was absolute confidence about site location. This prevented the radiance values from being mixed with other vegetation types within tamarisk pixels. At least one third of the tamarisk pixels were reserved for an independent set of accuracy assessment data.

Other vegetation pixels were also identified in the maps to provide detailed information on other types of vegetation most similar to tamarisk spectrally and to provide additional data for accuracy assessment of other vegetation types. Vegetation species of interest included multiple species of *Baccharis* only noted at the genus level, netleaf hackberry (*Celtis reticulate*), common reed (*Phragmites australis*), arrowweed (*Pluchea sericea*), honey mesquite (*Prosopis glandulosa*), coyote willow (*Salix exigua*), and mixed herbaceous vegetation. These species were identified separately as well as when mixed together. Care was given to insure that no tamarisks were located in these

pixels. Mixed vegetation pixels containing any assortment of vegetation other than tamarisks were also collected.

Image Processing

Final image classification for each study reach was performed in the following steps and is discussed in more detail in the following sub-sections. A supervised classification, Mahalanobis Distance approach, was used to detect all foliated tamarisks within the study areas in the 2009 image. Separate training pixels from the field-mapped tamarisk polygons were used from each reach along the river. The classification approach focused on identifying specific radiance values in the visible and NIR bands that together formed a unique signature for foliated tamarisks. NDVI, EVI, and LAI were also calculated for 2009 and stacked together with the original four bands to use in the supervised classification accuracy. A total vegetation mask was applied to each stacked image to only include vegetation pixels. The vegetation indices were also used in change detection analysis between 2009 and 2013.

The individual tiles that made up each study reach were combined together using a georeferenced mosaic function in ENVI software (ENVI Version 4.8. ITT Industries Inc., 2010, Boulder, CO). Six tiles were combined for the Lees Ferry reach, a total, while ten and eleven tiles were mosaicked together for the Kanab reach and the National reach, respectively. Due to the high resolution of the imagery, each study reach was divided into three sections (upper, middle and lower) for the purpose of image processing, classification, accuracy assessments and change detection analysis. The results for each

section were then combined to give the values for the reach as a whole. Table 3 shows the river extents encompassed by each river section.

Table 3: River extent for each study reach section

Study Reach and Section	km extent
Glen Canyon Upper	-25.4 to -15.3
Glen Canyon Middle	-15.3 to -3.4
Glen Canyon Lower	-3.4 to 6.0
Kanab Upper	216.6 to 226.6
Kanab Middle	226.6 to 236.6
Kanab Lower	236.6 to 250.6
National Upper	255.2 to 270.0
National Middle	270.0 to 279.9
National Lower	279.9 to 290.5

The radiance values in bands 1 (Blue), 3 (Red), and 4 (NIR) in the reach mosaics were then converted to reflectance values using the following empirically-derived regression Equations determined by Davis (2012). Data was kept was floating point values during all Equations to insure that no rounding errors occurred during the band math Equations.

Band 1 (blue)

Equation 4

$y = 1776.1893x + 144.0200$

Equation 5

x = (float(b1)-144.0200)/1776.1893

Band 3 (red)

Equation 6

y = 4530.1347x + 7.3981

Equation 7

x = (float(b3)-7.3981)/4530.1347

Band 4 (NIR)

Equation 8

y = 3582.1859x + 12.2268

Equation 9

x = (float(b4)-12.2268/3582.1859

The reflectance bands were then used to calculate NDVI, EVI, and LAI for each study reach and visited sites that were outside of the study reaches. The band math Equations used to calculate NDVI, EVI and LAI are given below (Equations 10, 11 and 12):

Equation 10

NDVI = (float(b4)-float(b3))/(float(b4)+float(b3))

Equation 11

EVI = 2.5× (float(b4)-float(b3))/(float(b4)+(6× float(b3))-(7.5× float(b1))+1)

where b4 = NIR band, b3 = RED band, and b1 = BLUE band.

LAI was also calculated using the band math function in ENVI with the following Equation (Nagler et al. 2014):

Equation 12

LAI = 8.74× float(b6)-0.68

where b6 = EVI band

The NDVI and EVI values were multiplied by a scale factor of 1,000 to bring the values to a similar scale of the original four radiance values. LAI was multiplied by a scale factor of 250 to bring values similar to the original four radiance values as well. It was hoped the scaling operations would bring the vegetation index values more in line with the original four band imagery, and limit possible issues in the ENVI classification when comparing bands with highly different values. The scaled vegetation index bands were then stacked in the same order to the mosaicked reaches, where NDVI band was band 5, EVI became band 6, and LAI band 7.

Vegetation masks were applied to each image stack. Gross vegetation mosaicked images, based on their NDVI pixel values were mosaicked from gross vegetation tiles created by Sankey et al. (2015). Gross vegetation files held only two values, 0 for non-

vegetation pixels and 255 for vegetation pixels. Vegetation mask files were created from each mosaicked vegetation layer, converting vegetation value of 255 to 1 and mask values to Not-a-Number (NaN). Tamarisk polygons still contained mixed and shadowed pixels after insuring no ground pixels were accidentally included in the tamarisk polygons.

Training and Validation Data

The field-mapped tamarisk polygons were separated randomly as either training or validation polygons. Two thirds of the polygons were reserved as training polygons, while the remaining third were reserved as validation polygons. Pixels were randomly generated within each set of training and validation tamarisk polygons to create a pure set of tamarisk pixels to be used in training supervised classifications and also to accurately assess the classification with pure validation pixels. These randomly generated pixels were inspected individually and moved within the tamarisk polygon if a randomly generated pixel fell in mixed or shadowed pixels. To improve supervised classification accuracy, only pure tamarisk pixels were used for training and validation purposes. Identification of pure pixels avoided any mixed pixels and pixels that were in deep shadows. Mixed pixels were easily identified, because these pixels were more earth toned, compared to the green vegetation. Mixed pixels and deep shadow pixels were identified visually. Mixed and deeply shadowed pixels were avoided because these pixels added greater uncertainty to the classification.

In Glen Canyon, 66 tamarisk trees were used to derive training pixels, and 38 for validation pixels. In Kanab reach, 9 trees were used to derive training pixels, and 5 for

validation. In National reach, 3 separate trees were used to derive both training and validation pixels. Glen Canyon had more visited areas which allowed for collection of more training and validation data. The upper, middle, and lower sections of Glen Canyon used 1000 pixels each, divided equally between training and validation for tamarisk classification. Kanab and National each utilized one different set of 500 training pixels for each respective reach. This was done by storing the training data as an ENVI statistics file with covariance calculated. Statistics for tamarisk training Regions of Interest (ROI) were calculated including covariance statistics in ENVI for supervised classifications of subgroups that did not have tamarisk training data. For example, tamarisk training data from the upper section of Kanab reach was used to classify tamarisk in the middle and lower sections of Kanab reach. These statistics files were called upon using the endmember collection tool in ENVI to use the statistics file for tamarisks that were within the study reach, but not within the particular study section to carry out the Mahalanobis classification. Having fewer training tamarisks to base the training data on for Kanab and National may have limited the scope of the training data. The lack of ground truth tamarisk points for Kanab and National meant that randomly identified tamarisk pixels were used instead, just as non-tamarisk pixels were identified in this way for all three study reaches. Table 4 shows the total numbers of training and validation pixels used for each reach.

Creation of Accuracy Assessment Samples

Supervised classification accuracy was assessed by identifying tamarisk and non-tamarisk pixels for each reach. Randomly generated vegetation pixels were created from a USGS dataset of total vegetation mask as an ROI layer for each reach and were then categorized as tamarisk, non-tamarisk, unidentified, or ignored pixels for accuracy assessment. The random points were then used to assess the accuracies of the Mahalanobis Distance classifications of foliated tamarisks for the 2009 dataset. Producer's accuracy, user's accuracy, and overall accuracy were calculated for tamarisk and non-tamarisk classes for each section. Spectrally mixed and shadowed pixels were not chosen from the ground truth tamarisk polygons. Pixels were also ignored if they could not be identified with a neighboring pure vegetation pixel or were part of processing errors (e.g. water riffles). Pixels that could not be classified as tamarisk or non-tamarisk due to the size of the vegetation or the inability of the analyst were considered unidentified.

Table 4: Total tamarisk and non-tamarisk validation pixels used in accuracy assessments. Tamarisk points used at Glen Canyon were ground truth points. All other validation pixels were identified using the 2009 USGS overflight imagery and ENVI software.

Study Reach	Tamarisk	Non-Tamarisk
Glen Canyon	1500	1500
Kanab	900	900
National	1022	1022

Supervised Classification

A range of Mahalanobis Distance settings were tested for each reach to identify the most appropriate distance setting value. The Mahalanobis Distance settings used for each reach are listed in Table5. The Mahalanobis Distance refers to the number of standard deviations from the mean values of the training data are used. Increasing this distance setting will increase the amount of vegetation pixels that will be classified as tamarisks. Sieve operations were then applied to each reach, which removed tamarisk classifications of less than 11 pixels. A connectivity value of 4 was found to be more useful in targeting areas of sparse classification than the default value of 8. These sparse classified areas generally occurred when a small number of pixels from non-tamarisk vegetation were classified as tamarisks. For example, dry land shrubs would often have a small number of tamarisk classified pixels near the center of the shrub that shared similar band values to the tamarisk training data. This created many sets of small erroneous tamarisk classifications that needed to be removed. Next, clump operations were applied to each reach. After initial visual and accuracy assessment, dilate and erode parameters of 3 within the clump function showed the most balanced results. Classified images were examined in tandem with standard RGB images and ROIs were manually created among areas of high tamarisk misclassification. These ROIs were then used to remove the misclassified pixels and create a final classification map for the year 2009.

Table 5: Mahalanobis distance settings applied for each study area section. Sites in bold text have training data that was used from within the data extent.

Site	Mahalanobis Distance Setting
Glen Upper	4.8
Glen Middle	3.2
Glen Lower	2.7
Kanab Upper	3
Kanab Middle	3.2
Kanab Lower	3.6
National Upper	4.9
National Middle	4
National Lower	5.2

Change Detection Analysis

The same vegetation indices were created for the 2009 and 2013 overflight data to allow for accurate change detection after the supervised classification was completed. The 2013 vegetation layers were created in the same fashion and ordered in the same way as described previously for the 2009 data. The difference with the 2013 dataset is that no vegetation mask was applied, since this layer was only used for change detection and not in a supervised classification. Once the 2013 dataset was completed, it was stacked with the 2009 completed dataset.

Change detection analysis was implemented to compare the 2009 image with the 2013 image using NDVI and EVI bands. All tamarisk pixels that decreased in NDVI or

EVI greatly over the 4-year time period were identified as tamarisk decrease. In this comparison, a ratio of 150% decrease in NDVI or EVI bands from 2009 to 2013 was classified as tamarisk decrease (Sankey et al. 2016) using the following band math Equations:

Equation 13

(2009NDVI/2013NDVI) gt1.5

Equation 14

(2009EVI/2013EVI) gt1.5

These ratio results are referred to in this thesis as NDVI or EVI declined pixels. This relatively strict ratio only identified pixels that had declined noticeably from 2009 to 2013. The numbers of declined tamarisk pixels were compared against the number of originally classified tamarisk pixels in 2009, and comparison results were summarized within short, 0.16-km long thiessen polygons based on GCMRC river centerline points (Sankey et al., 2015). Completing change detection analysis within these polygons enabled more detailed identification of change in tamarisks across the study area.

Use of Beetle Point Data

Collection of tamarisk beetle data is detailed in the report by Johnson et al. 2012. Field-mapped point data were collected by park staff and researchers of known beetle populations identified from 2010 to 2012 (Johnson et al. 2012). Although beetle sampling ranged from 2010 through 2012, the most concerted effort at beetle sampling

took place in 2011 from April – September. Beetle sampling locations were always at least 1.5 km apart (Johnson et al. 2012). Surveys were conducted using five sweep net passes at each site, and counting the number of adult beetles, early and late stage larvae beetle larvae, beetle eggs, as well as the presence or absence of ants and ladybugs which are known to prey on tamarisk beetles. The preferred amount of visits to each site was three, but due to logistic restrictions, some sites were visited one or two times.

The beetle observation points were used to identify the relationship between declined tamarisk stands and beetle populations. The beetle points were given a buffer radius of 100 meters (Meng et al., 2012) and a larger radius of 150 m was also evaluated. The radii for each beetle population point was created using the buffer tool in ArcGIS 10.2 and overlaid with the change detection product to identify which buffered beetle points intersected with tamarisk pixels that have declined NDVI//EVI values. The percent of beetle points that intersected with the declined tamarisk stands were compared against the declined pixels that fell outside of the buffered points. This buffer analysis data was also compared against beetle observation points that did not identify any beetles. Non-beetle points and their corresponding buffers were erased using the beetle presence buffer layers to avoid any overlap of tamarisk vegetation change pixels. Both presence and absence buffers were also merged together to prevent duplicate counting of overlapping buffer areas. Numbers of adult, early and late larvae tamarisk beetles from the research data were added to the .16 km Thiessen polygon river segments. This allowed for regression and t-test analysis within the river segments between observed or non-observed beetle data and the relation to percent NDVI or EVI decline in a river segment.

Light Model

A solar insolation model developed by Yard et al. (2005) that estimates maximum and minimum duration of direct and diffuse (indirect) solar insolation at GCMRC river centerline points was used. The model takes into account topography of the canyon, as well as the movement of the sun during each day of the year. The sun rise and set times for the model are based on civil sun rise and sun set. This system starts sun rise when the center of the sun is still 6 degrees below the horizon, and similarly sun set is when the center of the sun is 6 degrees below the horizon. The points begin at Glen Canyon Dam and are recorded every hectometer. The .16 km river segment dataset developed was combined with this solar model to provide relative values for viewshed, total, direct and diffuse solar values associated with each river segment. This solar data was used to analyze the relationships with declined tamarisk pixels as well as presence or absence beetle data.

Statistical Analysis for tamarisk decline and beetle observations

Using IBM SPSS Statistics 23 software, simple and multiple linear regression modeling was carried out to identify the relationship of environmental variables with the dependent variables identified as the level of tamarisk percent NDVI or EVI decline for each study reach. Analysis was based on the .16-km river segments (thiessen polygons). Environmental variables tested for each reach were: river segment (location along the river), initial area of tamarisk in square meters (tamarisk area), number of adult beetles surveyed, number of late larvae stage beetles, number of early larvae stage beetles,

viewshed, average minutes of total sunlight, direct sunlight and scattered sunlight received each year. Viewshed values ranged from 0 (no horizon visible at points) to 1 (full horizon visibility). Total, direct and diffuse sunlight values were averaged for an entire year in minutes. Total sunlight refers to the average total of both diffuse and direct sunlight. Diffuse sunlight refers to the average minutes of scattered sunlight, while direct sunlight refers to the average minutes of direct sunlight for the segment. The various life stages of the tamarisk beetle were tested separately in order to gain a better understanding of whether or not beetle larvae could act as a more accurate predictor of tamarisk defoliation rather than adult tamarisk beetles. Linear regression values were provided for each simple variable regression model completed, along with the model containing the highest Adjusted R^2value. The step wise forward approach was used when testing for a model with the highest Adjusted R^2 value.

Multiple regression analysis to predict NDVI or EVI decline in greenness was carried out with and without beetle observation data for each study reach. This was due to many river segments not containing beetle survey data. Therefore a separate regression analysis was carried out with the tamarisk beetle survey data. Adult tamarisk beetles were always used when building multiple regression models. These analyses were carried out in order to identify if a model predicting the amount of tamarisk defoliation could be developed. Multivariate models predicting percent NDVI or EVI tamarisk decline using step wise forward approach were compared against an automatic modeling method using SPSS in order to identify if the same variables were chosen, and also to identify if there was a noticeable change in the final Adjusted R^2 value. The automatic

modeling method carried out transformation on all variables, as well as removal and replacement of outliers. This method allowed for a relatively independent approach to identify if transformation of data was necessary.

The same environmental variables were also analyzed using the step wise forward approach to look for a relationship to adult tamarisk beetle observations as the dependent variable in the study reaches as a possible means to predict future tamarisk beetle occurrence. Independent T-tests were also carried out by converting the all beetle values into a presence and absence dataset. Each separate class of beetle observation was also combined into an all types presence/absence data set. Tamarisk beetle data was also converted into a presence/absence data set to carry out independent t-tests through SPSS to identify if there was a significant relationship between the presence of the tamarisk beetles, the other independent variables, as well as the percent of NDVI or EVI decline.

Chapter 4 - Results

The initial tamarisk classification for 2009 had errors due in part to deeply shaded areas created from the upper level canopy shading and ecosystem companion species. A separate accuracy assessment was, therefore, performed for each classification step: i) initial classification, ii) sieve applied, iii) clump applied, and iv) manual editing. Accuracy assessment was performed separately for each of the three reaches of the dataset: 1) Glen Canyon, 2) Kanab, and 3) National.

Tamarisk Classification: Glen Canyon Reach

The initial Mahalanobis classification in Glen Canyon had an overall accuracy of 80% (Table 6). Tamarisk producer's and user's accuracies were 77% and 85%, respectively. Non-tamarisk producer's and user's accuracies were 83% and 74%, respectively. After the sieve operation was implemented in the Glen Canyon study area, overall accuracy increased from 80% to 82% (Table 7). Accuracy values became evenly distributed between producer's and user's accuracy for both tamarisk and non-tamarisk. Producer's accuracy improved for tamarisk to 82%, while non-tamarisk producer's accuracy decreased to 82%. User's accuracy of tamarisk decreased to 82% after the sieve operation, while non-tamarisk vegetation increased to 81%.

The clump operation further increased the overall accuracy from 82% to 84% (Table 8). The clump function increased tamarisk user's accuracy from 82% to 92% and non-tamarisk producer's accuracy to 91%. Producer's accuracy decreased in the tamarisk class after the clump operation to 80%, while non-tamarisk producer's accuracy increased to 91%. User's accuracy of tamarisk increased to 92% after the clump operation, and

decreased to 77% for non-tamarisk vegetation. Manually erasing large improperly classified non-tamarisk areas increased overall accuracy from 84% to 87% (Table 9). User's accuracy for tamarisk remained the same at 92%, while non-tamarisk increased to 83%. Producer's accuracy for tamarisk increased to 84%, and non-tamarisk remained the same at 91%. Figures 4 and 5 show two examples of the processing steps carried out on the tamarisk classifications.

Table 6: Glen Canyon Initial Mahalanobis Classification

	Reference Data			
Classification	Tamarisk	Non-tamarisk	Total	**User's accuracy**
Tamarisk	1275	225	1500	**85%**
Non-tamarisk	387	1113	1500	**74%**
Total	1662	1338	3000	
Producer's accuracy	**77%**	**83%**		
Overall accuracy			**80%**	

Table 7: Glen Canyon sieve operation applied

	Reference Data			
Classification	Tamarisk	Non-tamarisk	Total	**User's accuracy**
Tamarisk	1237	263	1500	**82%**
Non-tamarisk	279	1221	1500	**81%**
Total	1516	1484	3000	
Producer's accuracy	**82%**	**82%**		
Overall accuracy			**82%**	

Table 8: Glen Canyon clump operation applied

Reference Data				
Classification	Tamarisk	Non-tamarisk	Total	**User's accuracy**
Tamarisk	1380	120	1500	**92%**
Non-tamarisk	349	1151	1500	**77%**
Total	1729	1271	3000	
Producer's accuracy	**80%**	**91%**		
Overall accuracy			**84%**	

Table 9: Glen Canyon final classification with manual erase applied

Reference Data				
Classification	Tamarisk	Non-tamarisk	Total	**User's accuracy**
Tamarisk	1380	120	1500	**92%**
Non-tamarisk	261	1239	1500	**83%**
Total	1641	1359	3000	
Producer's accuracy	**84%**	**91%**		
Overall accuracy			**87%**	

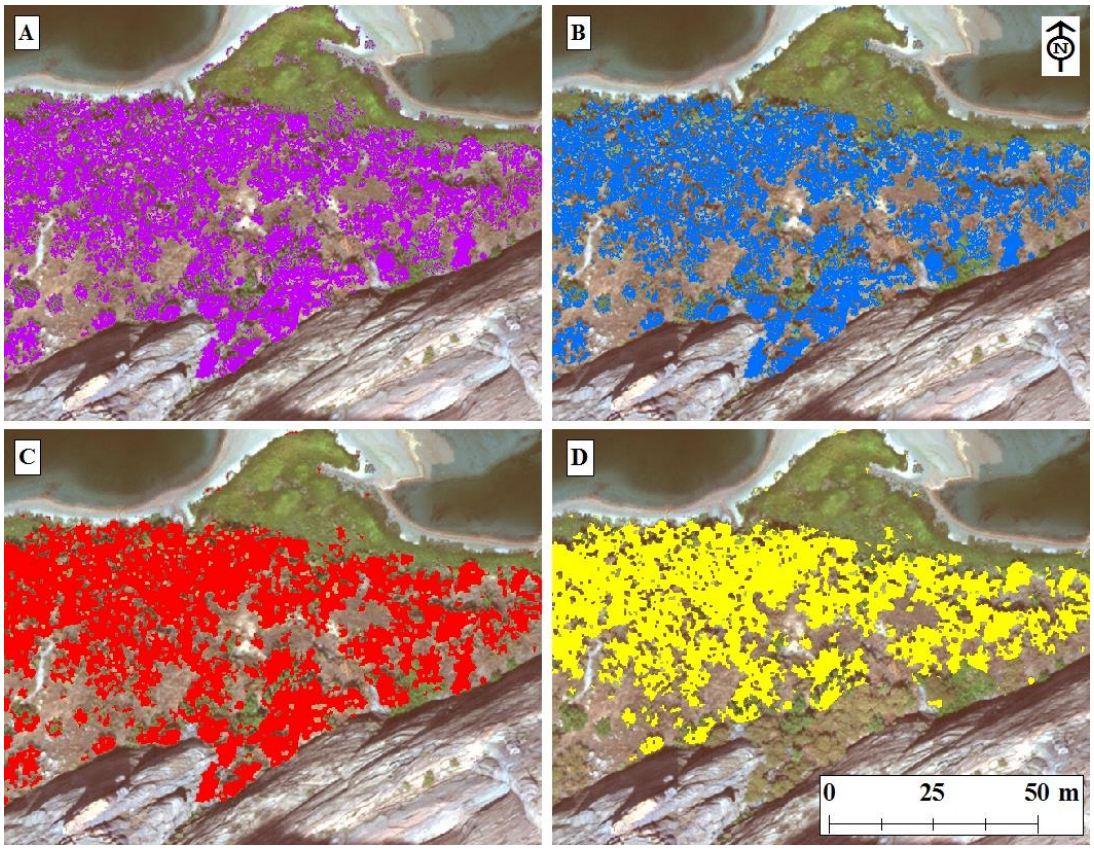

Figure 4: Tamarisk classification of the Glen Canyon study area at -12.2 km (-7.6 mile). Results of four different, consecutive processing steps that are used across the study area: 1) Initial Mahalanobis classification (Panel A), 2) Sieve operation applied to the output of the initial classification which removed any pixel groupings less than 11 pixels (Panel B), 3) Clump operation that is applied to the output of the sieve operation, which fills in gaps in the classification (Panel C), and 4) Manual erase operation to remove incorrectly classified vegetation.

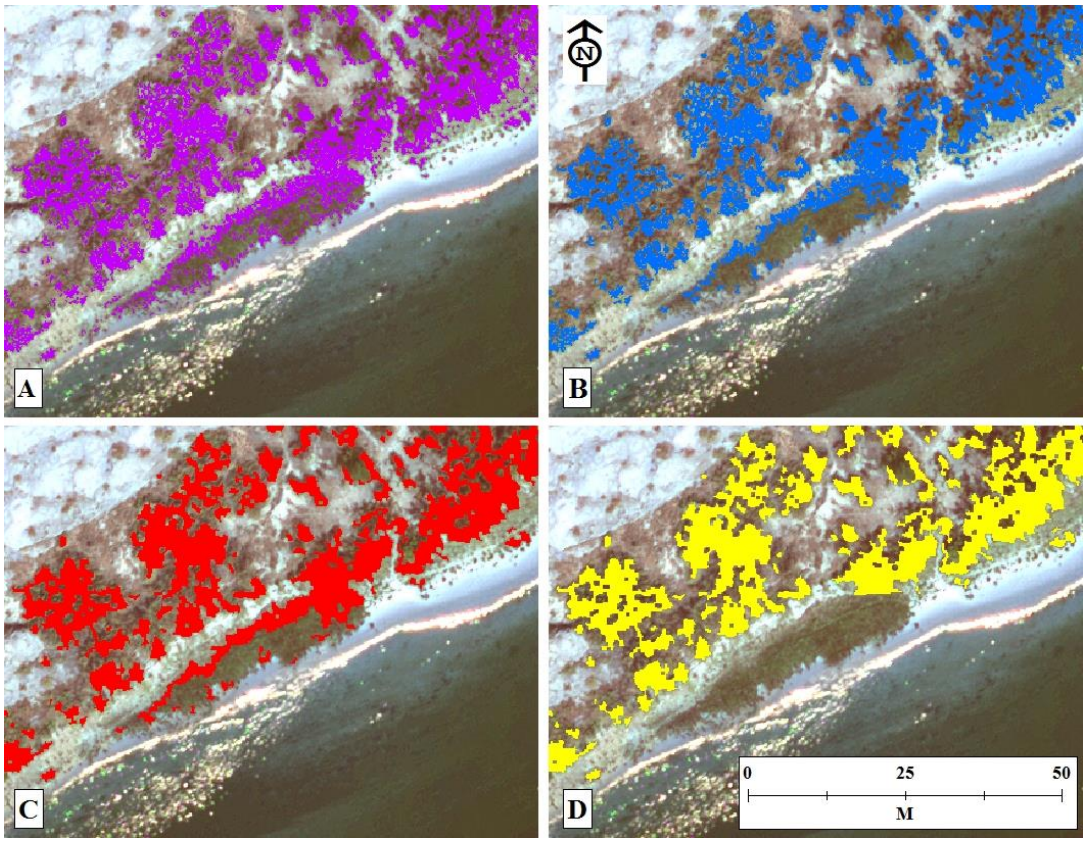

Figure 5: Site in Glen Canyon at -14.5 km (-9 Mile) Results of four different, consecutive processing steps that are used across the study area: 1) Initial Mahalanobis classification (Panel A), 2) Sieve operation applied to the output of the initial classification which removed any pixel groupings less than 11 pixels (Panel B), 3) Clump operation that is applied to the output of the sieve operation, which fills in gaps in the classification (Panel C), and 4) Manual erase operation to remove incorrectly classified vegetation.

Tamarisk Classification: Kanab Reach

The initial Mahalanobis classification of the Kanab reach had an overall accuracy of 72% (Table 10). Tamarisk producer's and user's accuracies were 73% and 71%, respectively. Non-tamarisk producer's and user's accuracies were 72% and 73%, respectively. After the sieve operation was implemented in the Kanab study area, overall accuracy increased to 75% (Table 11). Producer's accuracy improved for tamarisk to 78%, while non-tamarisk producer's accuracy stayed the same at 72%. User's accuracy of tamarisk decreased to 69% after the sieve operation, while non-tamarisk vegetation increased to 81%.

The clump operation further increased the overall accuracy to 77% (Table 12). The clump function increased tamarisk user's accuracy to 76% and decreased non-tamarisk user's accuracy to 78%. Producer's accuracy stayed the same in the tamarisk class from the clump operation at 78%, while non-tamarisk producer's accuracy increased to 77%. User's accuracy of tamarisk increased to 76% after the clump operation, while non-tamarisk vegetation decreased to 78%. Manually erasing large improperly classified non-tamarisk areas increased overall accuracy to 83% (Table 13). User's accuracy for tamarisk remained the same at 76%, while non-tamarisk increased to 89%. Producer's accuracy for tamarisk increased to 87%, and non-tamarisk increased to 79%.

Table 10: Kanab Initial Mahalanobis Classification

Reference Data				
Classification	Tamarisk	Non-tamarisk	Total	**User's accuracy**
Tamarisk	641	259	900	**71%**
Non-tamarisk	243	657	900	**73%**
Total	884	916	1800	
Producer's accuracy	**73%**	**72%**		
Overall accuracy			**72%**	

Table 11: Kanab sieve operation applied

Reference Data				
Classification	Tamarisk	Non-tamarisk	Total	**User's accuracy**
Tamarisk	617	283	900	**69%**
Non-tamarisk	175	725	900	**81%**
Total	792	1008	1800	
Producer's accuracy	**78%**	**72%**		
Overall accuracy			**75%**	

Table 12: Kanab clump operation applied

Reference Data				
Classification	Tamarisk	Non-tamarisk	Total	**User's accuracy**
Tamarisk	686	214	900	**76%**
Non-tamarisk	194	706	900	**78%**
Total	880	920	1800	
Producer's accuracy	**78%**	**77%**		
Overall accuracy			**77%**	

Table 13: Kanab final classification with manual erase applied

Reference Data				
Classification	Tamarisk	Non-tamarisk	Total	**User's accuracy**
Tamarisk	686	214	900	**76%**
Non-tamarisk	99	801	900	**89%**
Total	785	1015	1800	
Producer's accuracy	**87%**	**79%**		
Overall accuracy			**83%**	

Tamarisk Classification: National Reach

The initial Mahalanobis classification of the National reach had an overall accuracy of 58% (Table 14). Tamarisk producer's and user's accuracies were both 58%. Non-tamarisk producer's and user's accuracies were also both 58%. After the sieve operation was implemented in the National study area, overall accuracy increased to 60% (Table 15). User's accuracy for tamarisk declined to 55%, and increased to 65% for non-tamarisk. Producer's accuracy increased to 61% and 59% for tamarisk and non-tamarisk respectively.

The clump operation further increased the overall accuracy to 62% (Table 16). The clump function increased tamarisk user's accuracy to 65% and non-tamarisk user's accuracy declined to 60%. Producer's accuracy increased in the tamarisk class after the sieve operation to 62%, while non-tamarisk producer's accuracy increased to 63% after the sieve operation. Manually erasing large improperly classified non-tamarisk areas increased overall accuracy to 72% (Table 17). The final user's accuracy for tamarisk

remained 65% but increased to 79% for non-tamarisk. Producer's accuracy increased to 76% and 69% for tamarisk and non-tamarisk respectively.

Table 14: National Initial Mahalanobis Classification

	Reference Data			
Classification	Tamarisk	Non-tamarisk	Total	**User's accuracy**
Tamarisk	592	430	1022	**58%**
Non-tamarisk	428	594	1022	**58%**
Total	1020	1024	2044	
Producer's accuracy	**58%**	**58%**		
Overall accuracy			**58%**	

Table 15: National sieve operation applied

	Reference Data			
Classification	Tamarisk	Non-tamarisk	Total	**User's accuracy**
Tamarisk	559	463	1022	**55%**
Non-tamarisk	355	667	1022	**65%**
Total	914	1130	2044	
Producer's accuracy	**61%**	**59%**		
Overall accuracy			**60%**	

Table 16: National clump operation applied

	Reference Data			
Classification	Tamarisk	Non-tamarisk	Total	**User's accuracy**
Tamarisk	661	361	1022	**65%**
Non-tamarisk	411	611	1022	**60%**
Total	1072	972	2044	
Producer's accuracy	**62%**	**63%**		
Overall accuracy			**62%**	

Table 17: National final classification with manual erase applied

Reference Data				
Classification	Tamarisk	Non-tamarisk	Total	**User's accuracy**
Tamarisk	667	361	1028	**65%**
Non-tamarisk	215	807	1022	**79%**
Total	882	1168	2050	
Producer's accuracy	**76%**	**69%**		
Overall accuracy			**72%**	

Change Detection: NDVI decline in Glen Canyon Reach

A total of 28.6 ha were classified as tamarisk in the Glen Canyon reach in 2009. Of this area, 30% had experienced tamarisk decline by 2013, when using the NDVI decline ratio (Table 18). Summarizing tamarisk NDVI decline by .16 km (0.1 mile) river segments showed a range of tamarisk decline from 2% to 70% along the Glen Canyon reach (Appendix A). On average, the 0.16 km segments had 23% decline in the area classified as tamarisk in 2009. The five highest 0.16 km segments of % NDVI decline from greatest % NDVI decline were located at river segments -11.4, -3.5, -16.3, -18.2 and -4.8. Often, the largest tamarisk stands mapped in 2009 showed the largest amount of decline in area. To gain a better understanding of the effectiveness of the Glen Canyon NDVI change detection image, Table 19 shows that the image correctly identified 700 out of a total 735 tamarisk validation pixels that met the NDVI change ratio. The change detection image also incorrectly included 31 out of 177 non-tamarisk pixels that also met the NDVI change ratio.

Table 18: Tamarisk change in Glen Canyon from 2009 to 2013 using NDVI analysis.

	Number pixels	Hectares	Percent
No change	4,970,217	19.9	70%
Decline	2,177,707	8.7	30%
Total	7,147,924	28.6	100%

Table 19: Validation pixels comparing amount of declined tamarisk and non-tamarisk pixels using the complete vegetation change image and tamarisk classification change image for Glen Canyon reach using NDVI analysis.

	Classification Layers	
Vegetation Type	NDVI change layer	Tamarisk Classification NDVI Change
Tamarisk No Change	765	800
Tamarisk Decline	735	700
Non-tamarisk No Change	1323	1469
Non-tamarisk Decline	177	31

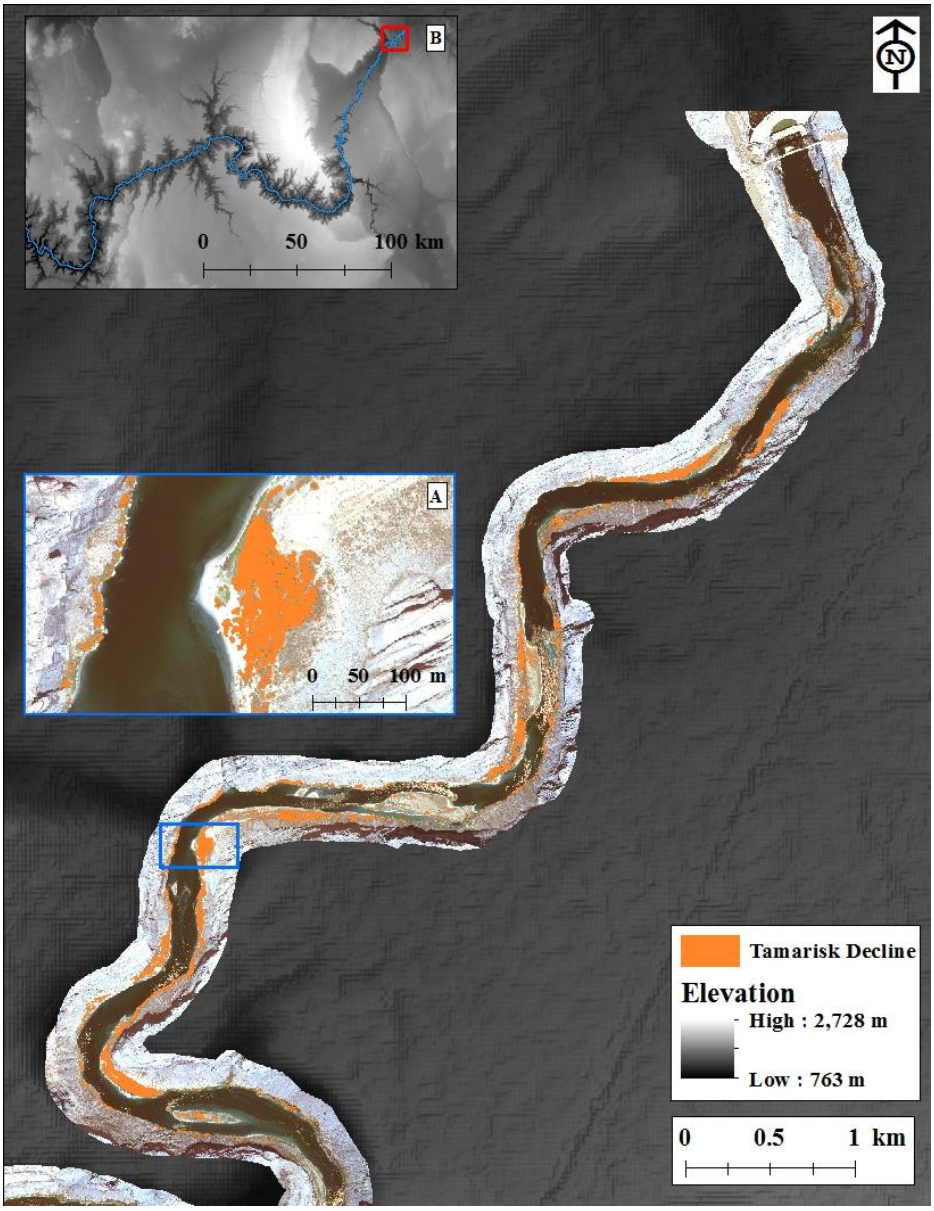

Figure 6: Upper portion of Glen Canyon reach from -25.4 to -15.3 km showing the areas of tamarisk NDVI decline from 2009 to 2013. Elevation image is an ASTER dataset, overlaid by the 2009 USGS overflight imagery. Panel A shows Ferry Swale at -17.7 km and panel B shows the Glen Canyon study reach.

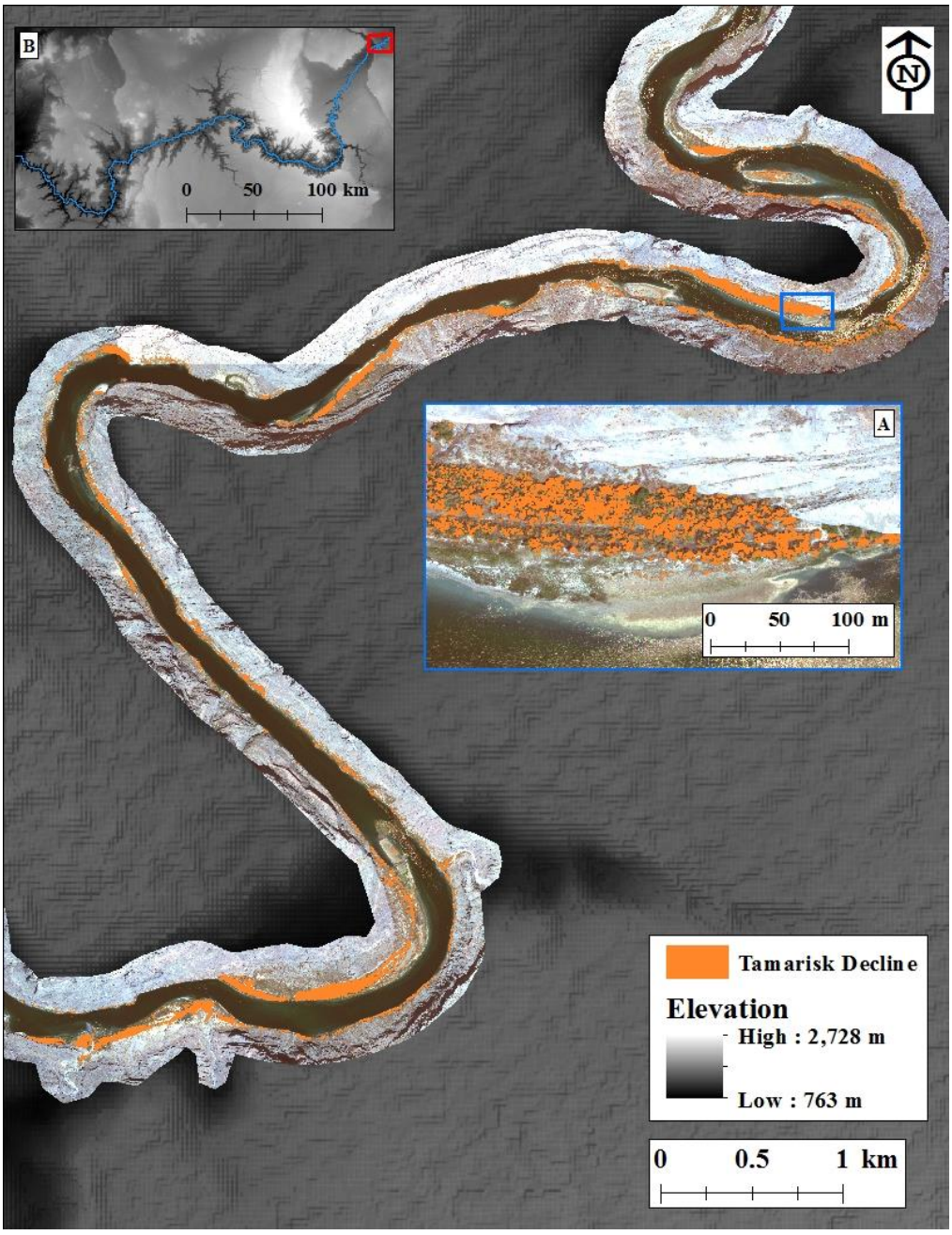

Figure 7: Middle portion of Glen Canyon reach from -15.3 to -3.4 km showing the areas of tamarisk NDVI decline from 2009 to 2013. Elevation image is an ASTER dataset, overlaid by the 2009 USGS overflight imagery. Panel A shows a close up view of tamarisk decline at -13.7 km and panel B shows the study reach.

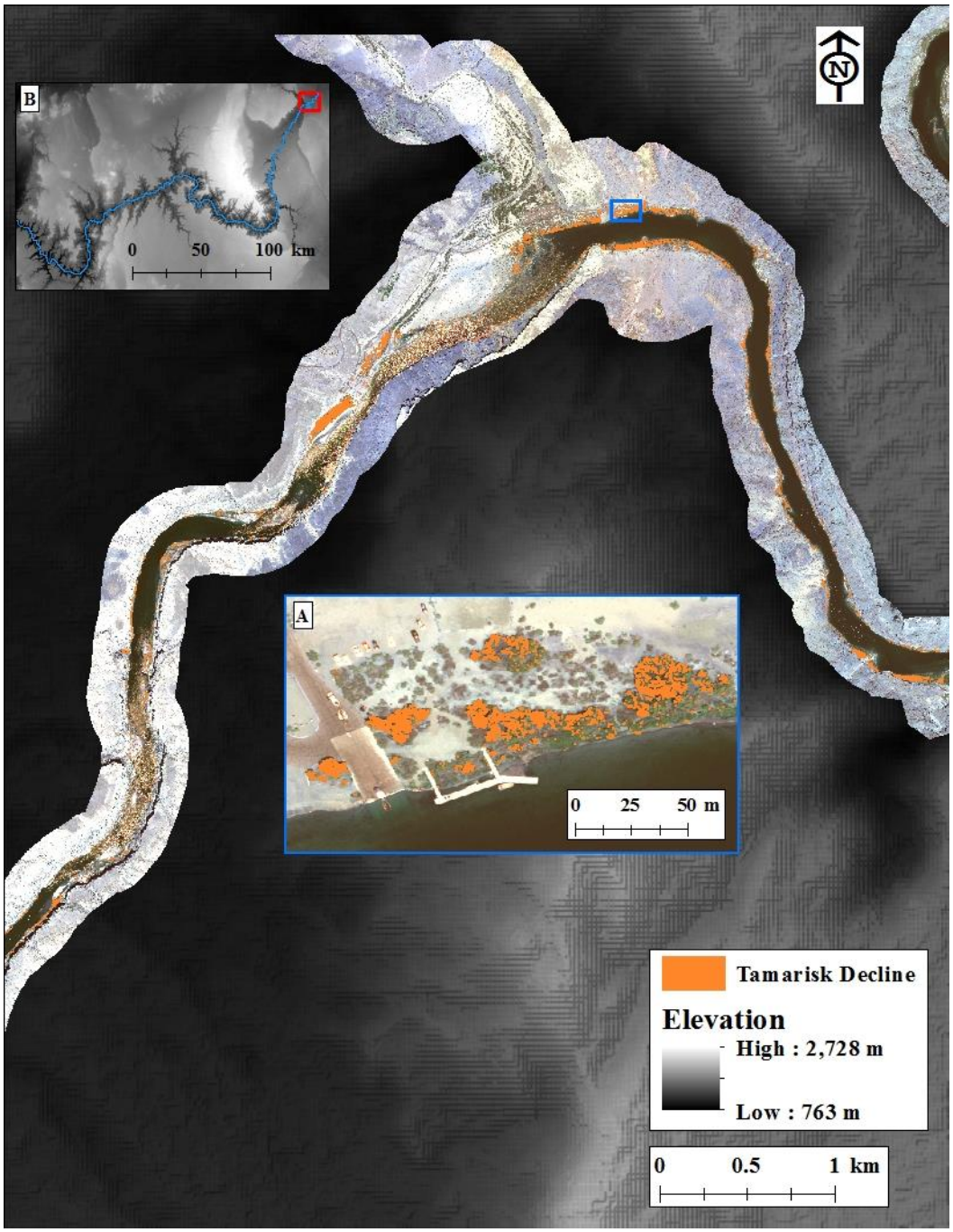

Figure 8: Lower portion of Glen Canyon reach from -3.4 to 6 km showing the areas of tamarisk NDVI decline from 2009 to 2013. Elevation image is an ASTER dataset, overlaid by the 2009 USGS overflight imagery. Panel A shows a close up view of tamarisk decline at Lees Ferry 0 km and panel B shows the study reach.

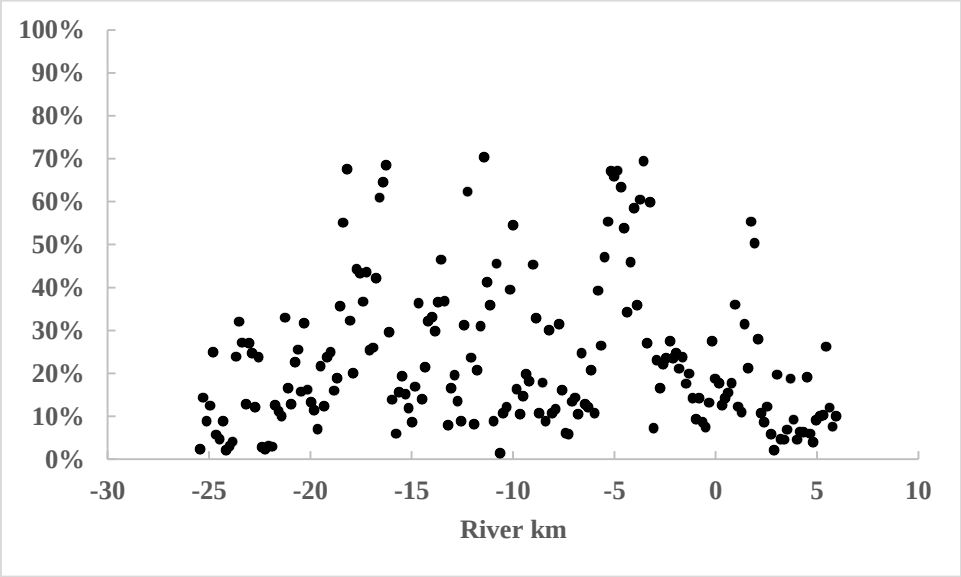

Figure 9: Figure 9: Percent of tamarisk by river segment with NDVI decline per 0.16 km river segment. Glen Canyon Dam is ~ -25 km. Lees Ferry is at 0 km.

Change Detection: EVI decline Glen Canyon Reach

Sixty-five percent of the area classified as tamarisk in the Glen Canyon reach in 2009 (28.6 ha) experienced tamarisk decline by 2013, when using the EVI decline ratio (Table 20). Over twice the area of tamarisk were listed as declined by the EVI ratio compared against the NDVI decline ratio. Identifying tamarisk EVI decline by .16 km (0.1 mile) segments shows a range of tamarisk decline along the river corridor for Glen Canyon (Appendix B) from 6% to 96% of the area classified as tamarisk in 2009. On average, EVI decline was observed in 54% of the area classified as tamarisk in 2009 across the river segments. The five highest km segments of % EVI decline in rank order were located at river segments -16.3, -16.6, -16.4, -18.2 and -18.3. To gain a better understanding of the effectiveness of the Glen Canyon EVI change detection image, Table 21 shows that the image correctly identified 1233 out of a total 1315 tamarisk validation pixels that met the EVI change ratio. The change detection image also incorrectly included 85 out of 422 non-tamarisk pixels that also met the EVI change ratio.

Table 20: Tamarisk change in Glen Canyon from 2009 to 2013 using EVI analysis.

	Number pixels	Hectares	Percent
No Change	2,504,366	10	35%
Decline	4,643,558	18.6	65%
Total	7,147,924	28.6	100%

Table 21: Validation pixels comparing amount of declined tamarisk and non-tamarisk pixels using total vegetation change image and tamarisk classification change image for Glen Canyon reach using EVI analysis.

	Classification Layers	
Vegetation Type	EVI change layer	Tamarisk Classification EVI Change
Tamarisk No Change	185	267
Tamarisk Decline	1315	1233
Non-tamarisk No Change	1078	1415
Non-tamarisk Decline	422	85

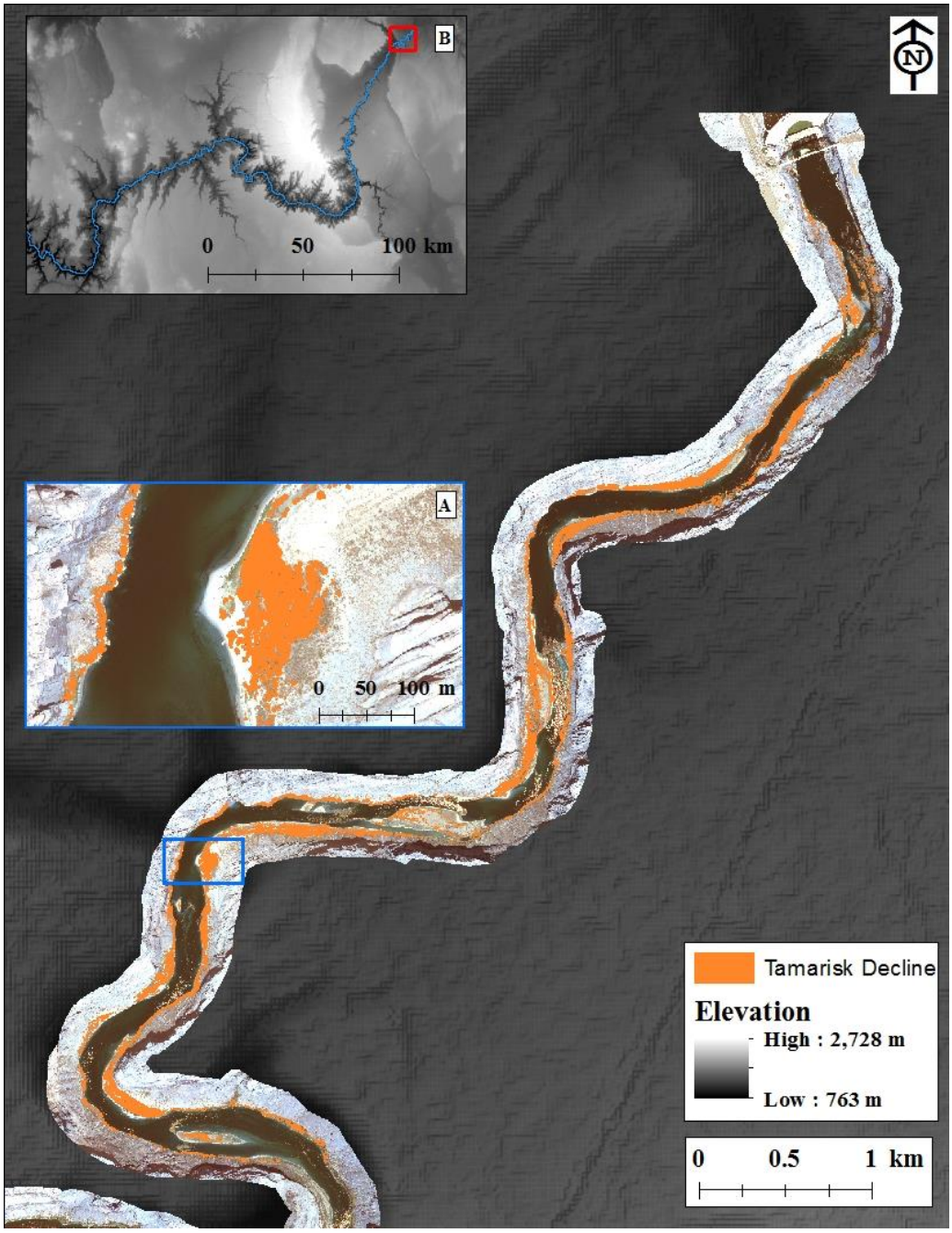

Figure 10: Upper portion of Glen Canyon reach from -25.4 to -15.3 km showing the areas of tamarisk EVI decline from 2009 to 2013. Elevation image is an ASTER dataset, overlaid by the 2009 USGS overflight imagery. Panel A shows Ferry Swale at -17.7 km and panel B shows the Glen Canyon study reach.

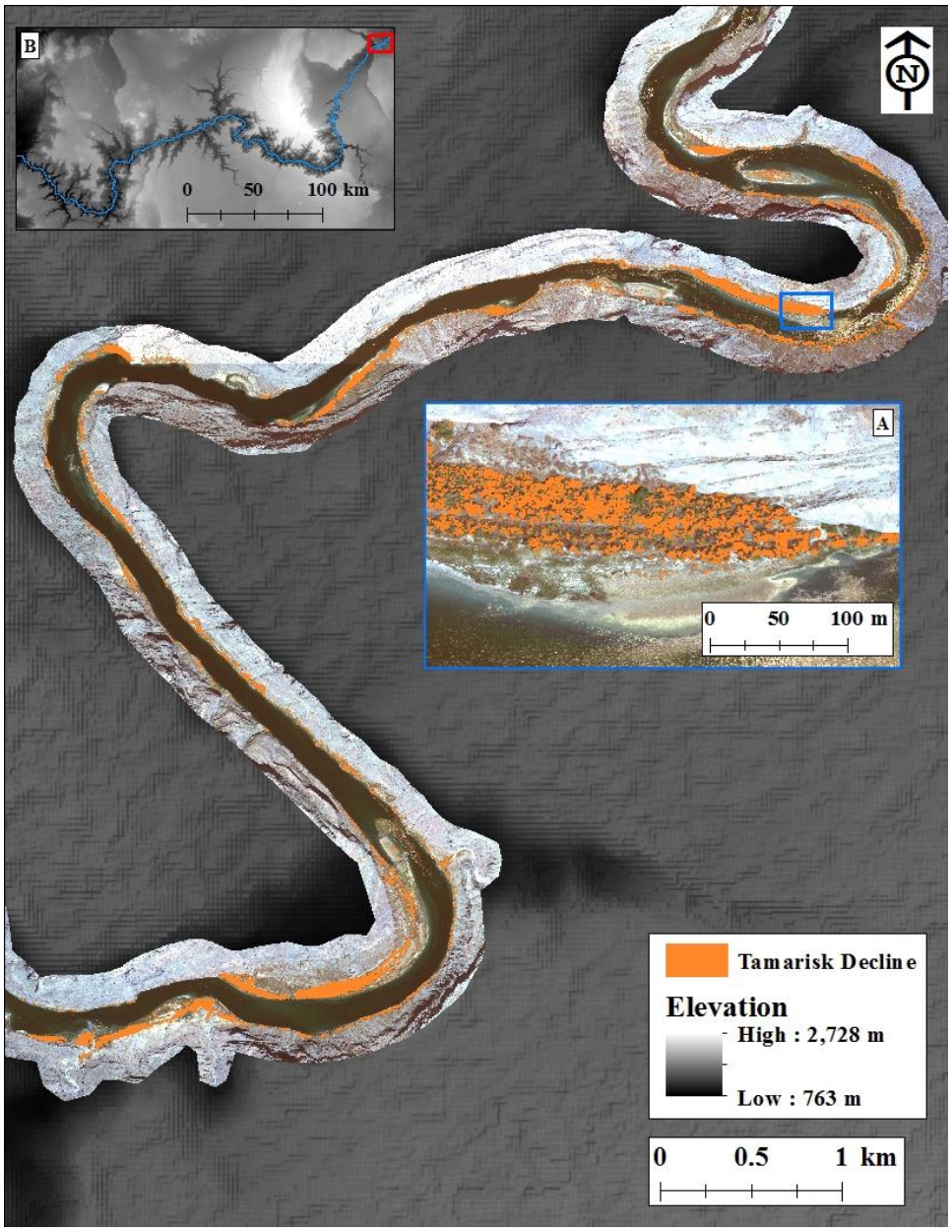

Figure 11: Middle portion of Glen Canyon reach from -15.3 to -3.4 km showing the areas of tamarisk EVI decline from 2009 to 2013. Elevation image is an ASTER dataset, overlaid by the 2009 USGS overflight imagery. Panel A shows a close up view of tamarisk decline at -13.7 km and panel B shows the study reach.

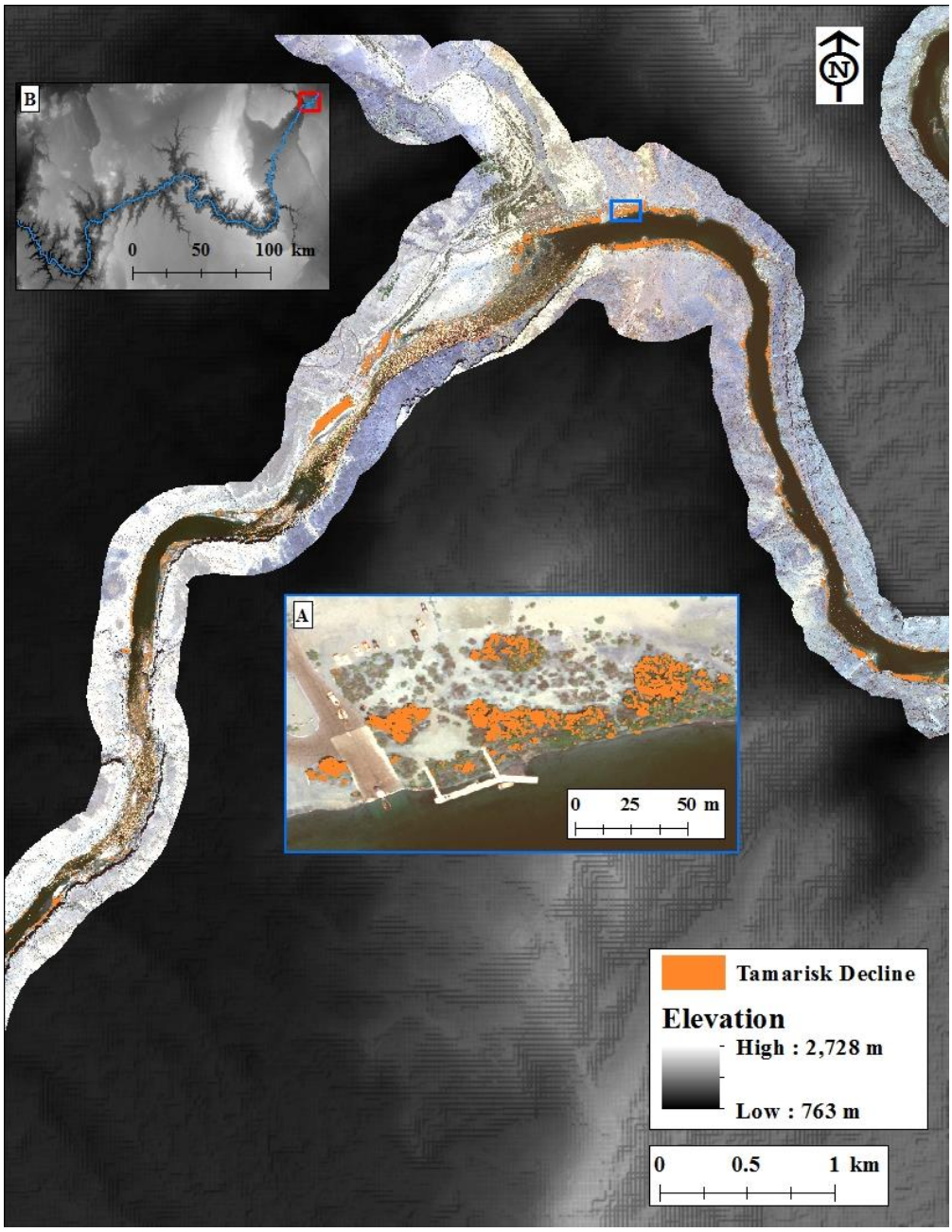

Figure 12: Lower portion of Glen Canyon reach from -3.4 to 6 km showing the areas of tamarisk EVI decline from 2009 to 2013. Elevation image is an ASTER dataset, overlaid by the 2009 USGS overflight imagery. Panel A shows a close up view of tamarisk decline at Lees Ferry 0 km and panel B shows the study reach.

Change Detection: NDVI decline in Kanab Reach

A total of 5.1 ha were classified as tamarisk in the Kanab reach in 2009. 21% of this area had experienced tamarisk decline by 2013, when using the NDVI decline ratio (Table 22). NDVI decline for Kanab averaged 22% (Appendix C). The range of NDVI decline for Kanab was from 2% to 69% for the 0.16 km river segments. The five segments with highest percentage NDVI decline were 243.3, 243.2, 231.7, 231.9, and 241.4. Kanab creek located at km 231.7 had the third highest percent NDVI decline of 61%. The five segments with the most area of NDVI decline were 231.7, 221.8, 227.6, 227.4 and 227.9 composed a .21 ha area, or 19% of the total tamarisk area. This area decline can also be viewed as .8 km of the total 33.5 km river length accounted for 19% of the tamarisk decline area. To gain a better understanding of the effectiveness of the Kanab NDVI change detection image, Table 23 shows that the image correctly identified 127 out of a total 178 tamarisk validation pixels that met the NDVI change ratio. The change detection image also incorrectly included 23 out of 203 non-tamarisk pixels that also met the NDVI change ratio.

Table 22: Tamarisk change in Kanab from 2009 to 2013 using NDVI analysis.

	Number pixels	Hectares	Percent
No Change	1,000,618	4	79%
Decline	271,258	1.1	21%
Total	1,271,876	5.1	100%

Table 23: Validation pixels comparing amount of declined tamarisk and non-tamarisk pixels using total vegetation change image and tamarisk classification change image for Kanab reach using NDVI analysis.

	Classification Layers	
Vegetation Type	NDVI change layer	Tamarisk Classification NDVI Change
Tamarisk No Change	722	773
Tamarisk Decline	178	127
Non-tamarisk No Change	697	877
Non-tamarisk Decline	203	23

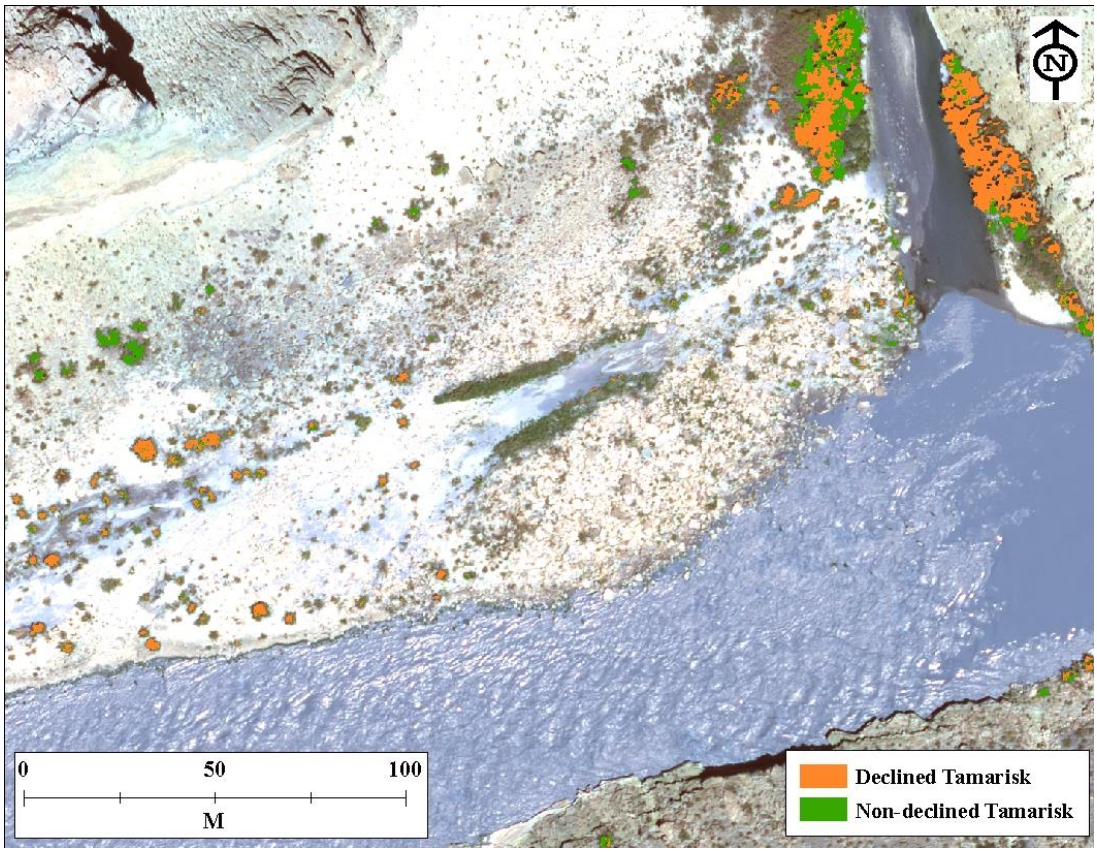

Figure 13: Tamarisk with NDVI decline overlaid with the remaining green tamarisk at the Kanab Creek confluence located at km 231.7 (mile 144). Base image is the 2009 USGS overflight image used in the classification. Kanab Creek has been identified as a point of entrance for the tamarisk beetle as the beetles traveled down Kanab Creek from Utah (Makarick, 2016).

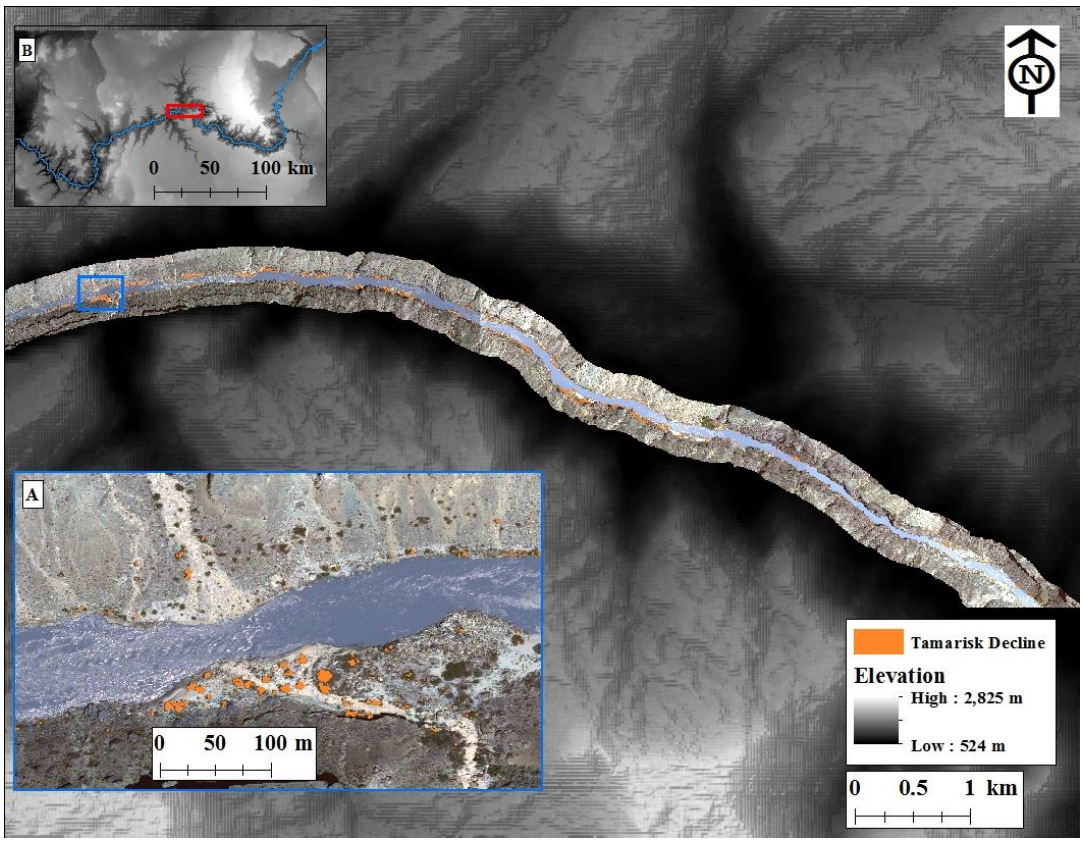

Figure 14: Upper portion of Kanab reach from 216.6 to 226.6 km showing the areas of tamarisk NDVI decline. Elevation image is an ASTER dataset, overlaid by the 2009 USGS overflight imagery. Panel A shows a close up view of tamarisk decline at 226.1 km and panel B shows the study reach.

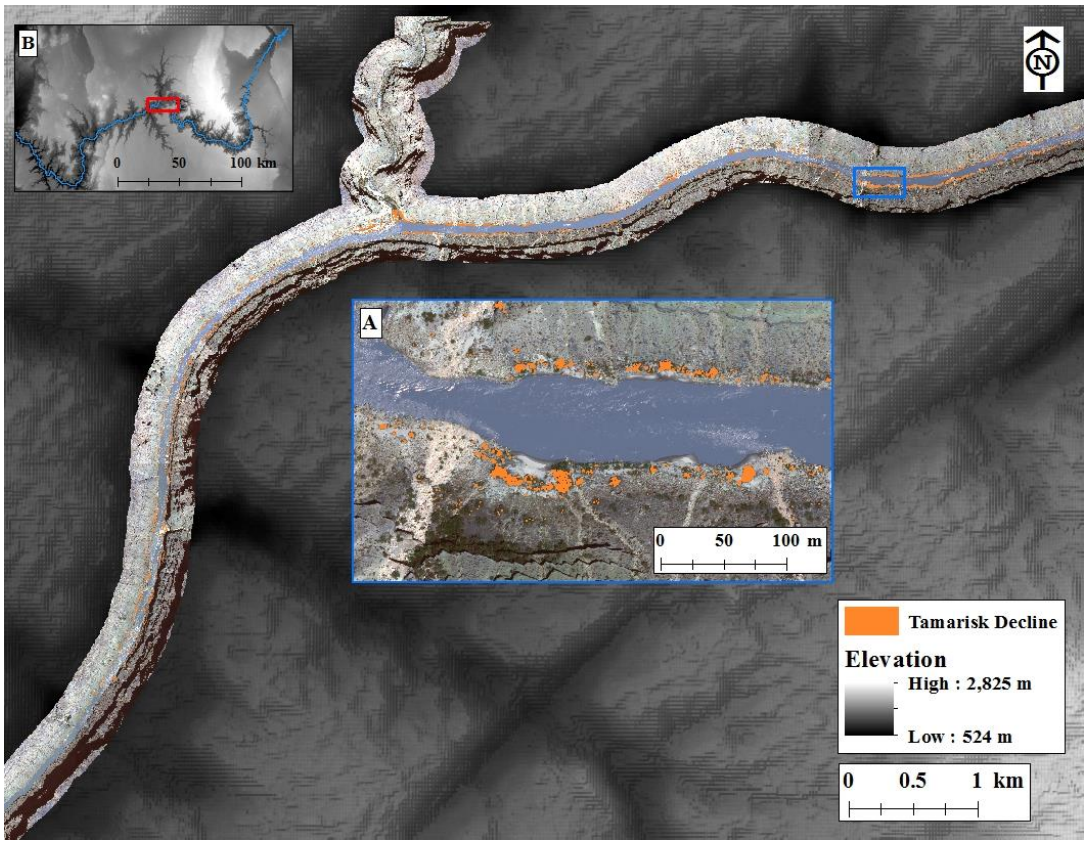

Figure 15: Middle portion of Kanab reach from 226.6 to 236.6 km showing the areas of tamarisk NDVI decline. Kanab Creek is visible in the midway in the image and had the highest percent of NDVI declined tamarisks in one area in all of Kanab reach. Elevation image is an ASTER dataset, overlaid by the 2009 USGS overflight imagery. Panel A shows a close up view of tamarisk decline at 227.9 km and panel B shows the study reach.

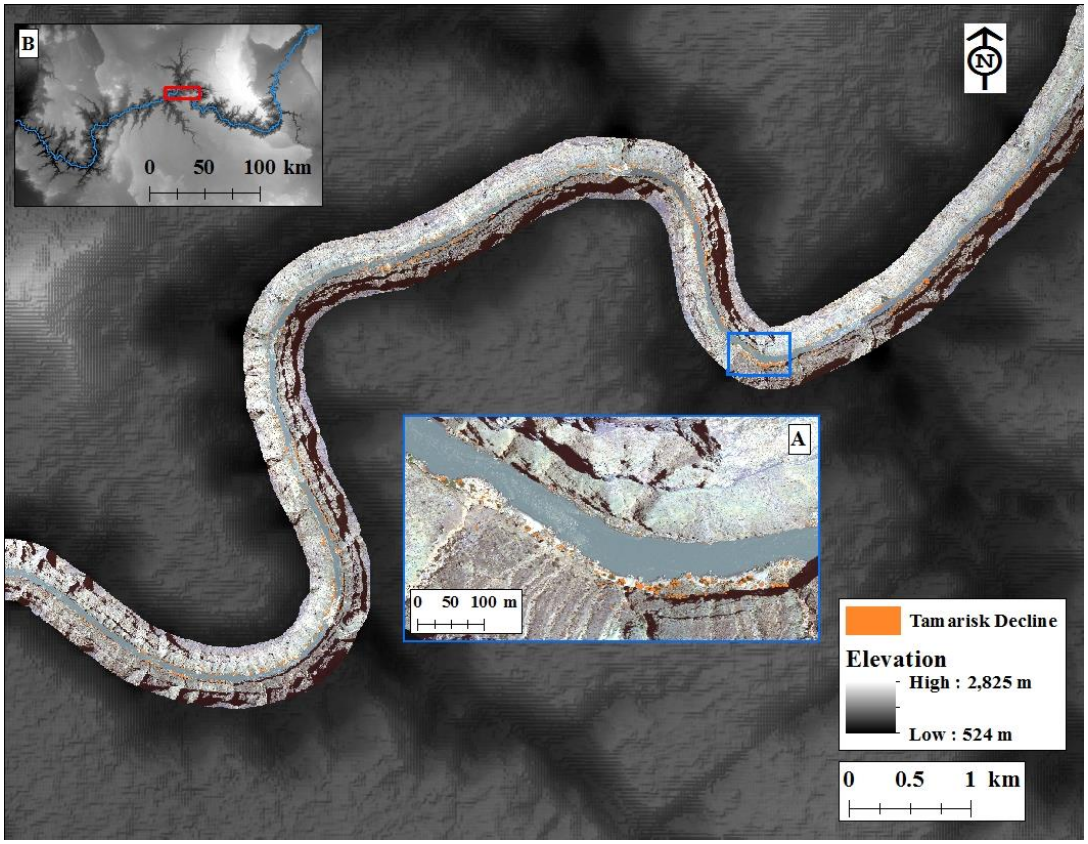

Figure 16: Lower portion of Kanab reach from 236.6 to 250.6 km showing the areas of tamarisk NDVI decline. Elevation image is an ASTER dataset, overlaid by the 2009 USGS overflight imagery. Panel A shows a close up view of tamarisk decline at 239.6 km and panel B shows the study reach.

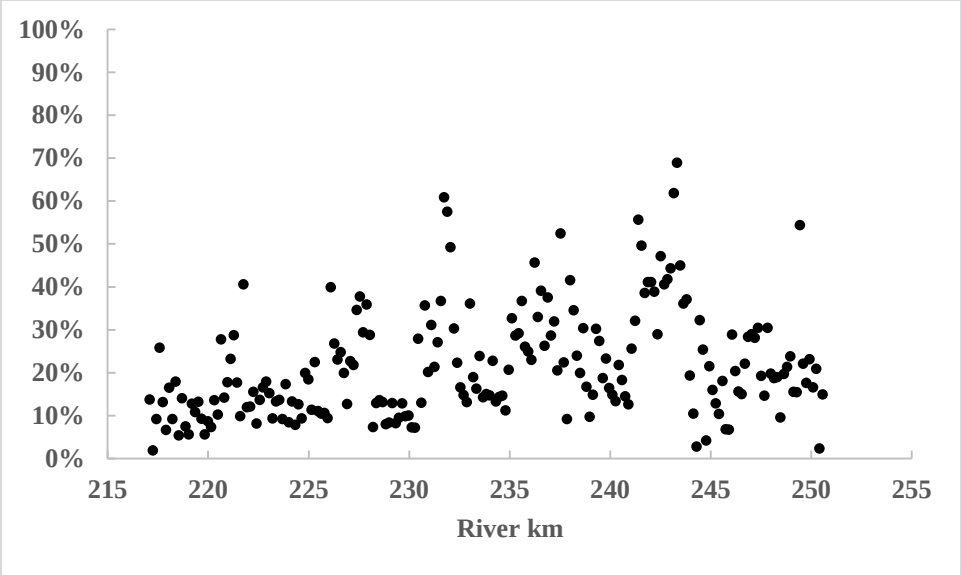

Figure 17: Percent tamarisk NDVI decline through Kanab study area by .16 km segments

Change Detection: EVI decline in Kanab Reach

A total of 5.1 ha was classified as tamarisk in the Kanab reach in 2009. 8% of this area had experienced tamarisk decline by 2013, when using the EVI decline ratio (Table 24). EVI decline averaged 8%. EVI decline values ranged from 0% to 97% in the 0.16 km river segments. The five segments with highest EVI decline percentages were 243.2, 243.0, 243.3, 221.8, and 241.2. The five segments with the most area of EVI decline were 221.8, 231.7, 221.1, 221.3, and 221.6. These five segments totaling .8 km of the total 33.5 km river length had a total ha area decline of .11 or 28% of the total area declined. To gain a better understanding of the effectiveness of the Kanab EVI change detection image, Table 25 shows that the image correctly identified 45 out of a total 60 tamarisk validation pixels that met the EVI change ratio. The change detection image

also incorrectly included 13 out of 65 non-tamarisk pixels that also met the EVI change ratio.

Table 24: Tamarisk change in Kanab from 2009 to 2013 using EVI analysis.

	Number pixels	Hectares	Percent
No Change	1,174,635	4.7	92%
Decline	97,241	0.4	8%
Total	1,271,876	5.1	100%

Table 25: Validation pixels comparing amount of declined tamarisk and non-tamarisk pixels using total vegetation change image and tamarisk classification change image for Kanab reach using EVI analysis.

	Classification Layers	
Vegetation Type	EVI change layer	Tamarisk Classification EVI Change
Tamarisk No Change	840	855
Tamarisk Decline	60	45
Non-tamarisk No Change	835	887
Non-tamarisk Decline	65	13

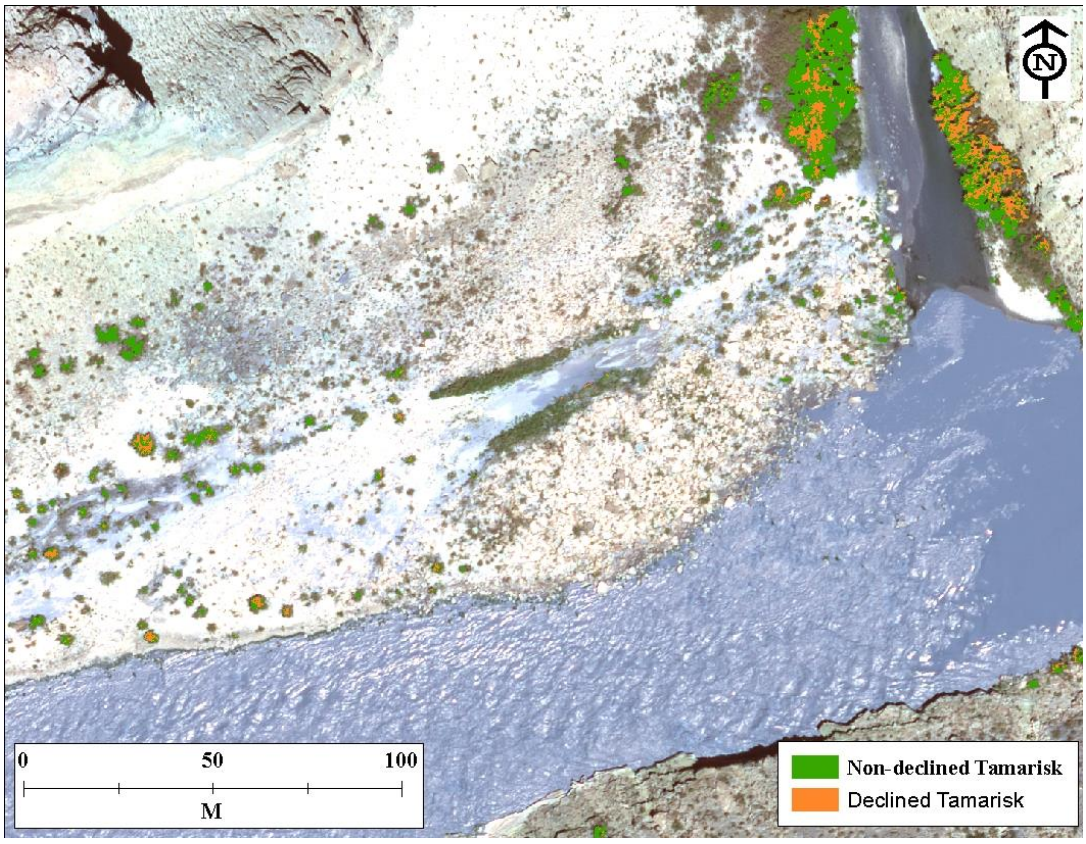

Figure 18: Tamarisk with EVI decline overlaid with the remaining green tamarisk at the Kanab Creek confluence located at km 231.7 (mile 144). Base image is the 2009 USGS overflight image used in the classification. Kanab Creek has been identified as a point of entrance for the tamarisk beetle as the beetles traveled down Kanab Creek from Utah (Makarick, 2016).

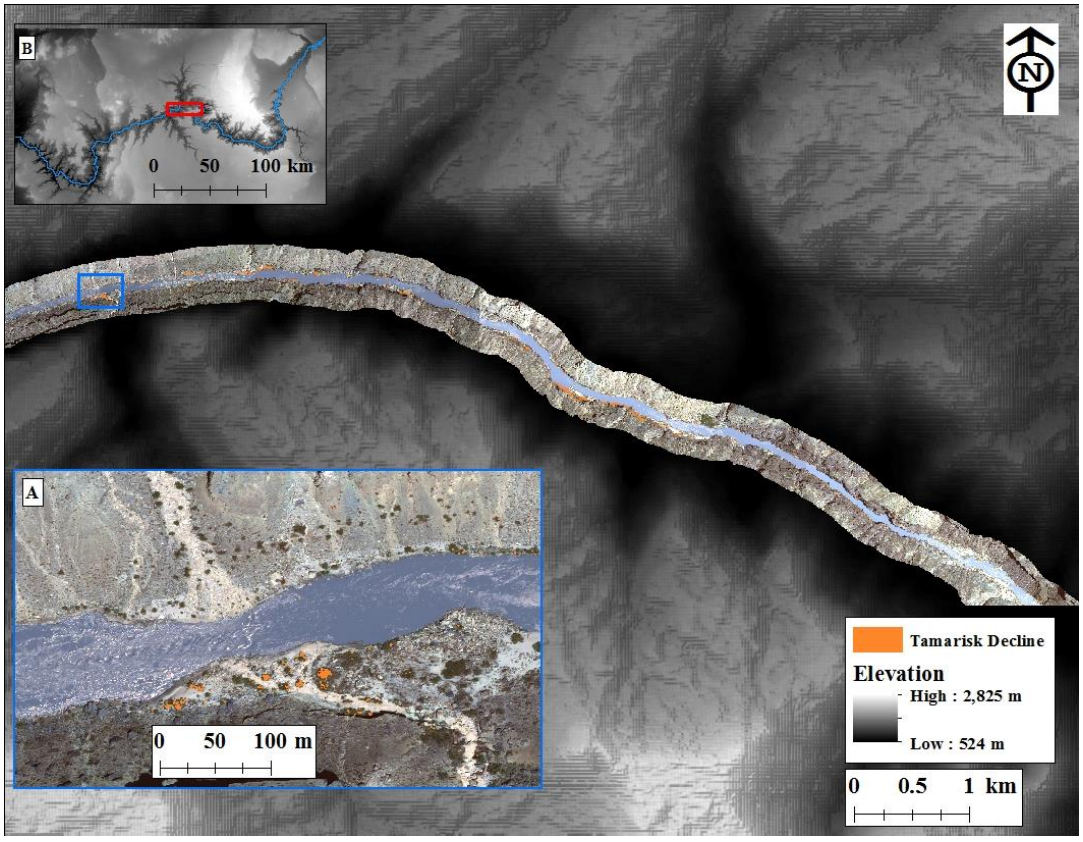

Figure 19: Upper portion of Kanab reach from 216.6 to 226.6 km showing the areas of tamarisk EVI decline. Elevation image is an ASTER dataset, overlaid by the 2009 USGS overflight imagery. Panel A shows a close up view of tamarisk decline at 226.1 km and panel B shows the study reach.

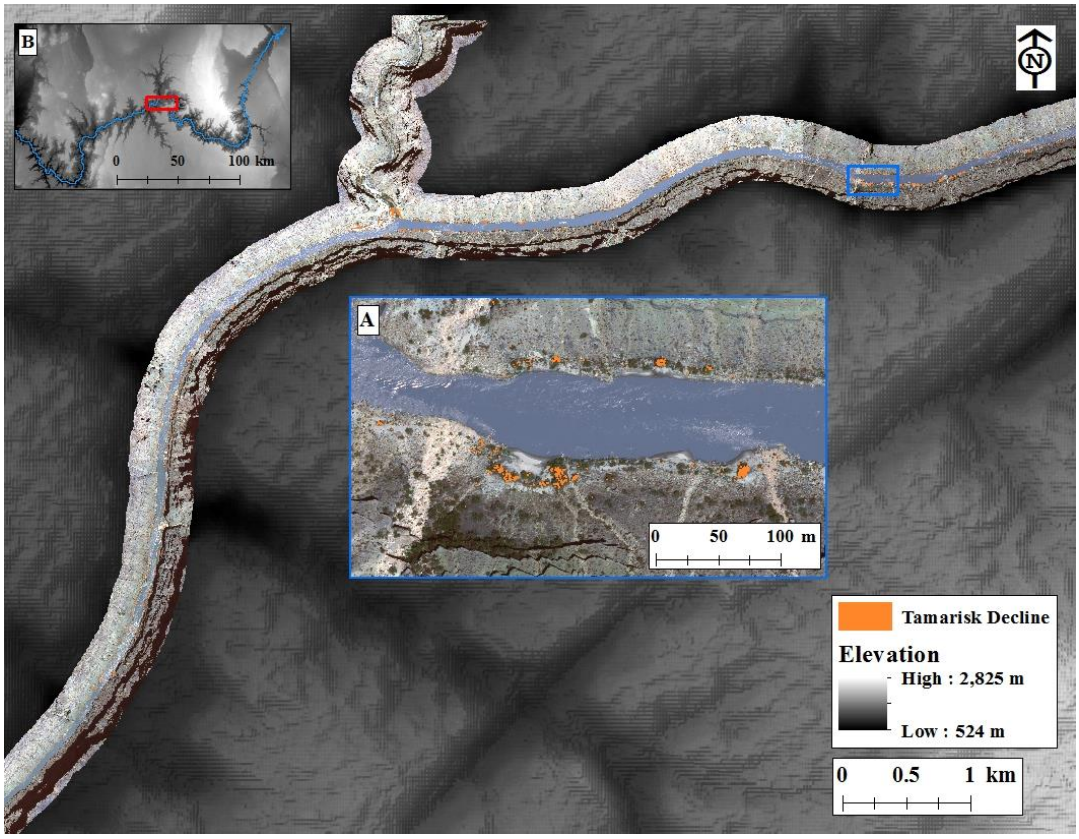

Figure 20: Middle portion of Kanab reach from 226.6 to 236.6 km showing the areas of tamarisk EVI decline. Kanab Creek is visible in the midway in the image and had the highest percent of EVI declined tamarisks in one area in all of Kanab reach. Elevation image is an ASTER dataset, overlaid by the 2009 USGS overflight imagery. Panel A shows a close up view of tamarisk decline at 227.9 km and panel B shows the study reach.

Figure 21: Lower portion of Kanab reach from 236.6 to 250.6 km showing the areas of tamarisk EVI decline. Elevation image is an ASTER dataset, overlaid by the 2009 USGS overflight imagery. Panel A shows a close up view of tamarisk decline at 239.6 km and panel B shows the study reach.

Change Detection: NDVI decline in National Reach

A total of 24.6 ha were classified as tamarisk in the National reach in 2009. Twelve percent (2.9 ha) of this area experienced tamarisk decline by 2013, when using the NDVI decline ratio (Table 26). NDVI decline averaged 14%. NDVI decline ranged from 3% to 82%. The five segments with highest percent NDVI decline were 268.8, 268.9, 256.7, 260.2 and 259.6. The five segments with the most area declined were 268.9, 268.8,

289.4, 286.6, and 289.5. The five segments with the most area declined account for .4 ha or 14% of the total 2.9 ha declined area. The NDVI decline located at river km 268.8 (mile 167) is National Canyon. The high rate of decline at this area is attributed to a flash flood, and not tamarisk beetles. In July 2012 a flash flood removed nearly all of the vegetation from the debris fan at the confluence of National Canyon with the Colorado River. To gain a better understanding of the effectiveness of the National NDVI change detection image, Table 27 shows that the image correctly identified 99 out of a total 179 tamarisk validation pixels that met the NDVI change ratio. The change detection image also incorrectly included 27 out of 129 non-tamarisk pixels that also met the NDVI change ratio.

Table 26: Tamarisk change in National from 2009 to 2013 using NDVI analysis.

	Number pixels	Hectares	Percent
No Change	5,427,545	21.7	88%
Decline	722,836	2.9	12%
Total	6,150,381	24.6	100%

Table 27: Validation pixels comparing amount of declined tamarisk and non-tamarisk pixels using total vegetation change image and tamarisk classification change image for National reach using NDVI analysis.

	Classification Layers	
Vegetation Type	NDVI change layer	Tamarisk Classification NDVI Change
Tamarisk No Change	838	918
Tamarisk Decline	179	99
Non-tamarisk No Change	891	993
Non-tamarisk Decline	129	27

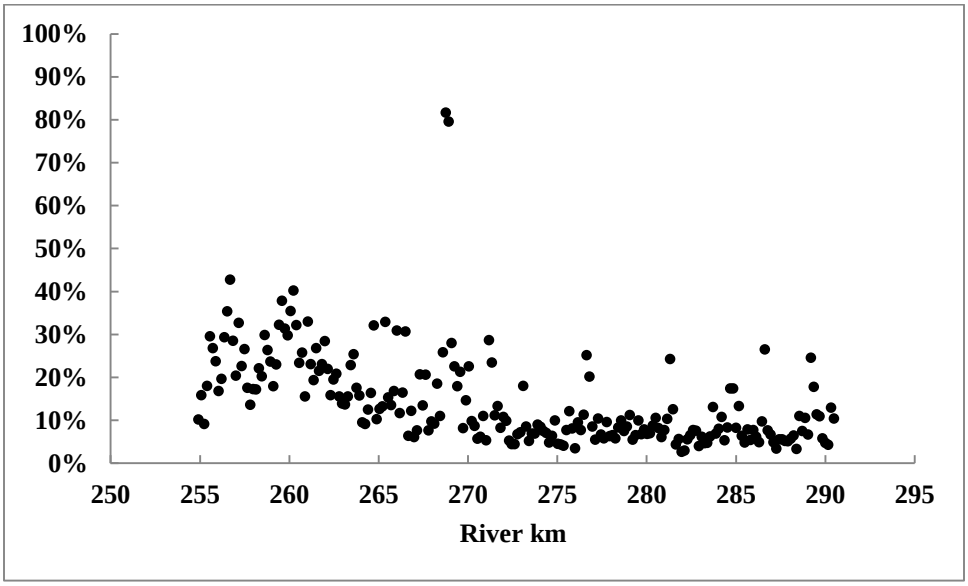

Figure 22: Percent tamarisk NDVI decline through National study area by .16 km segments

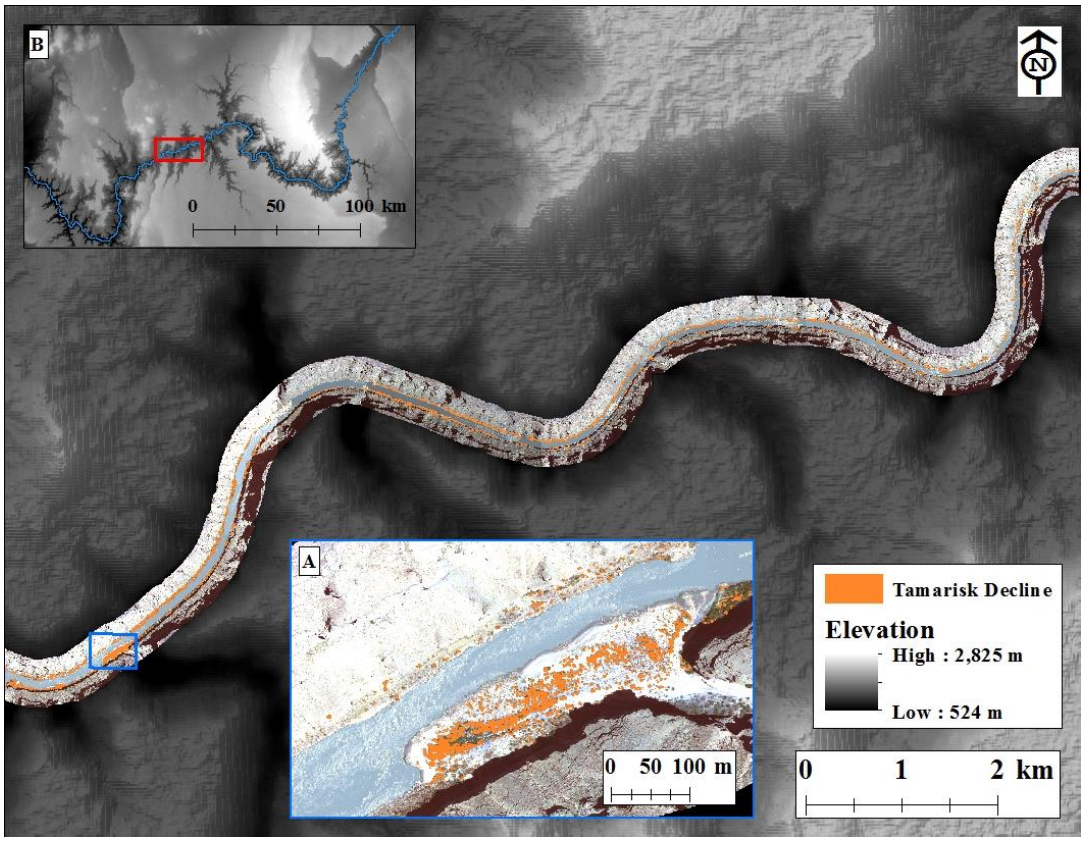

Figure 23: Upper portion of National reach from 255.2 to 270.0 km showing the areas of tamarisk NDVI decline. Elevation image is an ASTER dataset, overlaid by the 2009 USGS overflight imagery. Panel A shows a close up view of tamarisk decline at National Canyon (268.8 km) and panel B shows the study reach.

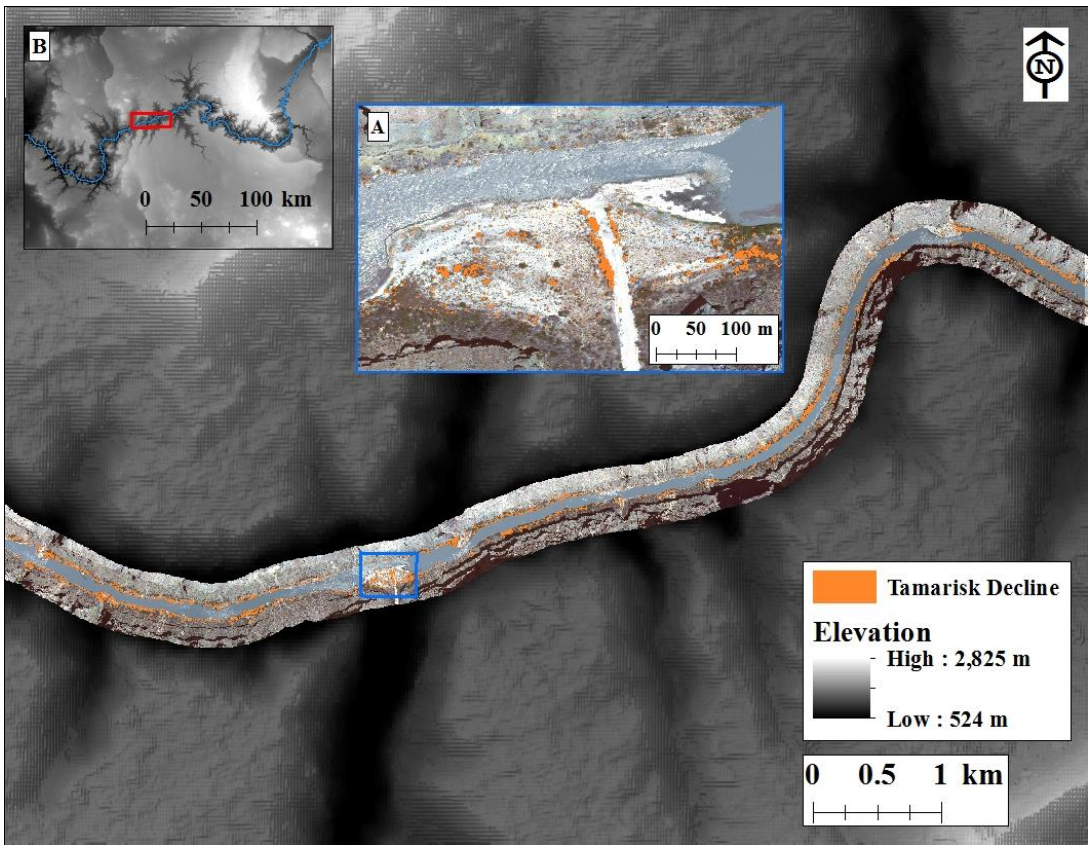

Figure 24: Middle portion of National reach from 270.0 to 279.9 km showing the areas of tamarisk NDVI decline. Elevation image is an ASTER dataset, overlaid by the 2009 USGS overflight imagery. Panel A shows a close up view of tamarisk decline at 276.6 km and panel B shows the study reach.

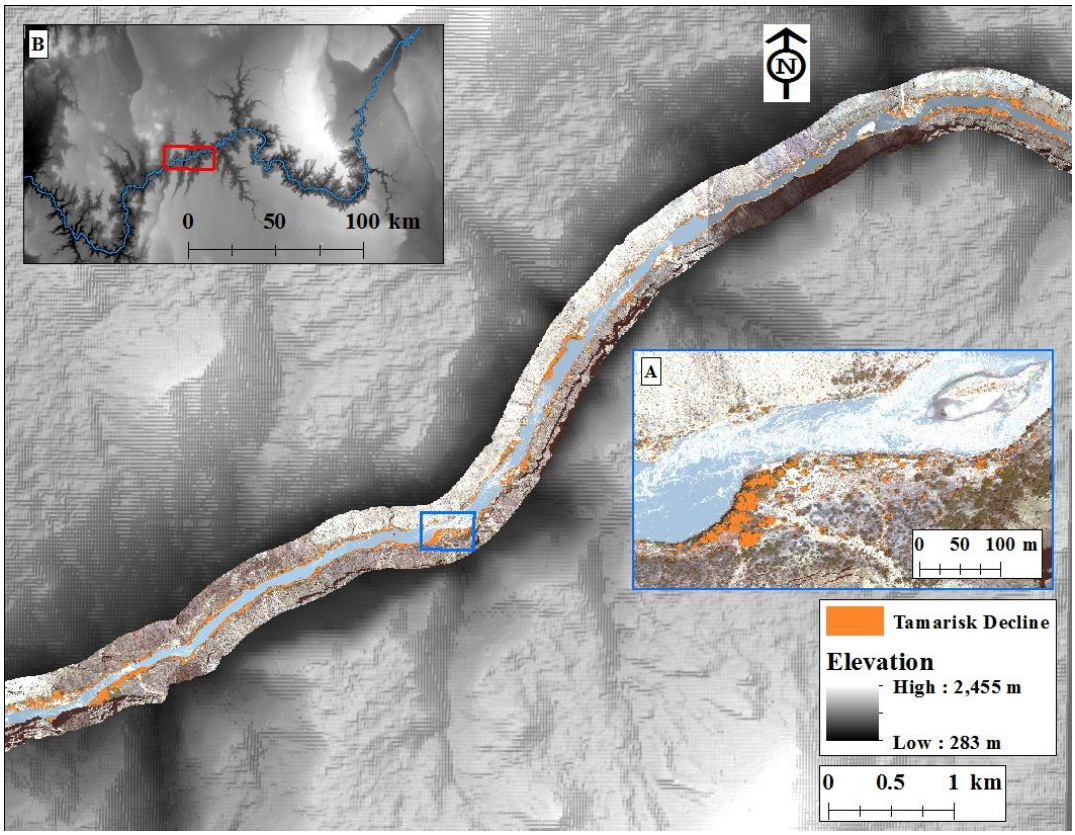

Figure 25: Lower portion of National reach from 279.9 to 290.5 km showing the areas of tamarisk NDVI decline. Elevation image is an ASTER dataset, overlaid by the 2009 USGS overflight imagery. Panel A shows a close up view of tamarisk decline at 286.5 km and panel B shows the study reach.

Change Detection: EVI decline in National Reach

A total of 24.6 ha were classified as tamarisk in the National reach in 2009. Eight percent of this area experienced tamarisk decline by 2013, when using the EVI decline ratio (Table 28). EVI decline averaged 8%. EVI decline ranged from 1% to 35.4%. The five highest EVI decline percent segments were 257.5, 286.6, 257.2, 272.1, and 257.3. The five segments with the greatest decline in area based on EVI decline in rank order

were 286.6, 289.4, 289.2, 275.7, and 288.6. The five segments with the highest EVI decline relating to area totaled .27 ha or 14% of the total declined area. To gain a better understanding of the effectiveness of the National EVI change detection image, Table 29 shows that the image correctly identified 75 out of a total 143 tamarisk validation pixels that met the EVI change ratio. The change detection image also incorrectly included 15 out of 85 non-tamarisk pixels that also met the EVI change ratio.

Table 28: Tamarisk change in National from 2009 to 2013 using EVI analysis.

	Number pixels	Hectares	Percent
No Change	5,648,298	22.6	92%
Decline	502,083	2.0	8%
Total	6,150,381	24.6	100%

Table 29: Validation pixels comparing amount of declined tamarisk and non-tamarisk pixels using total vegetation change image and tamarisk classification change image for National reach using EVI analysis.

	Classification Layers	
Vegetation Type	EVI change layer	Tamarisk Classification EVI Change
Tamarisk No Change	874	942
Tamarisk Decline	143	75
Non-tamarisk No Change	935	1005
Non-tamarisk Decline	85	15

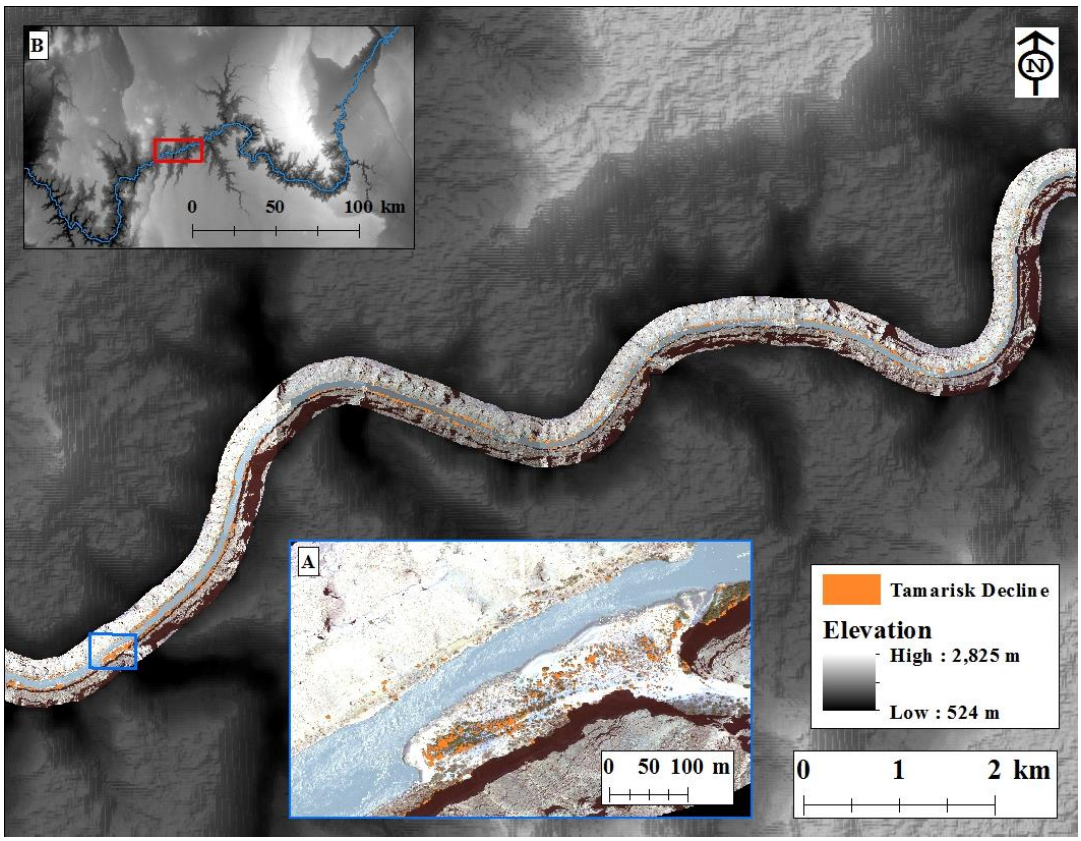

Figure 26: Upper portion of National reach from 255.2 to 270.0 km showing the areas of tamarisk EVI decline. Elevation image is an ASTER dataset, overlaid by the 2009 USGS overflight imagery. Panel A shows a close up view of tamarisk decline at National Canyon (268.8 km) and panel B shows the study reach.

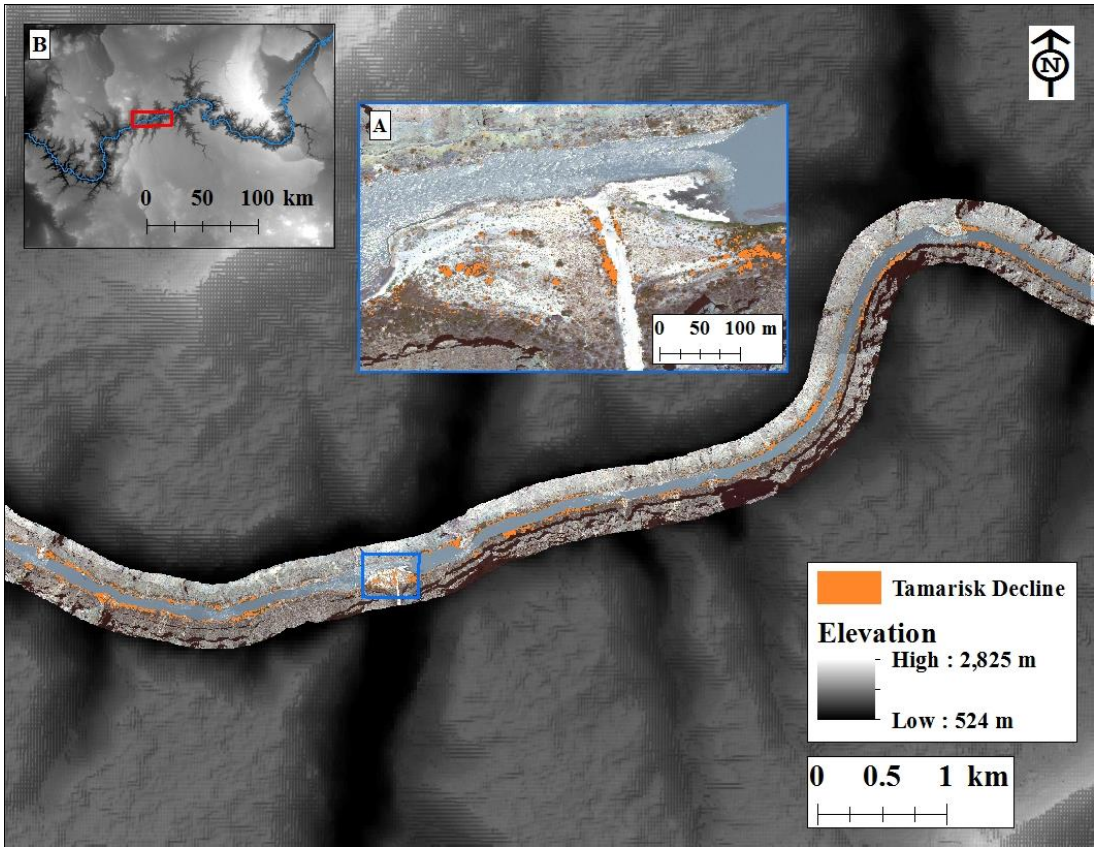

Figure 27: Middle portion of National reach from 270.0 to 279.9 km showing the areas of tamarisk EVI decline. Elevation image is an ASTER dataset, overlaid by the 2009 USGS overflight imagery. Panel A shows a close up view of tamarisk decline at 276.6 km and panel B shows the study reach.

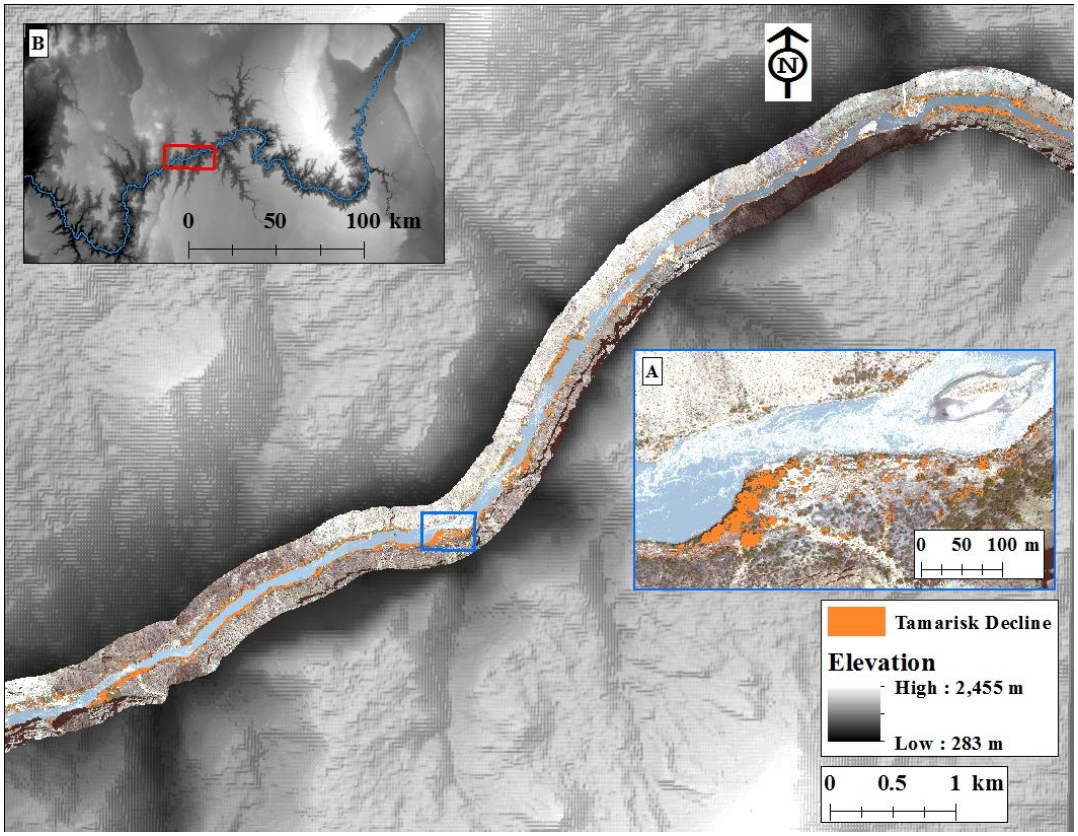

Figure 28: Lower portion of National reach from 279.9 to 290.5 km showing the areas of tamarisk EVI decline. Elevation image is an ASTER dataset, overlaid by the 2009 USGS overflight imagery. Panel A shows a close up view of tamarisk decline at 286.5 km and panel B shows the study reach.

Relationship of beetle observation data with NDVI and EVI decline: Glen Canyon

Analysis of 100 meter beetle and non-beetle buffer points showed that 5% more pixels in beetle buffers showed NDVI decline rates greater than 50% (i.e., 39% of the buffered point area) when compared against non-beetle buffers (i.e., 34% of the buffered point area) (Table 30). EVI analysis of the same buffer points showed that 15% less

pixels in beetle buffers experienced decline rates greater than 50% (i.e., 63% of the buffered point area) when compared against non-beetle buffers (i.e., 78% of the buffered point area) (Table 31). Analysis of 150 meter beetle and non-beetle buffer points showed that 7% more pixels in beetle buffers showed NDVI decline rates greater than 50% (i.e., 39% of the buffered point area) when compared against non-beetle buffers (i.e., 32% of the buffered point area) (Table 30). EVI analysis of the same buffer points showed that 12% less pixels in beetle buffers experienced decline rates greater than 50% (i.e., 63% of the buffered point area) when compared against non-beetle buffers (i.e., 75% of the buffered point area) (Table 31).

Table 30: Percent NDVI change for 100 m and 150 m buffer Tables using observed adult or no adult beetles for Glen Canyon.

	100 m beetle	100 m non-beetle	150 m beetle	150 m non-beetle
No change %	61%	66%	61%	68%
Decline %	39%	34%	39%	32%
Total %	100%	100%	100%	100%

Table 31: Percent EVI change for 100 m and 150 m buffer Tables using observed adult or no adult beetles for Glen Canyon.

	100 m beetle	100 m non-beetle	150 m beetle	150 m non-beetle
No change %	37%	22%	37%	25%
Decline %	63%	78%	63%	75%
Total %	100%	100%	100%	100%

Relationship of beetle observation data with NDVI and EVI decline: Kanab

Analysis of 100 meter beetle and non-beetle buffer points showed that 5% more pixels in beetle buffers showed NDVI decline rates greater than 50% (i.e., 23% of the buffered point area) when compared against non-beetle buffers (i.e., 18% of the buffered point area) (Table 32). EVI analysis of the same buffer points showed that 1% more pixels in beetle buffers showed EVI decline rates greater than 50% (i.e., 9% of the buffered point area) when compared against non-beetle buffers (i.e., 8% of the buffered point area) (Table 33). Analysis of 150 meter beetle and non-beetle buffer points showed that 4% more pixels in beetle buffers showed NDVI decline rates greater than 50% (i.e., 22% of the buffered point area) when compared against non-beetle buffers (i.e., 18% of the buffered point area) (Table 32). EVI analysis of the same buffer points showed that 1% more pixels in beetle buffers showed EVI decline rates greater than 50% (i.e., 9% of the buffered point area) when compared against non-beetle buffers (i.e., 8% of the buffered point area) (Table 33).

Table 32: Percent NDVI change for 100 m and 150 m buffer Tables using observed adult or no adult beetles for Kanab.

	100 m beetle	100 m non-beetle	150 m beetle	150 m non-beetle
No change %	77%	82%	78%	82%
Decline %	23%	18%	22%	18%
Total %	100%	100%	100%	100%

Table 33: Percent EVI change for 100 m and 150 m buffer Tables using observed adult or no adult beetles for Kanab.

	100 m beetle	100 m non-beetle	150 m beetle	150 m non-beetle
No change %	91%	92%	91%	92%
Decline %	9%	8%	9%	8%
Total %	100%	100%	100%	100%

Relationship of beetle observation data with NDVI and EVI decline: National

Analysis of 100 meter beetle and non-beetle buffer points showed 1% less pixels in beetle buffers showed NDVI decline rates greater than 50% (i.e., 14% of the buffered point area) when compared against non-beetle buffers (i.e., 15% of the buffered point area) (Table 34). EVI analysis of the same buffer points showed that 1% more pixels in beetle buffers showed EVI decline rates greater than 50% (i.e., 9% of the buffered point area) when compared against non-beetle buffers (i.e., 8% of the buffered point area) (Table 35). Analysis of 150 meter beetle and non-beetle buffer points showed 2% less pixels in beetle buffers showed NDVI decline rates greater than 50% (i.e., 13% of the buffered point area) when compared against non-beetle buffers (i.e., 15% of the buffered point area) (Table 34). EVI analysis of the same buffer points showed that both beetle and non-beetle buffered points had 8% of the area showing decline rates greater than 50% (Table 35).

Table 34: Percent NDVI change for 100 m and 150 m buffer Tables using observed adult or no adult beetles for National.

	100 m beetle	100 m non-beetle	150 m beetle	150 m non-beetle
No change %	86%	85%	87%	85%
Decline %	14%	15%	13%	15%
Total %	100%	100%	100%	100%

Table 35: Percent EVI change for 100 m and 150 m buffer Tables using observed adult or no adult beetles for National.

	100 m beetle	100 m non-beetle	150 m beetle	150 m non-beetle
No change %	91%	92%	92%	92%
Decline %	9%	8%	8%	8%
Total %	100%	100%	100%	100%

Statistical Analysis: Summary NDVI and EVI decline

Viewshed and diffuse daylight simple regression models had P-values that were less than 0.1 across all reaches with NDVI percent change (Table 36). Using EVI decline percentages, river segment and diffuse daylight had simple regression models had P-values that were less than 0.1 across all reaches (Table 38). Comparing the multivariate models with the highest adjusted R^2 against the models created using the automatic modeling method in SPSS showed very little change in the adjusted R^2 value of the models. The percent NDVI decline models without using beetle observation data included the same variables for Glen Canyon and Kanab study reaches, while the

automatic model for National included the viewshed variable. The difference in model fit between the manual and automatic multivariate models varied no more than 0.043 for the Adjusted R^2 value. The percent EVI decline models without using beetle observation data used the same variables for National study reach. Variables predicting EVI decline for Glen Canyon and Kanab varied slightly (Table 38). All models had very similar Adjusted R^2 values, with a maximum difference of 0.034. The histograms for the manual forward stepwise multivariate models showed no obvious residuals trends and the histograms appeared relatively normal with a slight right skew across all study reaches (Appendices K and L). Including beetle observation variables into the multivariate manual and automatic models also showed very little difference between the model fit.

Comparing manual multivariate models and automatic multivariate models while using beetle observation data was inconclusive for both Kanab and National reaches, because the automatic model immediately excluded all of the beetle data due to creating a worse model. For Glen Canyon NDVI percent decline, a slightly different model was adopted that used early larvae instead of adult beetle, while holding all the same environmental variables. The Adjusted R^2 values for both the manual and automatic model were only 0.001 apart from each other.

Table 36: Summary of simple regression models for each reach showing P-values for each variable in relation to the study reach for percent NDVI decline. Full information on simple regression models found in Appendix I. Columns highlighted in bold print have P-values of less than 0.1 across all reaches. Values less than 0.1 are also bolded.

P-Value	River Segment	Tamarisk Area	**Viewshed**	Total Daylight	**Diffuse Daylight**	Direct Daylight	Adult Beetle	Early Larvae	Late Larvae
Glen Canyon	0.801	**0.000**	**0.068**	0.117	**0.076**	0.284	0.247	0.518	**0.075**
Kanab	**0.000**	0.826	**.000**	0.012	**0.000**	**0.000**	0.942	0.49	0.678
National	**0.000**	**0.000**	**.000**	**0.000**	**0.000**	**0.006**	0.846	0.571	0.376

Table 37: Table showing the variables used in the multivariate model with highest model fit for predicting percent NDVI decline for manual and automatic multivariate models. '*******' where P < 0.001, '******' where P<0.01, '*****' where P<.05,'·' where P<0.1.

Reach and Method	River Segment	Tamarisk Area	Viewshed	Total Daylight	Diffuse Daylight	Direct Daylight
Glen Canyon Manual		0.000***	0.006**	0.000***		
Glen Canyon Automatic		0.000***	0.062·	0.000***		
Kanab Manual	0.054·	0.017*	0.003**		0.000***	
Kanab Automatic	0.082·	0.023*	0.004**		0.000***	
National Manual	0.000*******				0.075·	0.002******
National Automatic	0.000*******		0.278		0.061·	0.005******

Table 38: Summary of simple regression models for each reach showing P-values for each variable in relation to the study reach for percent EVI decline. Full information on simple regression models found in Appendices J – O. Columns highlight in bold print have P-values of less than .1 across all reaches.

P-Value	**River Segment**	Tamarisk Area	Viewshed	Total Daylight	**Diffuse Daylight**	Direct Daylight	Adult Beetle	Early Larvae	Late Larvae
Glen Canyon	**0.000**	**0.000**	**0.000**	**0.000**	**0.000**	**0.000**	**0.077**	0.584	**0.013**
Kanab	**0.005**	0.411	**0.086**	**0.032**	**0.002**	**0.045**	0.717	**0.051**	0.622
National	**0.090**	0.572	0.686	0.469	**0.081**	0.180	0.506	0.666	0.662

Table 39: Table showing the variables used in the multivariate model with highest model fit for predicting percent EVI decline for manual and automatic multivariate models. '***' where P < 0.001, '**' where P<0.01, '*' where P<.05,'·' where P<0.1.

Reach and Method	River Segment	Tamarisk Area	Viewshed	Total Daylight	Diffuse Daylight	Direct Daylight
Glen Canyon Manual		0.000***	0.000***		0.000***	0.096·
Glen Canyon Automatic	0.000***	0.000***	0.000***	0.037*		0.063·
Kanab Manual		0.134	0.148	0.007**	0.287	
Kanab Automatic	0.001**			0.011*		
National Manual	0.013*	0.252		0.010*	0.803	0.002**
National Automatic	0.000***	0.243		0.011*		0.002**

Statistical Analysis: Glen Canyon NDVI and EVI decline

Simple regression analysis using tamarisk NDVI change as the dependent variable showed that the three variables with the highest Adjusted R^2 values were tamarisk area, minutes of diffuse daylight and adult beetles (Appendix I). Tamarisk area was the only variable of the simple regression models when P <= 0.05. A multiple regression model (Equation 15) incorporating tamarisk area, total day length, and viewshed (P-value of 0.000, 0.000 and .006 respectively) achieved the highest Adjusted R^2 value of 0.369 (Standard Error of the Estimate is 13.6%) (Table 40). A multiple regression model (Equation 16) including the adult tamarisk beetle, early larvae, late larvae, tamarisk area, total day length, and viewshed (P-value of 0.400, 0.215, 0.040, 0.006, 0.005, 0.013) achieved an Adjusted R^2 of 0.418 (Standard Error of the Estimate is 16.1%) (Table 41).

Equation 15: multiple regression model with highest model fit for predicting percent tamarisk NDVI decline for Glen Canyon

%NDVI decline = $--1.52\times10^5$+ 0.008×tamarisk area + 211×total day length – 38.8×viewshed

Equation 16: multiple regression model with highest model fit for predicting percent tamarisk NDVI decline for Glen Canyon using beetle collection data

%NDVI decline = -2.80×10^5 - .013×adult beetle + 0.041×early larvae - 0.337×late larvae + 0.007×tamarisk area + 389×total day length – 104×viewshed

Table 40: Equation 15 (No Beetle used in multivariate regression). '*******' where P < 0.001, '******' where P<0.01, '*****' where P<.05,'·' where P<0.1.

Independent variable	Unstandardized Coefficient B	Std. Error (Unstandardized)	Standardized Coefficient Beta	t	P (Sig)
Constant	-1.52×10^5	3.17×10^4	0.000	-4.786	0.000***
Tamarisk Area	0.008	0.001	0.585	9.964	0.000***
Total Daylight	211	44	0.297	4.787	0.000***
Viewshed	-39	14	-0.170	-2.798	0.006*

Table 41: Equation 16 (Beetle used in multivariate regression). '*******' where P < 0.001, '******' where P<0.01, '*****' where P<.05,'·' where P<0.1.

Independent variable	Unstandardized Coefficient B	Std. Error (Unstandardized)	Standardized Coefficient Beta	t	P (Sig)
Constant	-2.80×10^5	9.27×10^4	0.000	-3.017	0.005**
Adult Beetle	-0.013	0.015	-0.112	-0.854	0.400
Tamarisk Area	0.007	0.002	0.411	2.963	0.006**
Total Daylight	389	129	0.452	3.018	0.005**
Viewshed	-104	39.3	-0.422	-2.637	0.013*
Late Larvae	-0.337	0.157	-0.296	-2.149	0.040
Early Larvae	0.041	0.032	0.189	1.265	0.215

Simple regression analysis using tamarisk EVI change as the dependent variable showed that all variables had P-values < 0.05 except for adult beetle, and early larvae (Appendix J). A multiple regression model (Equation 17) incorporating tamarisk area, viewshed, diffuse day length and direct day length (P-value of 0.000, 0.000, 0.000 and 0.096 respectively) achieved the highest Adjusted R^2 value of .526 (Standard Error of the

Estimate is 16.1%) (Table 42). A multiple regression model including the adult tamarisk beetle, early larvae, late larvae, tamarisk area, river segment, total day length and viewshed (P-value of 0.315, 0.032, 0.022, 0.011, 0.148, 0.204, and 0.057 respectively) achieved an Adjusted R^2 of .601 (Standard Error of the Estimate is 18.2%) (Equation 18) (Table 43).

Equation 17: multiple regression model with highest Adjusted R^2 value for predicting percent tamarisk EVI decline for Glen Canyon

%EVI decline = -1.37×10^5 +.010× tamarisk area – 104× viewshed + 175× diffuse day length + .032× direct day length

Equation 18: multiple regression model with highest Adjusted R^2 value for predicting percent tamarisk EVI decline for Glen Canyon using beetle collection data

%EVI decline = -1.84×10^5 - .018× total adult + .082× early larvae - .451× late larvae + .008× tamarisk area - .970× river segment + 255× total day length – 104× viewshed

Table 42: Equation 17 (No Beetle used in multivariate regression). **'***'** where P < 0.001, **'**'** where P<0.01, **'*'** where P<.05,'·' where P<0.1.

Independent variable	Unstandardized Coefficient B	Std. Error (Unstandardized)	Standardized Coefficient Beta	t	P (Sig)
Constant	-1.37×10^5	3.82×10^4	0.000	-3.579	0.000***
Tamarisk Area	0.010	0.001	0.520	9.980	0.000***
Viewshed	-104	25	-0.331	-4.108	0.000***
Diffuse Daylight	175	49	0.229	3.583	0.000***
Direct Daylight	0.032	0.019	0.122	1.672	0.096·

Table 43: Equation 18 (Beetle used in multivariate regression). **'***'** where P < 0.001, **'**'** where P<0.01, **'*'** where P<.05,'·' where P<0.1.

Independent variable	Unstandardized Coefficient B	Std. Error (Unstandardized)	Standardized Coefficient Beta	t	P (Sig)
Constant	-1.84×10^5	1.42×10^5	0.000	-1.298	0.204
Adult Beetle	-0.018	0.017	-0.111	-1.021	0.315
Tamarisk Area	0.008	0.003	0.345	2.695	0.011*
River Segment	-0.970	0.654	-0.340	-1.484	0.148
Late Larvae	-0.451	0.187	-0.290	-2.409	0.022*
Early Larvae	0.082	0.036	0.278	2.251	0.032*
Total Daylight	255	197	0.218	1.299	0.204
Viewshed	-104	52	-0.310	-1.982	0.057·

Statistical Analysis: Kanab NDVI and EVI decline

Simple regression analysis using tamarisk NDVI change as the dependent variable showed that river segment, tamarisk area, viewshed, total daylight, diffuse daylight and direct daylight were all significant variables (Appendix I). The three simple regression models with the highest Adjusted R^2 were viewshed, diffuse daylight and direct daylight. A multiple regression model (Equation 19) incorporating viewshed, diffuse day length, tamarisk area and river segment (P-value of 0.003, 0.000, 0.017 and 0.054 respectively) achieved the highest Adjusted R^2 value of 0.182 (Standard Error of the Estimate is 11.4%) (Table 44). A multiple regression model including adult beetle, late larvae, viewshed, river segment, tamarisk area, and diffuse day length (Equation 20) (P-value of 0.224, 0.1, 0.000, 0.063, 0.153 and 0.167 respectively) achieved an Adjusted R^2 value of 0.211 (Standard Error of the Estimate is 12.4%) (Table 45).

Equation 19: multiple regression model with highest model fit for predicting percent tamarisk NDVI decline for Kanab

%NDVI decline = -2.10×10^4- 57× viewshed + 27× diffuse day length + 0.009× tamarisk area -.399× river segment

Equation 20: multiple regression model with highest model fit for predicting percent tamarisk NDVI decline for Kanab using beetle collection data

%NDVI decline = $-1.54-2.10\times10^4$+ 0.045× adult beetle - 0.055× late larvae - 129× viewshed - 0.769× river segment + 0.008× tamarisk area + 20× diffuse day length

Table 44: Equation 19 (No Beetle used in multivariate regression). **'***' where P < 0.001, **'**'** where P<0.01, **'*'** where P<.05,**'.'** where P<0.1.

Independent variable	Unstandardized Coefficient B	Std. Error (Unstandardized)	Standardized Coefficient Beta	t	P (Sig)
Constant	-2.10×10^4	5744	0.000	-3.651	0.000***
Viewshed	-57	19	-0.357	-3.033	0.003**
Diffuse Daylight	27	7	0.456	3.657	0.000***
Tamarisk Area	0.009	0.004	0.173	2.401	0.017*
River Segment	-0.399	0.206	-0.309	-1.938	0.054·

Table 45: Equation 20 (Beetle used in multivariate regression). '*' where P < 0.001, **'**'** where P<0.01, **'*'** where P<.05, **'·'** where P<0.1.

Independent variable	Unstandardized Coefficient B	Std. Error (Unstandardized)	Standardized Coefficient Beta	t	P (Sig)
Constant	$-1.54\text{-}2.10\times10^4$	$1.12\text{-}2.10\times10^4$	0.000	-1.378	0.172
Adult Beetle	0.045	0.037	0.128	1.226	0.224
Viewshed	-129	35	-0.776	-3.706	0.000***
River Segment	-0.769	0.408	-0.549	-1.885	0.063·
Late Larvae	-0.055	0.033	-0.176	-1.664	0.100
Tamarisk Area	0.008	0.005	0.166	1.445	0.153
Diffuse Daylight	20	14	0.306	1.395	0.167

Simple regression analysis using tamarisk EVI change as the dependent variable showed that the three highest Adjusted R^2 values came from the diffuse daylight, early larvae and river segment variables (Appendix J). Simple regression models with significant variables were river segment, total daylight, diffuse daylight, and direct

daylight (Appendix J). A multiple regression model (Equation 21) incorporating diffuse day length, total day length, viewshed and tamarisk area (Table 46) (P-value of 0.287, 0.007, 0.148 and 0.134 respectively) achieved the highest Adjusted R^2 value of .067 (Standard Error of the Estimate is 10.7%). Equation 22 shows a multiple regression model including adult beetle, early larvae, river segment, total day length, viewshed, and tamarisk area (P-value of 0.597, 0.130, 0.4, 0.006, 0.033, 0.081 respectively) achieved an Adjusted R^2 value of 0.119 (Standard Error of the Estimate is 8.5%) (Table 47).

Equation 21: multiple regression model with highest model fit for predicting percent tamarisk EVI decline for Kanab

%EVI decline = 6.06×10^4+ 7× diffuse day length - 91× total day length - 28× viewshed + 0.006× tamarisk area

Equation 22: multiple regression model with highest model fit for predicting percent tamarisk EVI decline for Kanab using beetle collection data

%EVI decline = 1.07×10^5+ 0.014× adult beetle - 0.051× early larvae -0.215× river segment -149× total day length – 80× viewshed + 0.006× tamarisk area

Table 46: Equation 21 (No Beetle used in multivariate regression). '*******' where P < 0.001, '******' where P<0.01, '*****' where P<.05,'·' where P<0.1.

Independent variable	Unstandardized Coefficient B	Std. Error (Unstandardized)	Standardized Coefficient Beta	t	P (Sig)
Constant	6.06×10^4	2.69×10^4	0.000	2.252	0.025*****
Diffuse Daylight	7	6	0.128	1.067	0.287
Total Daylight	-91	33	-0.273	-2.730	0.007******
Viewshed	-28	19	-0.197	-1.453	0.148
Tamarisk Area	0.006	0.004	0.119	1.505	0.134

Table 47: Equation 22 (Beetle used in multivariate regression). '*******' where P < 0.001, '******' where P<0.01, '*****' where P<.05,'·' where P<0.1.

Independent variable	Unstandardized Coefficient B	Std. Error (Unstandardized)	Standardized Coefficient Beta	t	P (Sig)
Constant	1.07×10^5	3.76×10^4	0.000	2.859	0.006******
Adult Beetle	0.014	0.027	0.061	0.531	0.597
Early Larvae	-0.051	0.033	-0.177	-1.532	0.130
River Segment	-0.215	0.254	-0.237	-0.846	0.400
Total Daylight	-149	52	-0.522	-2.860	0.006******
Viewshed	-80	37	-0.741	-2.170	0.033*****
Tamarisk Area	0.006	0.004	0.211	1.772	0.081·

Statistical Analysis: National NDVI and EVI decline

Simple regression analysis using tamarisk NDVI change as the dependent variable showed that river segment, tamarisk area, viewshed, total daylight, diffuse daylight, and direct daylight were all significant variables (Appendix I). The three simple regression models with the highest Adjusted R^2 were river segment, diffuse daylight and viewshed. A multiple regression model (Equation 23) incorporating river segment, direct day length, and diffuse day length (P-value of 0, 0.002, and 0.075 respectively) (Table 48) achieved the highest Adjusted R^2 value of 0.329 (Standard Error of the Estimate is 8.9%). A multiple regression model using adult beetles, early larvae, diffuse day length, direct day length, and river segment (P-value of 0.810, 0.237, 0.148, 0.080, and 0.192 respectively) (Table 49) had an Adjusted R^2 value of 0.180 (Standard Error of the Estimate is 11.6%) (Equation 24).

Equation 23: multiple regression model with highest model fit for predicting percent tamarisk NDVI decline for National

$$\%\text{NDVI decline} = -5.63\times10^{4} - 0.521\times \text{river segment} + 0.045\times \text{direct day length} + 72\times \text{diffuse day length}$$

Equation 24: multiple regression model with highest model fit for predicting percent tamarisk NDVI decline for Kanab using beetle collection data

$$\%\text{NDVI decline} = -9.58\times10^{4} + 0.008\times \text{adult beetle} + 0.059\times \text{early larvae} + 122\times \text{diffuse day length} + 0.054\times \text{direct day length} - 0.349\times \text{river segment}$$

Table 48: Equation 23 (No Beetle used in multivariate regression). **'***' where P < 0.001, **'**' where P<0.01, **'*'** where P<.05,**'·'** where P<0.1.

Independent variable	Unstandardized Coefficient B	Std. Error (Unstandardized)	Standardized Coefficient Beta	t	P (Sig)
Constant	-5.63×10^4	3.16×10^4	0.000	-1.781	0.076·
River Segment	-0.521	0.126	-0.496	-4.122	0.000***
Direct Daylight	0.045	0.014	0.220	3.215	0.002**
Diffuse Daylight	72	40	0.206	1.787	0.075·

Table 49: Equation 24 (Beetle used in multivariate regression). **'***' where P < 0.001, **'**' where P<0.01, **'*'** where P<.05,**'·'** where P<0.1.

Independent variable	Unstandardized Coefficient B	Std. Error (Unstandardized)	Standardized Coefficient Beta	t	P (Sig)
Constant	-9.58×10^4	6.57×10^4	0.000	-1.458	0.149
Adult Beetle	0.008	0.033	0.024	0.241	0.810
Diffuse Daylight	122	84	0.304	1.461	0.148
Direct Daylight	0.054	0.030	0.216	1.775	0.080·
River Segment	-0.349	0.265	-0.283	-1.316	0.192
Early Larvae	0.059	0.050	0.119	1.192	0.237

Simple regression analysis using tamarisk EVI change as the dependent variable showed that there were no significant variables (Appendix J). The three simple regression models with the highest Adjusted R^2 were river segment, diffuse daylight and direct daylight. A multiple regression model (Equation 25) incorporating diffuse day length, direct day length, total day length, river segment, and tamarisk area (P-value of 0.803, 0.002, 0.010, 0.013 and 0.252 respectively) (Table 50) achieved the highest

Adjusted R^2 value of 0.062 (Standard Error of the Estimate is 5.6%). A multiple regression model using adult beetle, direct day length, river segment, and total day length (P-value of 0.289, 0.008, 0.008, and 0.050) had the highest Adjusted R^2 value of 0.070 (Standard Error of the Estimate is 6.7%) when using beetle observation data (Equation 26) (Table 51).

Equation 25: multiple regression model with highest model fit for predicting percent tamarisk EVI decline for National

%EVI decline = 4.62×10^4+ 6× diffuse day length + 0.028× direct day length – 71× total day length - 0.237× river segment + 0.001× tamarisk area

Equation 26: multiple regression model with highest model fit for predicting percent tamarisk EVI decline for Kanab using beetle collection data

%EVI decline = 7.60×10^4+ 0.021× adult beetle + 0.048× direct day length - 0.283× river segment -106× total day length

Table 50: Equation 25 (No Beetle used in multivariate regression). '*******' where P < 0.001, '******' where P<0.01, '*****' where P<.05,'·' where P<0.1.

Table 50: Equation 25 (No Beetle used in multivariate regression). '***' where P < 0.001, '**' where P<0.01, '*' where P<.05,'·' where P<0.1.

Independent variable	Unstandardized Coefficient B	Std. Error (Unstandardized)	Standardized Coefficient Beta	t	P (Sig)
Constant	4.62×10^4	3.07×10^4	0.000	1.503	0.134
Diffuse Daylight	6	26	0.035	0.249	0.803
Direct Daylight	0.028	0.009	0.259	3.180	0.002**
Total Daylight	-71	27	-0.222	-2.605	0.010*
River Segment	-0.237	0.095	-0.428	-2.495	0.013*
Tamarisk Area	0.001	0.001	0.100	1.148	0.252

Table 51: Equation 26 (Beetle used in multivariate regression). '***' where P < 0.001, '**' where P<0.01, '*' where P<.05,'·' where P<0.1.

Independent variable	Unstandardized Coefficient B	Std. Error (Unstandardized)	Standardized Coefficient Beta	t	P (Sig)
Constant	7.60×10^4	3.82×10^4	0.000	1.992	0.050·
Adult Beetle	0.021	0.019	0.113	1.068	0.289
Direct Daylight	0.048	0.018	0.358	2.699	0.008*
River Segment	-0.283	0.104	-0.423	-2.729	0.008*
Total Daylight	-106	53	-0.255	-1.991	0.050·

Statistical Analysis Beetle Observation

The most beetle observations were made in 2011 for all study areas (Figure 29). For Glen Canyon beetle observations, most beetles were observed at or below Lees Ferry. The best models predicting adult tamarisks had very low model fits. The residual histograms for these models for Glen Canyon reach and National reach had acceptably low levels of right skew (Appendix M1 and M3). Kanab reach had a greater level of right skew present in the model (Appendix M2).

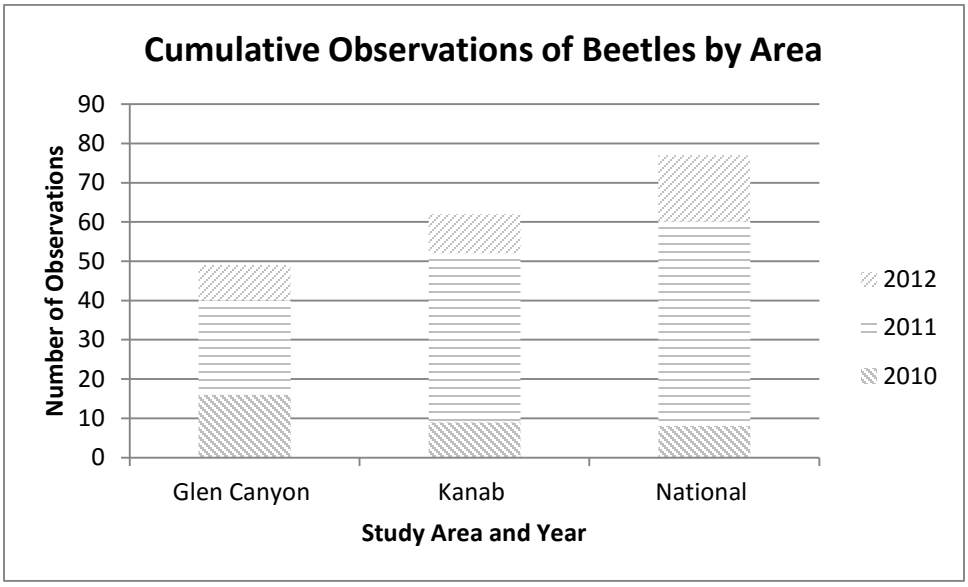

Figure 29: Cumulative observations by of beetles by year within each study area

Statistical Analysis Beetle Observation: Glen Canyon

Thirty-eight river segments contained beetle presence or absence data within the Glen Canyon reach. The presence or absence of adult beetles and larvae varied amongst river segments (Table 52). Simple regression models indicated that river segment, viewshed, total daylight, diffuse daylight and direct daylight have a significant

relationship to the presence of adult tamarisk beetles (Table 53) in Glen Canyon reach. Adult tamarisk beetles, early beetle larvae, and late beetle larvae did not have a significant relationship to the percent of NDVI (Table 54) or EVI tamarisk decline in Glen Canyon (Table 55). Simple regression models showed that average direct sunlight was the only significant predictor variable for adult tamarisk beetles (Table 56). The simple direct sunlight regression model (P-value of .04) proved to have the highest Adjusted R^2 value of .08 (Equation 27).

Equation 27: Simple regression model with best model for predicting adult tamarisk beetles for Glen Canyon

Adult Beetle = -174 + .58× direct day length

Table 52: Presence/absence of tamarisk beetle and larvae by river segments for Glen Canyon.

	Adult Beetle	Early Larvae	Late Larvae
Present	23	24	17
Absent	15	14	21

Table 53: Independent T-test comparing significance of variables to adult tamarisk beetle presented as presence/absence data for Glen Canyon. **'***' where P < 0.001, **'**'** where P<0.01, **'*'** where P<.05,**'·'** where P<0.1.

Variable	t	Degrees Freedom	Sig. (2-tailed)	Mean Difference	Std. Error Difference
River Segment	4.234	36.000	0.000***	11.760	2.777
Tamarisk Area	-1.791	36.000	0.082·	-725.004	404.793
Viewshed	2.856	36.000	0.007**	0.075	0.026
Total Daylight	3.109	36.000	0.004**	0.023	0.007
Diffuse Daylight	-4.283	36.000	0.000***	-0.040	0.009
Direct Daylight	2.287	36.000	0.028*	74.153	32.420
Early Larvae	2.224	22.029	0.037*	56.638	25.468
Late Larvae	2.454	22.070	0.022*	11.687	4.762

Table 54: Independent T-test comparing varying beetle life stages and the significance on percent NDVI decline for Glen Canyon. **'***' where P < 0.001, **'**'** where P<0.01, **'*'** where P<.05,**'·'** where P<0.1.

Variable	t	Degrees Freedom	Sig. (2-tailed)	Mean Difference	Std. Error Difference
Adult Beetle	0.122	36.000	0.903	0.87%	7.11%
Early Larvae	1.996	36.000	0.054·	13.64%	6.83%
Late Larvae	-0.909	36.000	0.370	-6.28%	6.91%
All Types	-0.496	36.000	0.623	-5.08%	10.24%

Table 55: Independent T-test comparing varying beetle life stages and the significance on percent EVI decline for Glen Canyon. **'***' where P < 0.001, **'**'** where P<0.01, **'*'** where P<.05,**'·'** where P<0.1.

Variable	t	Degrees Freedom	Sig. (2-tailed)	Mean Difference	Std. Error Difference
Adult Beetle	-1.614	35.562	0.115	-14.16%	8.78%
Early Larvae	3.023	36.000	0.005**	26.51%	8.77%
Late Larvae	-0.365	36.000	0.717	-3.47%	9.51%
All Types	-0.435	36.000	0.666	-6.08%	13.97%

Table 56: Independent variables predicting the dependent number of adult tamarisk beetles for Glen Canyon using simple regression models. **'***' where P < 0.001, **'**'** where P<0.01, **'*'** where P<.05,**'·'** where P<0.1.

Independent variable	Adjusted R^2	Unstandardized Coefficient B	Std. Error (Unstandardized)	Standardized Coefficient Beta	P (Sig)
River Segment	0.055	5.081	2.86	0.284	0.084·
Constant		88.3	33.0		0.011
Tamarisk Area	0.004	-0.025	0.024	-0.175	0.292
Constant		99.0	47.6		0.045
Viewshed	0.024	470	341.173	0.224	0.177
Constant		-273	242.401		0.268
Total Daylight	0.016	1523	1198	0.207	0.212
Constant		-1.10×10^6	8.63×10^5		0.212
Diffuse Daylight	0.047	-1444	856	-0.271	0.100
Constant		1.13×10^6	6.71×10^5		0.100
Direct Daylight	0.083	0.576	0.276	0.329	0.044*
Constant		-174	115		0.139
Early Larvae	-0.017	0.188	0.305	0.102	0.542
Constant		51.9	31.5		0.108
Late Larvae	-0.019	0.894	1.618	0.092	0.584
Constant		52.0	32.0		0.113

Statistical Analysis Beetle Observation: Kanab

Eighty, 0.16-km river segments contained beetle presence or absence data within Kanab reach. The presence or absence of adult beetles and larvae varied amongst river segments, with adult beetles being observed most often, and late larvae being observed with the least frequency (Table 57). None of the variables evaluated were found to have a significant relationship to the presence of adult tamarisk beetles (Table 58) in Kanab reach. Early larvae showed a significant relationship to EVI tamarisk decline in Kanab (Table 60). Simple regression models showed that average direct daylight was the only significant predictor variable for adult tamarisk beetles (Table 61). Multiple regression models were also carried out, but the simple direct sunlight regression model (P-value of .03) proved to have the highest Adjusted R^2 value of .046 (Equation 28).

Equation 28: simple regression model with best model for predicting adult tamarisk beetles for Kanab

Adult Beetle = -17.0 + .1× direct day length

Table 57: Presence/absence of tamarisk beetle and larvae by river segments Kanab.

Table 57: Presence/absence of tamarisk beetle and larvae by river segments Kanab.

	Adult Beetle	Early Larvae	Late Larvae	All Types
Present	46	42	34	56
Absent	34	38	46	24

Table 58: Independent T-test comparing significance of variables to adult tamarisk beetle presented as presence/absence data for Kanab. **'***' where P < 0.001, **'**'** where P<0.01, **'*'** where P<.05,**'·'** where P<0.1.

Variable	t	Degrees Freedom	Sig. (2-tailed)	Mean Difference	Std. Error Difference
River Segment	-1.152	78.000	0.253	-2.596	2.254
Tamarisk Area	1.875	76.437	0.065·	115.802	61.757
Viewshed	0.685	78.000	0.495	0.013	0.019
Total Daylight	0.351	78.000	0.726	0.003	0.007
Diffuse Daylight	-1.287	78.000	0.202	-0.062	0.048
Direct Daylight	1.124	78.000	0.264	23.530	20.934
Early Larvae	2.397	75.108	0.019**	15.357	6.406
Late Larvae	0.161	78.000	0.873	1.647	10.258

Table 59: Independent T-test comparing varying beetle life stages and the significance on percent NDVI decline for Kanab. **'***' where P < 0.001, **'**'** where P<0.01, **'*'** where P<.05,**'·'** where P<0.1.

Variable	t	Degrees Freedom	Sig. (2-tailed)	Mean Difference	Std. Error Difference
Adult Beetle	0.399	78.000	0.691	1.27%	3.18%
Early Larvae	-1.313	78.000	0.193	-4.10%	3.12%
Late Larvae	-1.113	78.000	0.269	-3.52%	3.16%
All Types	-0.075	78.000	0.941	-0.26%	3.44%

Table 60: Independent T-test comparing varying beetle life stages and the significance on percent EVI decline for Kanab. **'***' where P < 0.001, **'**'** where P<0.01, **'*'** where P<.05,**'·'** where P<0.1.

Variable	t	Degrees Freedom	Sig. (2-tailed)	Mean Difference	Std. Error Difference
Adult Beetle	-0.819	78.000	0.415	-1.68%	2.05%
Early Larvae	-2.579	57.151	0.013**	-5.17%	2.01%
Late Larvae	-1.802	78.000	0.075·	-3.64%	2.02%
All Types	-0.841	78.000	0.403	-1.86%	2.21%

Table 61: Independent variables predicting the dependent number of adult tamarisk beetles for Kanab using simple regression models. **'***' where P < 0.001, **'**'** where P<0.01, **'*'** where P<.05,**'·'** where P<0.1.

Independent variable	Adjusted R^2	Unstandardized Coefficient B	Std. Error (Unstandardized)	Standardized Coefficient Beta	P (Sig)
River Segment	0.031	-0.824	0.438	-0.208	0.064·
Constant		208	102		0.046
Tamarisk Area	-0.002	0.014	0.015	0.105	0.354
Constant		11.0	6.34		0.089
Viewshed	0.028	94.4	52.2	0.201	0.074·
Constant		-39	30.1		0.202
Total Daylight	-0.007	-95	141	-0.076	0.502
Constant		6.83×10^4	-1.01×10^5		0.502
Diffuse Daylight	0.036	-40	20.346	-0.219	0.051·
Constant		3.17×10^4	1.60×10^4		0.051
Direct Daylight	0.046	0.103	0.047	0.241	0.031**
Constant		-17.0	15.3		0.269
Early Larvae	0.125	0.467	0.133	0.369	0.001**
Constant		6.63	4.79		0.170
Late Larvae	0.014	0.143	0.098	0.163	0.148
Constant		12.6	4.72		0.009

Statistical Analysis Beetle Observation: National

86 river segments contained beetle presence or absence data within National reach (Table 62). The presence or absence of adult beetles and larvae varied amongst river segments (Table 62). T-Tests showed that diffuse daylight was found to have a significant relationship to the presence of adult tamarisk beetles (Table 63) in National reach. Adult tamarisk beetles, early beetle larvae and late beetle larvae did not have a significant relationship to the percent of NDVI (Table 64) or EVI tamarisk decline National (Table 65).

Simple regression analysis was carried out using adult tamarisk beetles as the dependent variable to learn whether any of the independent variables act as important predictors for adult beetle occurrence in National (Table 66). Simple regression models showed that none of the variables evaluated were significant predictors of adult tamarisk beetles. Multiple regression models were also carried out, but the simple total sunlight regression model (P-value of .28) proved to have the highest Adjusted R^2 value of .002 (Equation 29).

Equation 29: simple regression model with highest Adjusted R^2 value for predicting adult tamarisk beetles for National

Adult Beetle = $-1.93\times10^5+ 268\times$ total day length

Table 62: Presence/absence of tamarisk beetle and larvae by river segments National

	Adult Beetle	Early Larvae	Late Larvae	All Types
Present	55	48	40	62
Absent	31	38	46	24

Table 63: Independent T-test comparing significance of variables to adult tamarisk beetle presented as presence/absence data for National. **'***' where P < 0.001, **'**'** where P<0.01, **'*'** where P<.05,**'·'** where P<0.1.

Variable	t	Degrees Freedom	Sig. (2-tailed)	Mean Difference	Std. Error Difference
River Segment	1.525	84.000	0.131	3.531	2.315
Tamarisk Area	1.338	84.000	0.184	277.299	207.207
Viewshed	1.702	84.000	0.092·	0.015	0.009
Total Daylight	-0.167	84.000	0.868	-0.001	0.004
Diffuse Daylight	-2.158	84.000	0.034*	-0.015	0.007
Direct Daylight	1.280	84.000	0.204	14.694	11.477
Early Larvae	3.512	57.805	0.001**	14.794	4.213
Late Larvae	2.322	79.258	0.023	12.812	5.517

Table 64: Independent T-test comparing varying beetle life stages and the significance on percent NDVI decline for National. **'***' where P < 0.001, **'**'** where P<0.01, **'*'** where P<.05,**'·'** where P<0.1.

Variable	t	Degrees Freedom	Sig. (2-tailed)	Mean Difference	Std. Error Difference
Adult Beetle	-0.006	84.000	0.995	-0.02%	2.89%
Early Larvae	-1.342	84.000	0.183	-3.71%	2.77%
Late Larvae	-1.847	84.000	0.068·	-5.04%	2.73%
All Types	-0.742	84.000	0.460	-2.29%	3.09%

Table 65: Independent T-test comparing varying beetle life stages and the significance on percent EVI decline for National. **'***' where P < 0.001, '**' where P<0.01, '*' where P<.05,'·' where P<0.1.

Variable	t	Degrees Freedom	Sig. (2-tailed)	Mean Difference	Std. Error Difference
Adult Beetle	0.357	84.000	0.722	0.56%	1.57%
Early Larvae	-0.621	84.000	0.536	-0.94%	1.52%
Late Larvae	-1.205	84.000	0.231	-1.81%	1.50%
All Types	0.739	84.000	0.462	1.24%	1.68%

Table 66: Independent variables predicting the dependent number of adult tamarisk beetles for National using simple regression models. **'***' where P < 0.001, '**' where P<0.01, '*' where P<.05,'·' where P<0.1.

Independent variable	Adjusted R^2	Unstandardized Coefficient B	Std. Error (Unstandardized)	Standardized Coefficient Beta	P (Sig)
River Segment	-0.012	0.036	0.400	0.010	0.928
Constant		8.47	109		0.938
Tamarisk Area	-0.012	-0.001	0.004	-0.018	0.869
Constant		19.2	6.68		0.005
Viewshed	-0.012	-19	108	-0.019	0.861
Constant		29	59		0.627
Total Daylight	0.002	268	246	0.118	0.279
Constant		-1.93×10^5	1.77×10^5		0.279
Diffuse Daylight	-0.012	-22	131	-0.019	0.864
Constant		1.76×10^4	1.02×10^5		0.864
Direct Daylight	-0.012	-0.013	0.081	-0.018	0.871
Constant		22	22.9		0.340
Early Larvae	-0.005	0.124	0.162	0.083	0.445
Constant		16.9	4.51		0.000
Late Larvae	-0.012	-0.010	0.137	-0.008	0.940
Constant		18.4	4.45		0.000

Chapter 5 -Discussion

Tamarisk classification

Establishing a tamarisk classification with remote sensing techniques was a useful method to identify tamarisks and carry out a change detection study. The effectiveness of a tamarisk classification is influenced by the amount of data available to train and validate the classification, as well as the plant species and the abundance of each species in each reach. These factors meant that the tamarisk classification varied in accuracy among study reaches.

Initial tamarisk classifications were oriented toward achieving a balance between inclusion of tamarisk and exclusion of non-tamarisk pixels. It was helpful to test many different Mahalanobis distance settings to find the setting that worked best for a particular reach. As the distance setting was increased, producer's accuracy for tamarisk pixels increased as more tamarisks were correctly classified. The increase in distance setting also led to additional non-tamarisk pixels being included in the classification resulting in a lower tamarisk user's accuracy. This relationship was not strictly linear, which is why experimenting with different distance settings was important.

The tendency of the classification to omit non-tamarisk pixels varied among plant species. This classification had errors that were similarly reported by Ralston et al. (2008). For example, mesquites and acacias were especially difficult to classify correctly because the radiance values of tamarisks are very similar to these two species. This issue is indicated in the low classification accuracy of National reach where these two species

are abundant (Table 17). Visual inspection of the classifications showed that seep willows were partially classified as tamarisk, particularly the canopy edges of this vegetation type.

Post classification steps created a more accurate tamarisk classification. Sieve removed incorrectly classified non-tamarisk pixels with minimal loss to correctly classified tamarisk pixels (Tables 7, 11, and 15). Clump operations improved upon the sieve operation by removing gaps in the classified areas, and generally expanding to the borders of the classification to the edges of individual canopies and plant patches (Tables 8, 12, and 16). Manual removal of incorrectly classified non-tamarisk pixels was also an important step in removing large areas of vegetation types that were spectrally similar to tamarisks (Tables 9, 13, and 17).

Sieve operations removed single and small clustered pixels from the initial classification, resulting in a decrease of both correctly and incorrectly classified tamarisk pixels. The decrease in correctly identified tamarisk pixels is observed by the decline in tamarisk user's accuracy and non-tamarisk producer's accuracy as shown in the Glen Canyon reach (Table 7). The decrease in non-tamarisk vegetation pixels improved the classification by increasing non-tamarisk user's accuracy and tamarisk producer's accuracy. The overall accuracy increased in each study area from initial classification using the sieve operation because more incorrectly classified pixels were removed than correctly classified tamarisk pixels. Sparser classification pixels were more frequently present in non-tamarisk vegetation than tamarisk pixels and therefore were more susceptible to removal by the sieve operation.

Clump operations improved upon the sieve operation by growing the clusters of spatially adjacent pixels that remained from the sieve operation. Clump operations were useful in filling in unclassified gaps and borders in tamarisk canopies. Clump operations were not always able to completely fill in canopy gaps, and large groupings of shaded pixels were not always filled in completely. Clump operations also increased the incorrectly classified area of non-tamarisk vegetation. This result can be observed in the increase of tamarisk user's accuracy and decrease in producer's accuracy that resulted from the Clump operation. Additionally, non-tamarisk user's and producer's accuracy decreased and increased respectively (Tables 8 & 8, 11 & 12, and 15 & 16). Overall accuracy improved as a result of the clump operation because more tamarisks were correctly classified versus non-tamarisks being included in the tamarisk classification.

The final classification of manual removal of incorrectly classified tamarisk pixels was useful in removing large areas of incorrectly classified pixels from vegetation that were spectrally similar to tamarisk (Tables 9, 13, and 17). Removing these areas helped to provide more accurate values in the final tamarisk area, which was important for identifying the change in NDVI or EVI for these areas. Manual removal of incorrect classification was fairly time consuming, taking around 70 hours to complete for all reaches. Manual removal of incorrect classification sections was only possible given the high spatial resolution of this dataset. For manual removal to be effective, the operator needs to have good knowledge of both the local plant community, and the plants appearance in the high-resolution images being used.

The tamarisk classifications developed in this study may have utility outside of the prescribed study reach boundaries. The classifications used in each study reach may be useful in classifying tamarisks in other areas within the Grand Canyon where radiance values would be similar to the study reach tamarisks. I think factors that could contribute to similar radiance values would be proximity to the study reaches, as well as having similar orientations and topography. For example, I believe the Glen Canyon classification data could be useful up to river km 51.8. The orientation of the canyon is similar throughout this length of the canyon, distance to the training data is relatively close, and the canyon topology may be relatively similar. The Kanab and National study reaches may also have utility from 215.7 km to 302.6 km although much of this area is already encompassed in the two study reaches.

Classification Accuracy

Tamarisk classification accuracies varied greatly between the three reaches. Glen Canyon reach had the highest overall accuracy, while National reach had the lowest accuracy. This is likely due to a difference in available data and different plant communities. Glen Canyon reach had a final overall accuracy of 87%, which was very similar to the highest accuracies attained by the Meng et al. (2012) study of 86% and 88% using the Random Forest (RF) method and Disturbance Index (DI) method respectively. The Kanab reach had the second best classification with a final overall accuracy of 83% which was only a few percent below the highest accuracy scores of the Meng et al. (2012) study. National reach performed noticeably worse than the other two

reaches with a final accuracy of 72%, identical to the weakest classification in the Meng et al (2012) study using disturbances indexes.

Being unable to use ground truth tamarisk validation points for Kanab and National, as well as not using any ground truth points for non-tamarisk vegetation for any of the study reaches affected the accuracy assessments. As stated in the methods, not all randomly generated points were used in the accuracy assessments due to an inability to accurately identify the species using the 2009 imagery. The needed exclusion of some randomly generated points in each reach therefore does not provide a complete representation of the ratio of different vegetation species present in each reach. Identifying vegetation remotely using the 2009 USGS imagery was still a reasonable approach, given the very inaccessible reaches and the extreme difficulty of obtaining ground truth data for all randomly generated vegetation points.

Glen Canyon Classification Accuracy

The accuracy of the Glen Canyon tamarisk classification was the best of the three reach classifications and points to this classification being very useful for tamarisk identification and change detection in this study reach. The Glen Canyon reach final tamarisk producer's and user's accuracy was 84% and 92% (Table 9), noticeably higher than the vegetation classification carried out by Ralston et al. (2008) on the 2002 overflight imagery, in which an exact match for tamarisks had a producer's and user's accuracy of 53% and 58% respectively (Ralston et al. 2008). The Glen Canyon classification producer's accuracy of 84% was less when compared against both the DI and RF producer's accuracy which was as high as 100%, but the user's accuracy of 92%

performed better than the DI and RF user's accuracy of 77% and 79% respectively (Meng et al. 2012).

The Glen Canyon classification benefited from using three times the amount of training pixels than the other two reach classifications, as well as having a much greater number of tamarisks from which to select sampled pixels (Table 4). This allowed for more local training data to be used on the upper, middle, and lower sections of Glen Canyon. The number of tamarisks mapped also allowed for separate tamarisks to be used as ground truth validation points.

Kanab Classification Accuracy

The final Kanab reach classification had a producer's accuracy and user's accuracy of 87% and 76% respectively (Table 13). The accuracies of this classification show that this classification will also be helpful in change detection for this study area. The Kanab classification had higher producer's and user's accuracies than the Ralston et al. (2008) tamarisk classification. However, the Kanab producer's accuracy of 87% was still less than the Meng et al. (2012) study that was as much as 100%, while the user's accuracy of 76% was very similar to the DI and RF user's accuracy of 77% and 79%, respectively. Carrying out a manual erase of this reach was very useful in removing incorrectly classified vegetation, which improved the tamarisk producer's accuracy from 78% to 87% for the clump and final assessments, respectively.

National Classification Accuracy

The National reach classification performed noticeably worse than the other study reaches, but may still have some utility, though the change values identified in this study should be considered with more skepticism. The final classification had a producer's and user's accuracies of 76% and 65%, respectively (Table 17) which was higher than the Ralston et al. (2008) tamarisk classification accuracies. The National producer's accuracy of 76% was still less than the Meng et al. (2012) study that was as much as 100%, while the user's accuracy of 65% was over 10% less than the DI and RF user's accuracies of 77% and 79%, respectively. The classification in this reach had higher rates of commission error, due the high concentrations of mesquites and acacias observed in this study area, which resulted in a lower user's accuracy. This classification method had more difficulty correctly identifying tamarisk pixels, and experienced a higher omission error resulting in a lower producer's accuracy for National reach. The poor inclusion of tamarisk pixels is likely due to a lack of sufficient training data. The utility of the National classification is not as strong as the Glen Canyon classification. This difference in accuracy highlights the challenges in remotely classifying tamarisks in certain areas of Grand Canyon.

Change detection

Change detection results from 2009 to 2013 showed declines in both NDVI and EVI. The differences in decline percentages between reaches varied. Glen Canyon had the most area of decline (Tables 18 and 20), followed by National (Tables 26 and 28) and Kanab (Tables 22 and 24). NDVI and EVI change detection ratios of greater than 1.5 set

a high standard for what tamarisk pixels would be defined as having experienced decline. For all study areas, much of the tamarisk decline comes from relatively small areas within each reach. This is due to large healthy tamarisk stands being present at these areas prior to beetle arrival. It is important to recognize that this change detection method identified tamarisks that had declined severely. When viewing these areas of tamarisk decline with the USGS overflight data, tamarisk beetle impact was easily identified by tamarisks having a skeletal appearance with woody material remaining intact, but without accompanying foliage. Other events such as flooding or human caused removal by mechanical and chemical methods was also recorded in this study, but not identified separately. The tamarisk change detection imagery generated from this study quantifiably identifies large areas of tamarisk defoliation and possible mortality. This data can be used for precise ground monitoring of these areas to gather information on recreational impacts, the progression of new plant species into these areas, as well as identifying habitat impacts relating to bird species and provide direction for restoration activities as needed (Hultine et al. 2010, Malakoff, D. 1999, and Sogge et al. 2008).

Separating the Colorado River into short segments within each reach was beneficial for isolating tamarisk decline along the river (Appendices A through F). These segments enabled the creation of tamarisk decline Tables which will be very useful for the NPS and USGS. Creation of river segments also permitted statistical analysis on a finer scale for each reach. Furthermore, these river segments allowed viewing the change detection data in different ways. For example, NDVI/EVI decline could be viewed by the percent of tamarisks in a segment that met the decline threshold, or could be organized by

total area that met the decline threshold. The latter option allows managers to identify large areas of tamarisk NDVI/EVI decline.

Within tamarisk canopies experiencing decline there was often a mix of declined pixels, as well as pixels with no decline. This could mean that these tamarisks are in declining health due to beetle herbivory, but have not yet suffered mortality. There were also other tamarisks that showed 100% decline, possibly indicating mortality for that individual.

EVI decline rates were less than NDVI decline rates for both Kanab and National study reaches. Due to an unidentified error in EVI processing in Glen Canyon, many areas were identified as having EVI decline when this was not accurate. The cause appeared to be due to 2009 EVI values being larger than they should be, which led to the over classification of EVI decline. This issue seemed to be present throughout the entire study reach. The reason I believe the error is due to 2009 EVI levels in Glen Canyon is through comparing the tamarisk EVI change pixels in each study reach. The non-scaled mean 2009 EVI values for Glen Canyon, Kanab and National were .762, .509 and .453 respectively, while the 2009 non-scaled mean NDVI values for these same points were .534, .570, and .495 (Appendixes G, H, and I). Comparing these values shows that the primary outlying value is the Glen Canyon 2009 EVI value. The overly high 2009 EVI value for Glen Canyon, meant that when compared to the standard 2013 value, an unusually large area showed up as experiencing EVI decline. Multiple attempts were made at recalculating all EVI layers for each study reach, and the resulting bands were always the same. A possible method to address the high 2009 EVI levels for Glen

Canyon would have been to calculate a difference ratio between the 2009 Glen Canyon EVI values and the correct Kanab and National EVI values. This ratio could then have been applied to the 2009 Glen Canyon EVI values to bring them into a normal range.

The relatively strict NDVI/EVI change ratio threshold that was established helped to minimize the amount of non-tamarisk vegetation that met the ratio for decreased greenness, while also identifying tamarisks that had experienced noticeable decreases in the greenness of the pixels. The performance of the change detection images to capture all of the tamarisk validation pixels that met the NDVI or EVI change ratio threshold for each reach reflected the final 2009 tamarisk classification for each reach. The Glen Canyon reach change imagery captured the most declined tamarisk pixels while avoiding the most non-tamarisk pixels, followed by Kanab reach and finally National reach. It is possible since Kanab reach identified 71% of all NDVI tamarisk declined pixels that the total declined area for Kanab reach is being underestimated. This same possibility that National reach is underestimating the total declined area is also possible, because only 55% of declined validated pixels were captured. Another important observation gained from reviewing the validation pixels on their own is that more tamarisk pixels met both NDVI and EVI decline ratio thresholds than the non-tamarisk pixels. Combining all the reaches shows that 1092 out of 3417 tamarisk pixels met the NDVI decline ratio, while 509 out of 3420 non-tamarisk pixels met the same ratio. This information helps to highlight that at least twice as many tamarisk pixels experienced a noticeable decrease in greenness when compared to non-tamarisk pixels.

The average NDVI value of the tamarisk pixels that met the NDVI decline threshold in 2009 was 0.52, and in 2013 the mean value had decreased to 0.26 (Appendix G). This is a twofold decline in average NDVI values. This change in NDVI is much larger than the threshold set in the Dennison et al. (2009) study that focused on observing a 0.1 change in NDVI values. This lower threshold could also have been decided upon since the study used ASTER data with a resolution of 15m. It would be logical to assume that the high resolution pixels used in this study have a pure concentration of tamarisk pixels, while it is likely the 15m pixels in ASTER datasets would almost always have some mixture of ground values diluting the NDVI values. The changes to NDVI values observed in this study are similar to the Nagler et al. (2014) study using MODIS data where initial tamarisk NDVI values were somewhat higher at 0.65 and dropped to 0.2 after a defoliation event was observed in mid-summer.

Glen Canyon Change Detection

5.6 kilometers, or 18% of the total 31.5 km accounted for 64% of the total area of tamarisk NDVI decline (Appendix A) in Glen Canyon reach. These general river locations with high areas of tamarisk decline are located around -23 km, -21 km, -19 km through -16 km (Ferry Swale), -14 through -13 km (Horseshoe Bend), -11.3 km, -10 km, -5 km to -3 km, and 0 km (Lees Ferry). This highlights that much of the total declined tamarisk area is focused on a relatively small portion of this reach.

Kanab Change Detection

For the Kanab reach, the greatest area of NDVI decline was at Kanab Creek (231.7 km). Kanab creek alone account for 7.5% of the total area of tamarisk NDVI decline, and 61% of all tamarisks at this river segment had experienced NDVI decline (Appendix C). This segment was the second highest area for EVI decline, accounting for 8.1% of the total EVI declined area, and having 23.4% of all tamarisks at Kanab Creek experiencing EVI decline (Appendix D). This is logical because one point of entrance to the Colorado River in Grand Canyon for the tamarisk beetle was Kanab Creek, and beetles in this area would have had multiple years to impact tamarisks in this area. Kanab creek also had one of the largest areas of tamarisk in this reach and may have provided plenty of foliage for tamarisk beetles to prey on initially.

Four kilometers, or 12% of the total reach of 33.5 km accounted for 48% of the total area of tamarisk NDVI decline (Appendix C) in Kanab reach. The highest NDVI decline correlated with the areas of highest EVI decline, but the river segment ranking varied (Appendix C and D). For example, Kanab Creek had the second highest EVI decline, while the first highest was at km 221.8 (137.8 mile) which was the second highest NDVI decline area in Kanab reach. The highest areas of tamarisk decline were located at 239.6 upriver of Kanab Creek, and generally from below Kanab Creek around 231.7 km to 221 km.

National Change Detection

The highest percent decline in all of the study areas was located at National Canyon 268.8 km (167 mile) (Appendix E and F), but this decline was due to a flash flood that occurred in 2012, scouring away most of the vegetation. Beetles were also identified at National Canyon, but it is not possible to identify the impact of beetles at this location, due to the flash flood in 2012 removing nearly all vegetation.

3.4 km, or 9% of the total reach of 35.7 km accounted for 34% of the total area of tamarisk NDVI decline (Appendix E) in National reach. This also highlights tamarisk decline in National reach is more evenly distributed than the other two reaches, particularly when compared against Glen Canyon. The highest NDVI decline correlated with the areas of highest EVI decline, but the river segment ranking varied. The 21 river segments with the highest area of tamarisk decline were generally located around 289 km to 284 km, 275 km, and 271 km to 260 km (Appendix E and F).

Environmental Variables

During this study, it was observed that the tamarisk beetle observation data was Incomplete. Due likely to the lack of resources needed to mount beetle surveys along the Colorado River, multiple points used in the dataset were not visited repeatedly (Johnson et al. 2012), and likely lead to inaccurate representation of beetle absence. For example, Ferry Swale located at -18.2 km (-11.3 mile) which had 68% of tamarisk NDVI decline in the river segment with a total area decline of .31 hectares was surveyed for beetles in 2010 one time with no beetles observed (Appendix A). Given the quantitative values based on the NDVI decline for tamarisks at this site, as well as visual observation using

the 2013 dataset and seeing tamarisk decline indicative of tamarisk beetles, it is likely that beetles came to this point after the 2010 survey, but were not recorded, and therefore this river segment was analyzed as not having beetles present at the site. These types of omission errors potentially made statistical analysis using the beetle data inconclusive. For future use of this dataset, it is recommended to revisit sites that have been identified as having no beetles to confirm if this is the case or to update the area as having beetle impacts. Also, an assumption could be made to extend the presence of beetles past the .16km segments to account for the dispersal of beetles. For example, if one point is identified as containing beetles, it would be logical to assume that all segments within a certain radius would likely have beetles as well, because tamarisk beetles have been noted to travel long distances (DeLoach et al. 2004).

Environmental Variables Relating to Tamarisk Decline

Nine environmental variables were examined as potential factors contributing to tamarisk decline. These included river segment, initial tamarisk area, sun model data in the form of viewshed, average minutes of total sunlight in a year, average minutes of direct and indirect sunlight in a year, beetle count data in the form of adults, early and late stage larvae. Analysis of tamarisk decline was carried out with and without beetle data due to the temporal and spatial issues mentioned above.

Variables developed from the sun model held consistent positive or negative slopes throughout the study reaches for predicting percent tamarisk NDVI decline. Total sunlight and diffuse sunlight always had positive slopes, while direct sunlight and viewshed always had negative slope values. The total and diffuse sunlight values often

held very similar values indicating a strong correlation between these values, which helps to explain why both these variables maintained positive slopes. Viewshed and direct sunlight also appeared to be highly related to each other. This is because as viewshed increases, the skyline becomes more open, and therefore increases the amount of direct sunlight. It is less clear why these variables would have negative slopes, resulting in a lower tamarisk NDVI decline in areas with a more open viewshed resulting in more direct sunlight. One possibility is that tamarisks receiving greater rates of direct sunlight have increased vigor due to more efficient photosynthetic output than tamarisk in more shaded areas. It is also a possibility that using sun model data belonging to the center of the river as an approximation for each river segment is providing noticeably incorrect values for the amount of sunlight received in the areas along the river occupied by tamarisks.

Initial tamarisk area had a positive slope for predicting NDVI decline only in Glen Canyon, while Kanab and National study reaches had negative slope values. I believe it more reasonable to assume that a positive slope value would be correct for this variable, because increasing tamarisk area would provide increasing amounts of forage to sustain a tamarisk beetle population, which is what the positive slope for Glen Canyon indicates. The positive value for Glen Canyon is also likely related to the fact that there is a great deal more tamarisks found in this study reach, than compared with the Kanab and National Study reaches.

River segment had a positive slope for predicting NDVI decline in Kanab, while Glen Canyon and National had negative slope values. Negative slope values indicate a

decrease in tamarisk decline as the study reach continues downriver, while positive value indicates an increasing trend of tamarisk defoliation. It is possible the positive trend for Kanab is due to the tamarisk beetles coming from the Kanab Creek confluence. The negative value for Glen Canyon may make sense, because there was much more tamarisk closer to Glen Canyon Dam within the Glen Canyon National Recreation Area and much of the high values of percent tamarisk decline were located in this area. Therefore as the river segmented proceeded downriver away from these large areas of percent decline, tamarisk decline would decrease along a negative slope. For the National study area, the negative value could possibly indicate the decreasing effect of tamarisk beetles because they have not yet expanded to the more downriver portions of this study reach.

Initial tamarisk area was identified as a significant variable in simple regression models relating to percent NDVI/EVI decline by river segment for Glen Canyon, and for National when using NDVI decline data, but not EVI decline data (Tables 36, and 38). This might suggest that tamarisk beetles are targeting larger areas of tamarisks, rather than sparse tamarisk populations. Using percent decline values, rather than the total area of decline in this analysis addressed the more direct relationship between initial area and decline area that was observed in analysis.

River segments were a significant variable for simple regression models for Glen Canyon EVI decline, Kanab NDVI or EVI decline, and National NDVI decline (Tables 36, and 38). The Adjusted R^2 value NDVI decline for the Kanab and National reaches were 0.093 and 0.295 respectively. This indicated a weak but significant relationship in Kanab to river location, and a stronger relationship in the National reach. This could

indicate a relationship between tamarisk locations along the river and their likelihood to experience decline. The relationship of river segment to the Kanab reach could be due to tamarisk beetles originating from the Kanab Creek confluence (Makarick, 2016). River segment significance for National reach could be influenced by the flash flood that removed nearly all vegetation from this area.

Viewshed, average total daylight, average diffuse and direct daylight were all significant coefficients for simple regression models based on NDVI decline for Kanab and National reaches (Tables 36, and 38), while none of these were significant for Glen Canyon. River orientations for Kanab and National reaches are generally east-west, while Glen Canyon has a more north-south orientation. This, along with the topography of the canyon could indicate why these variables are significant for Kanab and National, but not Glen Canyon.

The simple regression model using late larvae counts as a predictor for percent tamarisk EVI in Glen Canyon decline was the only beetle model to show a P value less than .05 (Appendix J1). As discussed earlier, the EVI change detection layer for Glen Canyon reach is a questionable dataset and therefore so are any models relating to the EVI values for this reach. Independent T-tests examining the relationship of the presence or absence of tamarisk beetles and larvae found that early beetle larvae had a significant relationship to EVI decline in Kanab (Table 60). The multiple regression model for predicting percent NDVI decline in Glen Canyon (Equation 16) did exhibit a significant value for late larvae count (P-value of 0.040). This multiple regression model was one of the strongest models identified for any reach predicting percent NDVI decline. This was

the only multiple regression model to show significance of beetle data lowering tamarisk decline.

There are likely other variables that could help to predict the areas of tamarisk decline that were not used in this study. Analysis of declined pixels as they relate to a certain river flow level could be helpful in future studies. It is possible that tamarisks farther from the river may have additional difficulty accessing the water Table for the area and therefore have more difficulty recovering from beetle impacts.

The multivariate model without beetle observation for Glen Canyon NDVI decline makes sense ecologically. The positive coefficients of tamarisk area and total daylight would point to the greatest chance for tamarisk to decline due to an availability of tamarisks and sunlight. The viewshed variable was used in the majority of multivariate models, it is still puzzling why the slope for this variable is negative. The Kanab multivariate model for percent NDVI decline also makes sense. Using diffuse daylight instead of total daylight like Glen Canyon seems reasonable, because both variable have positive slopes and are correlated with each other. The addition of river segment for the Kanab reach could be explained due to the tamarisk beetle spreading from Kanab Creek itself as mentioned earlier. I think the multivariate model for percent decline without using beetle observation data is least likely. This model likely had a hard time developing accurate variables due to the poor initial classification of tamarisk, and the flood event that happened at National Canyon introduced a major point of severe NDVI decline that was not beetle related. I think this is the reason river segment shows up as a variable in the multivariate regression model for this reach.

Environmental Variables Relating to beetle observations

Direct daylight had a significant relationship ($P < .05$) with the presence and absence of adult tamarisk beetles for Glen Canyon and Kanab reaches. These models had low fits but may still indicate that tamarisk beetles have a preference for areas that have more direct sunlight. No regression models were able to adequately predict the occurrence of tamarisk beetles. This suggests that there are other unidentified factors that are a greater influence on the spread of the tamarisk beetle in Grand Canyon. It also indicates that a more temporally and spatially complete inventory of tamarisk beetles is needed. These results are somewhat similar to the Archambault et al. (2009) where low R^2 values were observed for sunlight variables, but different because these variables were sometimes significant. I believe as Archambault et al. (2009) concluded that there are other more important drivers not identified that are more strongly linked to beetle establishment.

Chapter 6 – Conclusion

High spatial resolution data allowed pure vegetation pixels to be located and was a critical part in accurately classifying tamarisk. Classification accuracies varied spatially due to the difference in training data, and the changing plant communities. The change in plant species and their abundance influenced the accuracy of tamarisk classifications, particularly when the abundance of spectrally similar plants such as acacias and mesquites increased. This high resolution data also allowed concise change detection analysis, being able to classify small tamarisk stands that would be difficult to detect with satellite imagery. High resolution data also enabled the pairing of small river segment data to allow specific identification of areas with high rates of tamarisk decline. Any future vegetation classification would benefit from more training data throughout Grand Canyon. Adding to the database for pure vegetation pixels created by Ralston et al. (2008) would help this process. This database could be expanded incrementally during river monitoring trips by USGS and NPS staff during annual surveys. The points in this database could be used as training and validation datasets for future classification efforts.

Additional methods and imagery should be employed to further tamarisk classification within Glen and Grand Canyons. LIDAR imagery could be beneficial in establishing height thresholds to exclude vegetation with different heights compared to tamarisks. Texture analysis could also be a beneficial method to separate vegetation that have similar spectral values. Fusion of spectral data, with these other types of data could improve tamarisk and other vegetation classifications in this area. For example, fusing the tamarisk classification generated with the high resolution USGS data with imagery

that has a greater temporal resolution could allow for tracking of beetle movements across individual years. For example, QuickBird data could be used with the tamarisk classification in this study to monitor the change in tamarisk stands during each year from 2009 to 2013. This would require scaling the .2 m USGS data to the QuickBird imagery resolution of 2.4 (Lillesand et al. 2008: 456) m which would allow monitoring of only larger tamarisk groupings. Another potential issue with using satellite data would be interference from the canyon topography, which could limit the amount of viewable area.

Tamarisk decline was spatially varied through the study reaches, with much of the total area of tamarisk decline occurring in relatively small, concentrated areas along the river. It could be beneficial for researchers and managers to establish a survey or monitoring routine at some of these locations. It could be useful to know if these areas are experiencing passive revegetation, and whether native or non-native vegetation are replacing tamarisks in these areas. Given the altered flow regimes for the Colorado River in this area, native riparian vegetation may likely have difficulty naturally colonizing an area (Hultine et al. 2010). It may be important for Grand Canyon National Park to develop restoration plans to mitigate the effects of tamarisk decline if native vegetation are not establishing readily. This is particularly important in southwest willow flycatcher habitat to promote native vegetation to act as nesting habitat to replace tamarisks.

I do not believe the statistical analysis generated from the tamarisk beetle data relating to tamarisk decline to be sufficiently accurate. The temporal coarseness of this dataset makes it very likely that beetles inhabited areas that were identified as beetle absences due to a lack of consistent surveys at locations every year or even multiple time

a year. Further consistent monitoring of tamarisk beetles would be helpful to identify where beetles are active.

Future tamarisk decline studies should focus on other reaches not encompassed in this study to gain a more complete picture of tamarisk decline in the Grand Canyon. Classification accuracies will likely vary considerably depending on the types of vegetation found in the area being classified. It would be worthwhile to test the efficacy of using the tamarisk training data developed in this study in the classification of other reaches of Grand Canyon, such as around the Little Colorado River. This would help researchers to understand how far the effective range of the tamarisk training data extends to, and also allow for further tamarisk change detection studies. As mentioned in the discussion, I believe proximity to the training data, canyon orientation and topography will be important factors in how well each set of training data performs.

References

Archambault, V., Auch, J., Landy, J., Rudy, G., and Seifert, C. (2009). Utilizing Remote Sensing to Supplement Ground Monitoring of *Diorhabda elongate* as a Control Agent for *Tamarix ramosissima* in Dinosaur National Monument. *ASPRS 2009 Annual Conference*.

Bay, R., and Sher, A. (2008). Success of Active Revegetation after *Tamarix* Removal in Riparian Ecosystems of the Southwestern United States: A Quantitative Assessment of Past Restoration Projects. *Restoration Ecology*, 16(1), 113-128

Bean, D., Dudley, T., and Keller, J. (2007). Seasonal Timing of Diapause Induction Limits the Effective Range of *Diorhabda elongate deserticola* (Coleoptera: Chrysomelidae) as a Biological Control Agent for Tamarisk (*Tamarix* spp.). *Environmental Entomology*, 36(1), 15-25.

Bean, D., Dalin, P., and Dudley, T. (2012). Evolution of critical day length for diapause induction enables range expansionof *Diorhabda carinulata*, a biological control agent against tamarisk (*Tamarix* spp.). *Evolutionary Applications*. 5, 511-523

Brock, J. (1994). *Tamarix* spp. (Salt Cedar), an Invasive Exotic Woody Plant in Arid and Semi-arid Riparian Habitats of Western USA. *Ecology and Management of Invasive Riverside Plants*, 27-43

Carruthers, R., Anderson, G., DeLoach, J., Knight, J., Ge, S., and Gong, P. (2006). Remote Sensing of Saltcedar Biological Control Effectiveness. *USDA Forest Service Proceedings RMRS-P-42CD*.

Davis, P. (2012). Airborne Digital-Image Data for Monitoring the Colorado River Corridor below Glen Canyon Dam, Arizona, 2009-Image-Mosaic Production and Comparison with 2002 and 2005 Image Mosaics. U.S. Geological Survey Open-File Report 2012-1139, 82 p. (Available at http://pubs.usgs.gov/of/2012/1139/.)

DeLoach, J., Carruthers, R., Dudley, T., Eberts, D., Kazmer, D., Knutson, A., Bean, D., Knight, J., Lewis, P., Milbrath, R., Tracy, J., Tomic-Carruthers N., Herr, J., Abbott, G., Prestwich, S., Harruff, G., Everitt, J., Thompson, D., Mityaev I., Jashenko, R., Li, B., Sobhian, R., Kirk, A., Robbins, T., and Delfosse, E. (2004). First results for control of saltcedar (*Tamarix* spp.) in the open field in the western United States. Proceedings of the XI International Symposium on Biological Control of Weeds: Canberra, Australia, CSIRO Entomology, P. 505-513.

Dennison, P., Nagler, P., Hultine, K., Glenn, E., and Ehleringer, J. (2009). Remote monitoring of tamarisk defoliation and evapotranspiration following saltcedar leaf beetle attack. *Remote Sensing of Environment*, 113, 1462-1472.

Fenner, P., Brady, W., and Patton, D. (1985). Effects of Regulated Water Flows on Regeneration of Fremont Cottonwood. *Journal of Range Management*, 38(2), 135-138.

Fletcher, R. (2013). Employing spatial information technologies to monitor biological control of saltcedar in West Texas. *Geocarto International*.

Glenn, E., Huete, A., Nagler, P., and Nelson, S. (2008). Relationship Between Remotely-sensed Vegetation Indices, Canopy Attributes and Plant Physiological Processes: What Vegetation Indices Can and Cannot Tell Us About the Landscape. *Sensors*, 8, 2136-2160

Healey, S., Cohen, W., Zhiqiang, and Y., Krankina, O. (2005). Comparison of Tasseled Cap-based Landsat data structures for use in forest disturbance detection. *Remote Sensing of Environment*, 97, 301-310.

Hultine, K., Belnap, J., van Riper III, C., Ehleringer, J., Dennison, P., Lee, M., Nagler, P., Snyder, K., Uselman, S., and West, J. (2010). Tamarisk biocontrol in the western United States: ecological and societal implications. *Ecol Environ*, 8(9), 467-474.

Johnson, M., Ralston, B.E., Jamison L., Makarick, L. and Holmes, J. (2012). 2011 Monitoring Tamarisk Foliage Removal by the Introduced Tamarisk Leaf Beetle (*Diorhabda carinulata*), and its Effects on Avian Habitat Parameters along the Colorado River in Grand Canyon National Park, Arizona, pp 71.

Lewis PA, Deloach CJ, Knutson AE, Tracy JL, Robbins TO (2003). Biology of *Diorhabda carinulata deserticola* (Coleoptera: Chrysomelidae), an Asian leaf beetle for biological control of saltcedars (*Tamarix* spp.) in the United States. *Biol Cont*, 27, 101–116

Lillesand, Thomas, Kiefer, Ralph, and Chipman, Jonathan. 2008. *Remote Sensing and Image Interpretation*. Hoboken. John Wiley & Sons, Inc.

Makarick, L., (2016). Personal Communication.

Malakoff, D., (1999). Plan to import exotic beetles drives some scientists wild. *Science*, v. 284, p. 1255.

Meng, R., Dennison, P., Jamison, R., van Riper, C., Nagler, P., Hultine, K., Bean, D., Dudley, T. (2012). Detection of Tamarisk Defoliation by the Northern Tamarisk Beetle Based on Multitemporal Landsat 5 Thematic Mapper Imagery. *GIScience & Remote Sensing*, 49(3), 510-537.

Minard, A. (2011). Grand Canyon National Park Ecosystem Threatened by Kazakhstan Beetle? http://news.nationalgeographic.com/news/2011/04/110421-national-parks-grand-canyon-water-tamarisk-flycatcher/. Accessed 08 November 2013

Nagler, P., Pearlstein, S., Glenn, P., Brown, T., Bateman, H., Bean, D., and Hultine, K. (2014). Rapid dispersal of saltcedar (*Tamarix* spp.) biocontrol beetles (*Diorhabda carinulata*) on a desert river detected by phenocams, MODIS imagery and ground observations. *Remote Sensing of Environment* , 140, 206-219.

National Park Service. (2015). Weather and Road Conditions. https://www.nps.gov/grca/planyourvisit/weather-condition.htm.

Pettorelli, N., Vik, J., Mysterud, A., Gaillard J., Tucker, C., and Stenseth, N., (2005). Using the satellite-derived NDVI to assess ecological responses to environmental change. *TRENDS in Ecology and Evolution*. 20(9), 503-510

Ralston, Barbara E., Davis, Philip A., Weber, Robert M., and Rundall, Jill M., (2008), A vegetation database for the Colorado River ecosystem from Glen Canyon Dam to the western boundary of Grand Canyon National Park, Arizona: U.S. Geological Survey Open-File Report 2008–1216, 37 p.

Rouse, J.W.J., Haas, R.H., Schell, J.A., Deering, D.W., (1974). Monitoring vegetation systems in the Great Plains with ERTS. In: Third ERTS Symposium, NASA SP-351, Washington DC. 309-317.

Sankey, JB, Ralston, B, Grams PE, Schmidt, JC., Cagney, L., (2015), Riparian vegetation, Colorado River and climate: Five decades of spatio-temporal dynamics in the Grand Canyon in response to river regulation. *Journal of Geophysical Research*, 120(8), 1532-1547; doi: 10.1002/2015JG002991

Sankey, T., R. Horne, A. Bedford, and J. Sankey. (2016), Remote sensing of tamarisk biomass, insect herbivory, and defoliation: novel methods in the Grand Canyon region, Arizona, USA. *Photogrammetric Engineering and Remote Sensing* (*In Print*)

Shafroth, P., Beauchamp, V., Briggs, M., Lair, K., Scott, M., and Sher, A. (2008). Planning Riparian Restoration in the Context of *Tamarix* Control in Western North America. *Restoration Ecology*, 16(1), 97-112

Shafroth, P., Friedman, J., and Ischinger, L. (1995). Effects of Salinity on Establishment of *Populus fremontii* (cottonwood) and *Tamarix ramosissima* (saltcedar) in Southwestern United States. *Great Basin Naturalist*, 55(1), 58-65

Snyder, K., Uselman, S., Jones, T., and Duke, S. (2010). Ecophysiological responses of salt cedar (*Tamarix spp.* L.) to the northern tamarisk beete (*Diorhabda carinulata* Desbrochers) in a controlled environment. *Biol Invasions*, 12, 3795-3808.

Sogge, M., Sferra, S., and Paxton, E., (2008). *Tamarix* as habitat for birds: Implicationsn for riparian restoration in the Southwestern United States:. *Restoration Ecology*, 16(1), 146-154

Stromberg, J., Lite, S., Marler, R., Paradzick, C., Shafroth, P., Shorrock D., White, J., and White M. (2007). Altered stream-flow regimes and invasive plant species: the *Tamarix* case. *Global Ecology and Biogeography*, 16, 381-393.

Stromberg, J. (1998). Dynamics of Fremont cottonwood (*Populus fremontii*) and saltcedar (*Tamarix chinensis*) populations along the San Pedro River, Arizona. *Journal of Arid Environments*, 40, 133-155.

Yard, M., Bennet, G., Mietz, S., Coggins, L., Stevens, L., Hueftle, S., Blinn, D., (2005). Influence of topographic complexity on solar insolation estimates for the Colorado River, Grand Canyon, AZ. *Ecological Modelling*, 183, 157-172

Appendix

Appendix A: NDVI decline in Glen Canyon by .16 km river segments

River segment kilometer	Tamarisk 2009 classification meters squared	Tamarisk NDVI decline meters squared	% tamarisk with NDVI decline
-25.4	73.2	1.72	2.3%
-25.3	30	4.28	14.3%
-25.1	205.32	18.12	8.8%
-24.9	250.88	31.04	12.4%
-24.8	381.08	94.6	24.8%
-24.6	1110.68	63.12	5.7%
-24.5	1790.6	83.24	4.6%
-24.3	766.6	67.48	8.8%
-24.1	1177.52	24.28	2.1%
-24.0	615.24	18.36	3.0%
-23.8	1426.44	57.24	4.0%
-23.7	2043.72	488.52	23.9%
-23.5	2167.72	692.8	32.0%
-23.3	1575.24	426.6	27.1%
-23.2	1899.12	241.96	12.7%
-23.0	2864.56	770.56	26.9%
-22.9	4063.64	1004.68	24.7%
-22.7	3631.2	437.52	12.0%
-22.5	2364	562.4	23.8%
-22.4	2268.96	63.68	2.8%
-22.2	2492.56	58.8	2.4%
-22.0	2546.64	78.04	3.1%
-21.9	2001.28	57.04	2.9%
-21.7	1330.44	166.12	12.5%
-21.6	920.56	102.4	11.1%
-21.4	982.72	98.52	10.0%
-21.2	3110.28	1023.28	32.9%
-21.1	1737.52	285.84	16.5%
-20.9	932.52	117.96	12.6%
-20.8	1265.56	284.92	22.5%
-20.6	2245.56	570.72	25.4%
-20.4	771.36	120.96	15.7%
-20.3	1470.44	464.8	31.6%
-20.1	392.36	63.32	16.1%

-20.0	328.64	43.4	13.2%
-19.8	436.88	49.76	11.4%
-19.6	1122.92	77.52	6.9%
-19.5	1351.4	291.64	21.6%
-19.3	1157.48	141.32	12.2%
-19.2	2243	533	23.8%
-19.0	4757.6	1181.88	24.8%
-18.8	2134.92	338.6	15.9%
-18.7	924.56	174.04	18.8%
-18.5	1908.48	679.92	35.6%
-18.3	3067.96	1688.92	55.1%
-18.2	4579.52	3091.56	67.5%
-18.0	1108.04	357.04	32.2%
-17.9	2488.92	499.4	20.1%
-17.7	2131.36	942.04	44.2%
-17.5	2300.84	994.28	43.2%
-17.4	2065.48	756.08	36.6%
-17.2	984.8	428.16	43.5%
-17.1	1318.48	334.2	25.3%
-16.9	889.28	230.56	25.9%
-16.7	1305.64	548.92	42.0%
-16.6	2367.12	1440.64	60.9%
-16.4	2430.8	1566.32	64.4%
-16.3	2088.76	1429.72	68.4%
-16.1	1341.44	396.16	29.5%
-15.9	2944.8	407	13.8%
-15.8	1368.48	80.56	5.9%
-15.6	1185.24	183.52	15.5%
-15.4	2708.92	521.68	19.3%
-15.3	2013.56	303.08	15.1%
-15.1	1865.16	221.6	11.9%
-15.0	1400.56	119.04	8.5%
-14.8	1100.88	185.24	16.8%
-14.6	2225.24	808.24	36.3%
-14.5	2245.76	311.32	13.9%
-14.3	1154.76	247.36	21.4%
-14.2	2524.48	809.04	32.0%
-14.0	3905.68	1286.44	32.9%
-13.8	4948.36	1471.48	29.7%
-13.7	3925.04	1434.04	36.5%
-13.5	4222.64	1960.12	46.4%

-13.4	2569	942.24	36.7%
-13.2	1071.2	84.48	7.9%
-13.0	1353.16	222.12	16.4%
-12.9	1569.4	306.96	19.6%
-12.7	618.56	82.88	13.4%
-12.6	726.24	64.4	8.9%
-12.4	1298.8	406	31.3%
-12.2	2473.04	1539.92	62.3%
-12.1	151.92	35.8	23.6%
-11.9	342.76	27.96	8.2%
-11.7	604.32	125.08	20.7%
-11.6	2109.12	651.92	30.9%
-11.4	3693.32	2592.88	70.2%
-11.3	3658.72	1508.72	41.2%
-11.1	3577.52	1283.24	35.9%
-10.9	985.28	86.44	8.8%
-10.8	126.56	57.6	45.5%
-10.6	3.2	0.04	1.3%
-10.5	45.28	4.84	10.7%
-10.3	501.24	60.56	12.1%
-10.1	630.12	248.56	39.4%
-10.0	2393.16	1302.52	54.4%
-9.8	1860.44	301	16.2%
-9.7	493.92	51.36	10.4%
-9.5	1260.84	184.16	14.6%
-9.3	652.44	129.08	19.8%
-9.2	616.72	111.92	18.1%
-9.0	1398.48	633.36	45.3%
-8.9	1507.16	494.88	32.8%
-8.7	933.36	99.36	10.6%
-8.5	1188.6	211.04	17.8%
-8.4	441.64	38.56	8.7%
-8.2	1176.88	353.72	30.1%
-8.0	946.04	101.92	10.8%
-7.9	796.04	91.92	11.5%
-7.7	1294.04	406.68	31.4%
-7.6	413.92	66.08	16.0%
-7.4	639.16	38.72	6.1%
-7.2	417.08	24.36	5.8%
-7.1	983.2	131.12	13.3%
-6.9	679.28	97	14.3%

-6.8	595.28	62.2	10.4%
-6.6	604	148.44	24.6%
-6.4	1883.44	241.72	12.8%
-6.3	2680.56	324.52	12.1%
-6.1	1642.68	341.16	20.8%
-6.0	1036.96	110.28	10.6%
-5.8	663.72	260.12	39.2%
-5.6	2144.08	565.68	26.4%
-5.5	2855.68	1342.64	47.0%
-5.3	4481.56	2477.48	55.3%
-5.1	5745.44	3850.16	67.0%
-5.0	2695.76	1772.92	65.8%
-4.8	1476.8	991.64	67.1%
-4.7	4593.6	2908.8	63.3%
-4.5	4434.08	2379.84	53.7%
-4.3	3057.12	1044.08	34.2%
-4.2	1172.96	536.84	45.8%
-4.0	3262.44	1907.76	58.5%
-3.9	3659.36	1312.56	35.9%
-3.7	2702.92	1631.4	60.4%
-3.5	1741.76	1207.76	69.3%
-3.4	411.56	110.72	26.9%
-3.2	1079.56	646.28	59.9%
-3.1	213.92	15.48	7.2%
-2.9	551.16	127.2	23.1%
-2.7	48.08	7.88	16.4%
-2.6	168.76	37.24	22.1%
-2.4	259.92	60.88	23.4%
-2.3	591.2	162.4	27.5%
-2.1	139.96	32.8	23.4%
-1.9	101.2	24.96	24.7%
-1.8	444	93.44	21.0%
-1.6	246.96	58.72	23.8%
-1.4	774.68	135.6	17.5%
-1.3	182.08	36.08	19.8%
-1.1	165.4	23.48	14.2%
-1.0	635.52	59.12	9.3%
-0.8	824.04	116.16	14.1%
-0.6	1109.68	95.16	8.6%
-0.5	2590.96	192.76	7.4%
-0.3	3603.4	474	13.2%

-0.2	3543.72	970.6	27.4%
0.0	1850.16	346.24	18.7%
0.2	1244.04	220.08	17.7%
0.3	2072.44	261.72	12.6%
0.5	598.52	84.6	14.1%
0.6	509.96	78.76	15.4%
0.8	407.84	71.88	17.6%
1.0	163.52	58.8	36.0%
1.1	395.24	48	12.1%
1.3	900.4	97.84	10.9%
1.4	1572.56	493.88	31.4%
1.6	381.8	80.84	21.2%
1.8	2692.72	1486.8	55.2%
1.9	2747.6	1383.8	50.4%
2.1	164.32	45.88	27.9%
2.3	63.68	6.76	10.6%
2.4	68.52	5.88	8.6%
2.6	322.16	39.28	12.2%
2.7	444.08	25.84	5.8%
2.9	885.4	17.64	2.0%
3.1	317.2	62.12	19.6%
3.2	843.8	38.44	4.6%
3.4	1068.6	48.28	4.5%
3.5	897.44	61.04	6.8%
3.7	543.52	101.6	18.7%
3.9	1582.76	145.2	9.2%
4.0	554.92	25	4.5%
4.2	476.72	30.44	6.4%
4.3	580.76	35.84	6.2%
4.5	263.68	50.4	19.1%
4.7	127.64	7.52	5.9%
4.8	112.56	4.36	3.9%
5.0	228.24	20.64	9.0%
5.1	298.24	29.52	9.9%
5.3	418.44	42.52	10.2%
5.5	485.56	127.08	26.2%
5.6	576.32	68.68	11.9%
5.8	444.6	33.48	7.5%
6.0	114.48	11.48	10.0%

Appendix B: EVI decline in Glen Canyon by .16 km river segments

River segment kilometer	Tamarisk 2009 classification meters squared	Tamarisk EVI decline meters squared	% tamarisk with EVI decline
-25.43	73.2	7.84	10.7%
-25.27	30	11.52	38.4%
-25.11	205.32	64.24	31.3%
-24.94	250.88	75.96	30.3%
-24.78	381.08	177.84	46.7%
-24.62	1110.68	325.6	29.3%
-24.46	1790.6	559.56	31.2%
-24.30	766.6	253.72	33.1%
-24.14	1177.52	395.84	33.6%
-23.98	615.24	220.16	35.8%
-23.82	1426.44	583.76	40.9%
-23.66	2043.72	1563.64	76.5%
-23.50	2167.72	1733.36	80.0%
-23.34	1575.24	1016.92	64.6%
-23.17	1899.12	1243.68	65.5%
-23.01	2864.56	2283.44	79.7%
-22.85	4063.64	3493.24	86.0%
-22.69	3631.2	3096.96	85.3%
-22.53	2364	2057.6	87.0%
-22.37	2268.96	1306.24	57.6%
-22.21	2492.56	1220.6	49.0%
-22.05	2546.64	1517.88	59.6%
-21.89	2001.28	821.56	41.1%
-21.73	1330.44	807.16	60.7%
-21.57	920.56	577.76	62.8%
-21.40	982.72	601.04	61.2%
-21.24	3110.28	2281.72	73.4%
-21.08	1737.52	1032.4	59.4%
-20.92	932.52	510.52	54.7%
-20.76	1265.56	986.2	77.9%
-20.60	2245.56	2010.96	89.6%
-20.44	771.36	539.48	69.9%
-20.28	1470.44	1286.68	87.5%

-20.12	392.36	264.28	67.4%
-19.96	328.64	198.96	60.5%
-19.79	436.88	177.44	40.6%
-19.63	1122.92	595.84	53.1%
-19.47	1351.4	892.6	66.1%
-19.31	1157.48	663.76	57.3%
-19.15	2243	1594.48	71.1%
-18.99	4757.6	3979.68	83.6%
-18.83	2134.92	1631.28	76.4%
-18.67	924.56	674.08	72.9%
-18.51	1908.48	1450.76	76.0%
-18.35	3067.96	2816.84	91.8%
-18.19	4579.52	4297.12	93.8%
-18.02	1108.04	849.48	76.7%
-17.86	2488.92	1904.4	76.5%
-17.70	2131.36	1633.56	76.6%
-17.54	2300.84	1928.08	83.8%
-17.38	2065.48	1802	87.2%
-17.22	984.8	784.4	79.7%
-17.06	1318.48	797.2	60.5%
-16.90	889.28	526.56	59.2%
-16.74	1305.64	1125.44	86.2%
-16.58	2367.12	2251.96	95.1%
-16.42	2430.8	2294.72	94.4%
-16.25	2088.76	1997.2	95.6%
-16.09	1341.44	787.68	58.7%
-15.93	2944.8	1105.24	37.5%
-15.77	1368.48	347.64	25.4%
-15.61	1185.24	536.36	45.3%
-15.45	2708.92	1723.52	63.6%
-15.29	2013.56	834.24	41.4%
-15.13	1865.16	893.96	47.9%
-14.97	1400.56	611.52	43.7%
-14.81	1100.88	601.76	54.7%
-14.65	2225.24	1638.6	73.6%
-14.48	2245.76	826.88	36.8%
-14.32	1154.76	712.4	61.7%
-14.16	2524.48	1891.92	74.9%
-14.00	3905.68	3528.24	90.3%
-13.84	4948.36	4423	89.4%
-13.68	3925.04	3398.36	86.6%

-13.52	4222.64	3571.64	84.6%
-13.36	2569	2025.44	78.8%
-13.20	1071.2	578.08	54.0%
-13.04	1353.16	947.64	70.0%
-12.87	1569.4	1143.72	72.9%
-12.71	618.56	406.04	65.6%
-12.55	726.24	426.6	58.7%
-12.39	1298.8	908.76	70.0%
-12.23	2473.04	2248.92	90.9%
-12.07	151.92	110.96	73.0%
-11.91	342.76	192.72	56.2%
-11.75	604.32	397.16	65.7%
-11.59	2109.12	1488.84	70.6%
-11.43	3693.32	3303.68	89.5%
-11.27	3658.72	2842.32	77.7%
-11.10	3577.52	2337.36	65.3%
-10.94	985.28	421.08	42.7%
-10.78	126.56	100	79.0%
-10.62	3.2	2.28	71.3%
-10.46	45.28	26.92	59.5%
-10.30	501.24	214.88	42.9%
-10.14	630.12	414.36	65.8%
-9.98	2393.16	1961.84	82.0%
-9.82	1860.44	907.4	48.8%
-9.66	493.92	206.36	41.8%
-9.50	1260.84	573.24	45.5%
-9.33	652.44	348.04	53.3%
-9.17	616.72	287.8	46.7%
-9.01	1398.48	1041.16	74.4%
-8.85	1507.16	1033.68	68.6%
-8.69	933.36	357.72	38.3%
-8.53	1188.6	505.48	42.5%
-8.37	441.64	200.68	45.4%
-8.21	1176.88	715.12	60.8%
-8.05	946.04	406.36	43.0%
-7.89	796.04	341.04	42.8%
-7.72	1294.04	901.2	69.6%
-7.56	413.92	184.12	44.5%
-7.40	639.16	139.28	21.8%
-7.24	417.08	74.84	17.9%
-7.08	983.2	478.04	48.6%

-6.92	679.28	278.88	41.1%
-6.76	595.28	175.68	29.5%
-6.60	604	312.48	51.7%
-6.44	1883.44	580.64	30.8%
-6.28	2680.56	1002.4	37.4%
-6.12	1642.68	949.32	57.8%
-5.95	1036.96	665.92	64.2%
-5.79	663.72	541.76	81.6%
-5.63	2144.08	1542.56	71.9%
-5.47	2855.68	2353.28	82.4%
-5.31	4481.56	3403.96	76.0%
-5.15	5745.44	4851.96	84.4%
-4.99	2695.76	2238.48	83.0%
-4.83	1476.8	1133.88	76.8%
-4.67	4593.6	3774.4	82.2%
-4.51	4434.08	3527.96	79.6%
-4.35	3057.12	2019.32	66.1%
-4.18	1172.96	739.48	63.0%
-4.02	3262.44	2352.76	72.1%
-3.86	3659.36	2137.32	58.4%
-3.70	2702.92	2066.72	76.5%
-3.54	1741.76	1449.16	83.2%
-3.38	411.56	214.52	52.1%
-3.22	1079.56	845.88	78.4%
-3.06	213.92	34.56	16.2%
-2.90	551.16	200.44	36.4%
-2.74	48.08	15.48	32.2%
-2.57	168.76	89	52.7%
-2.41	259.92	120.16	46.2%
-2.25	591.2	268.28	45.4%
-2.09	139.96	55.28	39.5%
-1.93	101.2	44.76	44.2%
-1.77	444	135.24	30.5%
-1.61	246.96	83.96	34.0%
-1.45	774.68	233.6	30.2%
-1.29	182.08	49.96	27.4%
-1.13	165.4	35.96	21.7%
-0.97	635.52	155.12	24.4%
-0.80	824.04	220	26.7%
-0.64	1109.68	344.16	31.0%
-0.48	2590.96	541.8	20.9%

-0.32	3603.4	1248.6	34.7%
-0.16	3543.72	2270.48	64.1%
0.00	1850.16	602.08	32.5%
0.16	1244.04	483.88	38.9%
0.32	2072.44	656.36	31.7%
0.48	598.52	201.64	33.7%
0.64	509.96	228.48	44.8%
0.80	407.84	193.48	47.4%
0.97	163.52	88.8	54.3%
1.13	395.24	90.76	23.0%
1.29	900.4	226.84	25.2%
1.45	1572.56	723.6	46.0%
1.61	381.8	132.52	34.7%
1.77	2692.72	2062.24	76.6%
1.93	2747.6	2032.8	74.0%
2.09	164.32	82.2	50.0%
2.25	63.68	15.64	24.6%
2.41	68.52	21.6	31.5%
2.57	322.16	67.6	21.0%
2.74	444.08	57.32	12.9%
2.90	885.4	50.76	5.7%
3.06	317.2	59.2	18.7%
3.22	843.8	71.52	8.5%
3.38	1068.6	67.6	6.3%
3.54	897.44	226.08	25.2%
3.70	543.52	302.56	55.7%
3.86	1582.76	285.72	18.1%
4.02	554.92	47.64	8.6%
4.18	476.72	78.2	16.4%
4.35	580.76	76.32	13.1%
4.51	263.68	78.36	29.7%
4.67	127.64	21.96	17.2%
4.83	112.56	9.68	8.6%
4.99	228.24	34.08	14.9%
5.15	298.24	41.84	14.0%
5.31	418.44	61.6	14.7%
5.47	485.56	211.92	43.6%
5.63	576.32	205.44	35.6%
5.79	444.6	70.08	15.8%
5.95	114.48	37.04	32.4%

Appendix C: NDVI decline in Kanab by .16 km river segments

River segment kilometer	Tamarisk 2009 classification meters squared	Tamarisk NDVI decline meters squared	% tamarisk with NDVI decline
217.1	103.36	14.16	13.7%
217.3	208.48	3.88	1.9%
217.4	215.24	19.8	9.2%
217.6	191.04	49.28	25.8%
217.7	176.04	23.12	13.1%
217.9	165.24	11	6.7%
218.1	259.16	42.72	16.5%
218.2	55.96	5.16	9.2%
218.4	15.44	2.76	17.9%
218.5	18.56	1	5.4%
218.7	41.44	5.8	14.0%
218.9	71.04	5.28	7.4%
219.0	152.72	8.52	5.6%
219.2	58.28	7.44	12.8%
219.4	38.88	4.2	10.8%
219.5	81.36	10.76	13.2%
219.7	184.88	17.12	9.3%
219.8	238.4	13.36	5.6%
220.0	38.92	3.36	8.6%
220.2	291.88	21.4	7.3%
220.3	289.24	39.36	13.6%
220.5	425.64	43.4	10.2%
220.6	460.32	127.84	27.8%
220.8	332.32	47.2	14.2%
221.0	412.96	73.32	17.8%
221.1	540.36	125.28	23.2%
221.3	408.44	117.24	28.7%
221.4	372.16	65.8	17.7%
221.6	1075.24	106.2	9.9%
221.8	933.4	378.32	40.5%
221.9	312.12	37.32	12.0%
222.1	228.48	27.64	12.1%
222.3	311.72	48.44	15.5%

222.4	359.44	29.24	8.1%
222.6	448.76	61.4	13.7%
222.7	209.36	34.68	16.6%
222.9	234.04	41.96	17.9%
223.1	85.44	13	15.2%
223.2	121.6	11.32	9.3%
223.4	337.76	44.76	13.3%
223.5	414.32	56.72	13.7%
223.7	645	59.24	9.2%
223.9	383.84	66.52	17.3%
224.0	102.52	8.68	8.5%
224.2	463.68	61.6	13.3%
224.3	648.08	50.64	7.8%
224.5	248	31.2	12.6%
224.7	1446.84	135.52	9.4%
224.8	316.8	63.04	19.9%
225.0	109.04	20.08	18.4%
225.1	132.28	14.96	11.3%
225.3	675	151.76	22.5%
225.5	194.6	21.48	11.0%
225.6	153.6	16	10.4%
225.8	627.24	66.64	10.6%
226.0	586.52	55.12	9.4%
226.1	680.12	271.2	39.9%
226.3	253.84	68.04	26.8%
226.4	233.08	53.76	23.1%
226.6	304.76	75.48	24.8%
226.8	623.04	124	19.9%
226.9	723.64	91.96	12.7%
227.1	542.56	123.08	22.7%
227.2	593.24	129.4	21.8%
227.4	910.12	315.24	34.6%
227.6	927.92	350	37.7%
227.7	618.28	181.88	29.4%
227.9	765.6	274.48	35.9%
228.0	909.76	262.24	28.8%
228.2	230.24	16.8	7.3%
228.4	186.2	24	12.9%
228.5	314.16	42.6	13.6%
228.7	396.72	52.04	13.1%
228.8	365.16	29.2	8.0%

229.0	476	39.92	8.4%
229.2	309.88	40.08	12.9%
229.3	171.96	14.08	8.2%
229.5	218.68	20.8	9.5%
229.7	824.76	106	12.9%
229.8	465.68	45.8	9.8%
230.0	191.2	19.08	10.0%
230.1	547.64	39.76	7.3%
230.3	410.36	29.4	7.2%
230.5	263.08	73.36	27.9%
230.6	198.48	25.72	13.0%
230.8	314.28	111.96	35.6%
230.9	273.52	55.08	20.1%
231.1	680.04	211.48	31.1%
231.3	715.12	152.76	21.4%
231.4	485.56	131.28	27.0%
231.6	625.08	229.44	36.7%
231.7	1339.32	815	60.9%
231.9	118.92	68.32	57.5%
232.1	366.28	180.28	49.2%
232.2	155.72	47.16	30.3%
232.4	94.8	21.12	22.3%
232.6	123.28	20.4	16.5%
232.7	173.68	25.72	14.8%
232.9	237.16	31.08	13.1%
233.0	194.48	70.16	36.1%
233.2	231.6	43.84	18.9%
233.4	219.24	35.6	16.2%
233.5	275.52	65.8	23.9%
233.7	76	10.84	14.3%
233.8	353.28	53.08	15.0%
234.0	295.16	43.28	14.7%
234.2	110.16	25.08	22.8%
234.3	171.52	22.84	13.3%
234.5	93.92	13.48	14.4%
234.6	122.28	17.84	14.6%
234.8	134.84	15.08	11.2%
235.0	230.2	47.64	20.7%
235.1	307.08	100.36	32.7%
235.3	147.52	42.28	28.7%
235.4	147.84	43.16	29.2%

235.6	163.92	60.2	36.7%
235.8	262.64	68.32	26.0%
235.9	78.92	19.64	24.9%
236.1	83.32	19.16	23.0%
236.3	29.96	13.68	45.7%
236.4	129.16	42.6	33.0%
236.6	29.88	11.68	39.1%
236.7	50.88	13.36	26.3%
236.9	91.6	34.36	37.5%
237.1	66.44	19.04	28.7%
237.2	64.72	20.68	32.0%
237.4	60.16	12.32	20.5%
237.5	3.36	1.76	52.4%
237.7	141.56	31.68	22.4%
237.9	36.92	3.4	9.2%
238.0	17.72	7.36	41.5%
238.2	176.36	60.88	34.5%
238.3	228.92	54.84	24.0%
238.5	159.16	31.76	20.0%
238.7	249.24	75.6	30.3%
238.8	70.84	11.84	16.7%
239.0	88.12	8.56	9.7%
239.1	120.28	17.84	14.8%
239.3	69.72	21.08	30.2%
239.5	175.8	48.08	27.3%
239.6	552.96	103.64	18.7%
239.8	161.2	37.48	23.3%
240.0	170.24	27.96	16.4%
240.1	121.16	18	14.9%
240.3	0.6	0.08	13.3%
240.4	50.52	11	21.8%
240.6	231.12	42.24	18.3%
240.8	270.6	39.12	14.5%
240.9	201.76	25.48	12.6%
241.1	247.84	63.48	25.6%
241.2	119.76	38.4	32.1%
241.4	53.36	29.68	55.6%
241.6	46	22.8	49.6%
241.7	85.96	33.12	38.5%
241.9	159.04	65.4	41.1%
242.0	112.16	46.08	41.1%

242.2	71.08	27.64	38.9%
242.4	53.48	15.48	28.9%
242.5	106.12	50	47.1%
242.7	35.6	14.44	40.6%
242.9	15.32	6.4	41.8%
243.0	29.52	13.08	44.3%
243.2	49.08	30.32	61.8%
243.3	38.32	26.4	68.9%
243.5	67.48	30.32	44.9%
243.7	96.68	34.92	36.1%
243.8	151.52	56.16	37.1%
244.0	165.52	32	19.3%
244.1	162.2	16.96	10.5%
244.3	27.28	0.76	2.8%
244.5	15.88	5.12	32.2%
244.6	20.32	5.16	25.4%
244.8	233.44	9.76	4.2%
244.9	143.12	30.8	21.5%
245.1	84.56	13.52	16.0%
245.3	10	1.28	12.8%
245.4	4.64	0.48	10.3%
245.6	15.72	2.84	18.1%
245.7	76.72	5.2	6.8%
245.9	91.56	6.16	6.7%
246.1	293.84	84.72	28.8%
246.2	140.84	28.64	20.3%
246.4	95.2	14.84	15.6%
246.6	101.24	15.2	15.0%
246.7	147.36	32.52	22.1%
246.9	118.52	33.56	28.3%
247.0	32.88	9.52	29.0%
247.2	190	53.44	28.1%
247.4	249.12	75.76	30.4%
247.5	169.68	32.64	19.2%
247.7	106.88	15.64	14.6%
247.8	69	21	30.4%
248.0	109.36	21.6	19.8%
248.2	46.32	8.68	18.7%
248.3	143.92	27.32	19.0%
248.5	170.84	16.28	9.5%
248.6	186	36.6	19.7%

248.8	149.36	31.84	21.3%
249.0	165.04	39.32	23.8%
249.1	350.16	54.4	15.5%
249.3	236.92	36.52	15.4%
249.4	39.68	21.56	54.3%
249.6	60.68	13.4	22.1%
249.8	124.92	21.96	17.6%
249.9	58.44	13.52	23.1%
250.1	11.84	1.96	16.6%
250.3	20.88	4.36	20.9%
250.4	31	0.72	2.3%
250.6	134.04	20.04	15.0%

Appendix D: EVI decline in Kanab by .16 km river segments

River segment kilometer	Tamarisk 2009 classification meters squared	Tamarisk EVI decline meters squared	% tamarisk with EVI decline
217.1	103.36	3.52	3.4%
217.3	208.48	0.72	0.3%
217.4	215.24	3.84	1.8%
217.6	191.04	21.44	11.2%
217.7	176.04	4.12	2.3%
217.9	165.24	2.72	1.6%
218.1	259.16	3.52	1.4%
218.2	55.96	1.24	2.2%
218.4	15.44	1.28	8.3%
218.5	18.56	3.8	20.5%
218.7	41.44	2.84	6.9%
218.9	71.04	8.2	11.5%
219.0	152.72	3.72	2.4%
219.2	58.28	10.24	17.6%
219.4	38.88	6.48	16.7%
219.5	81.36	6.52	8.0%
219.7	184.88	2.16	1.2%
219.8	238.4	1.76	0.7%
220.0	38.92	0.24	0.6%
220.2	291.88	8.8	3.0%
220.3	289.24	11.04	3.8%
220.5	425.64	7.56	1.8%
220.6	460.32	86.44	18.8%
220.8	332.32	27.44	8.3%
221.0	412.96	83.32	20.2%
221.1	540.36	153.12	28.3%
221.3	408.44	133.84	32.8%
221.4	372.16	61.8	16.6%
221.6	1075.24	107.44	10.0%
221.8	933.4	417.08	44.7%
221.9	312.12	6.36	2.0%
222.1	228.48	7.32	3.2%
222.3	311.72	33.04	10.6%
222.4	359.44	16.08	4.5%
222.6	448.76	8.92	2.0%

222.7	209.36	7.84	3.7%
222.9	234.04	6.08	2.6%
223.1	85.44	3.32	3.9%
223.2	121.6	6	4.9%
223.4	337.76	20.84	6.2%
223.5	414.32	15.2	3.7%
223.7	645	8.92	1.4%
223.9	383.84	19.44	5.1%
224.0	102.52	1.04	1.0%
224.2	463.68	20.96	4.5%
224.3	648.08	10.64	1.6%
224.5	248	8.12	3.3%
224.7	1446.84	100.56	7.0%
224.8	316.8	14.64	4.6%
225.0	109.04	6.16	5.6%
225.1	132.28	1.28	1.0%
225.3	675	40.36	6.0%
225.5	194.6	3.4	1.7%
225.6	153.6	2.68	1.7%
225.8	627.24	7.48	1.2%
226.0	586.52	6.24	1.1%
226.1	680.12	47.72	7.0%
226.3	253.84	16.64	6.6%
226.4	233.08	8.76	3.8%
226.6	304.76	8.8	2.9%
226.8	623.04	28.6	4.6%
226.9	723.64	22.8	3.2%
227.1	542.56	14.24	2.6%
227.2	593.24	14.96	2.5%
227.4	910.12	41.36	4.5%
227.6	927.92	71.28	7.7%
227.7	618.28	24.36	3.9%
227.9	765.6	57.04	7.5%
228.0	909.76	39	4.3%
228.2	230.24	0.28	0.1%
228.4	186.2	2.8	1.5%
228.5	314.16	2.28	0.7%
228.7	396.72	3.72	0.9%
228.8	365.16	3.24	0.9%
229.0	476	4.12	0.9%
229.2	309.88	7.68	2.5%

229.3	171.96	1.52	0.9%
229.5	218.68	0.8	0.4%
229.7	824.76	11.76	1.4%
229.8	465.68	2.64	0.6%
230.0	191.2	1.96	1.0%
230.1	547.64	7.08	1.3%
230.3	410.36	5.68	1.4%
230.5	263.08	37.2	14.1%
230.6	198.48	2.28	1.1%
230.8	314.28	31.12	9.9%
230.9	273.52	9.08	3.3%
231.1	680.04	70.52	10.4%
231.3	715.12	22.52	3.1%
231.4	485.56	13.24	2.7%
231.6	625.08	67	10.7%
231.7	1339.32	313.24	23.4%
231.9	118.92	18.08	15.2%
232.1	366.28	66.04	18.0%
232.2	155.72	21.36	13.7%
232.4	94.8	2.92	3.1%
232.6	123.28	1.64	1.3%
232.7	173.68	3.44	2.0%
232.9	237.16	4.52	1.9%
233.0	194.48	31.32	16.1%
233.2	231.6	5.2	2.2%
233.4	219.24	6.64	3.0%
233.5	275.52	13	4.7%
233.7	76	1.36	1.8%
233.8	353.28	13.28	3.8%
234.0	295.16	5.76	2.0%
234.2	110.16	5.56	5.0%
234.3	171.52	6.68	3.9%
234.5	93.92	5.2	5.5%
234.6	122.28	3.12	2.6%
234.8	134.84	2.92	2.2%
235.0	230.2	7.12	3.1%
235.1	307.08	18.96	6.2%
235.3	147.52	7.64	5.2%
235.4	147.84	11.32	7.7%
235.6	163.92	10.88	6.6%
235.8	262.64	15.32	5.8%

235.9	78.92	3.28	4.2%
236.1	83.32	2.2	2.6%
236.3	29.96	5.84	19.5%
236.4	129.16	14.88	11.5%
236.6	29.88	4.2	14.1%
236.7	50.88	1.96	3.9%
236.9	91.6	6.72	7.3%
237.1	66.44	2.68	4.0%
237.2	64.72	1.52	2.3%
237.4	60.16	1.4	2.3%
237.5	3.36	0.12	3.6%
237.7	141.56	6.04	4.3%
237.9	36.92	0.04	0.1%
238.0	17.72	0.4	2.3%
238.2	176.36	6.04	3.4%
238.3	228.92	6.04	2.6%
238.5	159.16	1.76	1.1%
238.7	249.24	10.68	4.3%
238.8	70.84	0.32	0.5%
239.0	88.12	0.76	0.9%
239.1	120.28	3.08	2.6%
239.3	69.72	0.88	1.3%
239.5	175.8	6.28	3.6%
239.6	552.96	17.84	3.2%
239.8	161.2	13.12	8.1%
240.0	170.24	17.76	10.4%
240.1	121.16	4	3.3%
240.3	0.6	0	0.0%
240.4	50.52	1.96	3.9%
240.6	231.12	15.52	6.7%
240.8	270.6	13.64	5.0%
240.9	201.76	12.24	6.1%
241.1	247.84	48.6	19.6%
241.2	119.76	51.68	43.2%
241.4	53.36	22.2	41.6%
241.6	46	17.8	38.7%
241.7	85.96	17.24	20.1%
241.9	159.04	25.64	16.1%
242.0	112.16	16.4	14.6%
242.2	71.08	9.84	13.8%
242.4	53.48	6.64	12.4%

242.5	106.12	12.92	12.2%
242.7	35.6	3.44	9.7%
242.9	15.32	2.68	17.5%
243.0	29.52	16.04	54.3%
243.2	49.08	47.48	96.7%
243.3	38.32	20.32	53.0%
243.5	67.48	9.64	14.3%
243.7	96.68	6.32	6.5%
243.8	151.52	17.16	11.3%
244.0	165.52	7.44	4.5%
244.1	162.2	2.48	1.5%
244.3	27.28	0.16	0.6%
244.5	15.88	1.32	8.3%
244.6	20.32	0.64	3.1%
244.8	233.44	2.72	1.2%
244.9	143.12	5.2	3.6%
245.1	84.56	1.16	1.4%
245.3	10	0.88	8.8%
245.4	4.64	0.08	1.7%
245.6	15.72	0.68	4.3%
245.7	76.72	0.92	1.2%
245.9	91.56	3.84	4.2%
246.1	293.84	48.12	16.4%
246.2	140.84	10.64	7.6%
246.4	95.2	5.12	5.4%
246.6	101.24	6.96	6.9%
246.7	147.36	14.12	9.6%
246.9	118.52	17.92	15.1%
247.0	32.88	11	33.5%
247.2	190	33.32	17.5%
247.4	249.12	58.16	23.3%
247.5	169.68	21.2	12.5%
247.7	106.88	8.2	7.7%
247.8	69	14.84	21.5%
248.0	109.36	10.68	9.8%
248.2	46.32	3.6	7.8%
248.3	143.92	15.52	10.8%
248.5	170.84	7.16	4.2%
248.6	186	17.84	9.6%
248.8	149.36	33.88	22.7%
249.0	165.04	22.52	13.6%

249.1	350.16	24.32	6.9%
249.3	236.92	27.6	11.6%
249.4	39.68	10.44	26.3%
249.6	60.68	5.76	9.5%
249.8	124.92	8.96	7.2%
249.9	58.44	5.6	9.6%
250.1	11.84	0.04	0.3%
250.3	20.88	1.64	7.9%
250.4	31	0.32	1.0%
250.6	134.04	5.64	4.2%

Appendix E: NDVI decline in National by .16 km river segments

River segment kilometer	Tamarisk 2009 classification meters squared	Tamarisk NDVI decline meters squared	% tamarisk with NDVI decline
254.9	21.72	2.2	10.1%
255.1	168.36	26.6	15.8%
255.2	133.12	12.16	9.1%
255.4	182.08	32.8	18.0%
255.6	89.12	26.32	29.5%
255.7	237.96	63.76	26.8%
255.9	277.12	65.68	23.7%
256.0	288.68	48.4	16.8%
256.2	162.28	31.88	19.6%
256.4	135.76	39.76	29.3%
256.5	130.88	46.24	35.3%
256.7	52.96	22.64	42.7%
256.9	44.12	12.56	28.5%
257.0	125.28	25.48	20.3%
257.2	101.56	33.16	32.7%
257.3	201.24	45.52	22.6%
257.5	265.32	70.52	26.6%
257.7	333.08	58.28	17.5%
257.8	201.64	27.32	13.5%
258.0	332.76	57.36	17.2%
258.1	344.6	59.12	17.2%
258.3	278.36	61.4	22.1%
258.5	606.56	122.8	20.2%
258.6	386.64	115.2	29.8%
258.8	298.92	78.72	26.3%
258.9	547.6	129.56	23.7%
259.1	491.16	87.88	17.9%
259.3	674.2	155.04	23.0%
259.4	432.24	139.12	32.2%
259.6	380.32	143.76	37.8%
259.7	121.64	38.08	31.3%
259.9	314.24	93.4	29.7%
260.1	277.44	98.36	35.5%
260.2	395.56	159.12	40.2%
260.4	930.52	299.32	32.2%
260.6	768	179.4	23.4%

260.7	618.92	159.16	25.7%
260.9	661.08	102.52	15.5%
261.0	451.72	148.92	33.0%
261.2	613.32	141.56	23.1%
261.4	545	105.28	19.3%
261.5	459.28	122.96	26.8%
261.7	462.8	99.52	21.5%
261.8	475.12	109.4	23.0%
262.0	353.72	100.4	28.4%
262.2	573.32	125.8	21.9%
262.3	609	96.4	15.8%
262.5	650.64	126.72	19.5%
262.6	697.52	145	20.8%
262.8	572.76	88.96	15.5%
263.0	409.52	56.76	13.9%
263.1	632.4	86.16	13.6%
263.3	1528.52	237.32	15.5%
263.4	787.8	179.68	22.8%
263.6	924.64	234.8	25.4%
263.8	809.12	141.64	17.5%
263.9	935.52	146.96	15.7%
264.1	1118.72	106.4	9.5%
264.3	1129.12	102.76	9.1%
264.4	908.44	113.4	12.5%
264.6	522.68	85.52	16.4%
264.7	57.76	18.52	32.1%
264.9	46.04	4.72	10.3%
265.1	300.72	38	12.6%
265.2	597.28	78.8	13.2%
265.4	101.52	33.4	32.9%
265.5	113.96	17.4	15.3%
265.7	151.04	20.36	13.5%
265.9	129.64	21.8	16.8%
266.0	435.76	134.64	30.9%
266.2	658.36	76.84	11.7%
266.3	1180.04	193.64	16.4%
266.5	1807.44	553.68	30.6%
266.7	1488.8	95.04	6.4%
266.8	1104.16	134.04	12.1%
267.0	1552.96	94.48	6.1%
267.2	1735.88	132.48	7.6%

267.3	1662.08	343.12	20.6%
267.5	1164.76	156.44	13.4%
267.6	1404.8	288.72	20.6%
267.8	1296.8	98.44	7.6%
268.0	1193.48	116.24	9.7%
268.1	1314.16	120.92	9.2%
268.3	1486.6	274.72	18.5%
268.4	1456.6	159.48	10.9%
268.6	1038.4	267.64	25.8%
268.8	1304.16	1064.76	81.6%
268.9	1342.12	1067.24	79.5%
269.1	412.28	115.28	28.0%
269.2	426.8	96.12	22.5%
269.4	908.76	162.56	17.9%
269.6	1150.64	244.48	21.2%
269.7	1137.32	92.88	8.2%
269.9	1967.64	287.84	14.6%
270.0	1047.4	236.32	22.6%
270.2	1003.12	97.92	9.8%
270.4	1066.24	92.48	8.7%
270.5	1538.48	87.04	5.7%
270.7	1520.76	93.72	6.2%
270.9	1621.52	177.96	11.0%
271.0	2142.2	112.88	5.3%
271.2	1238.72	354.72	28.6%
271.3	338.72	79.32	23.4%
271.5	34.6	3.84	11.1%
271.7	750.2	99.48	13.3%
271.8	1231.84	101.32	8.2%
272.0	539.12	58	10.8%
272.1	713.36	70.16	9.8%
272.3	1328.48	69.48	5.2%
272.5	824	36.24	4.4%
272.6	1100.88	48.4	4.4%
272.8	788.52	53.08	6.7%
272.9	1559	111.36	7.1%
273.1	1528.8	275.04	18.0%
273.3	1401.56	119.24	8.5%
273.4	1349.72	69.56	5.2%
273.6	1392.96	95.64	6.9%
273.7	798.88	54.92	6.9%

273.9	657.4	58.96	9.0%
274.1	695.48	58.68	8.4%
274.2	431.84	32.4	7.5%
274.4	480.84	33.76	7.0%
274.6	431.52	20.72	4.8%
274.7	290.28	18.48	6.4%
274.9	636.24	63.12	9.9%
275.0	895.96	40.28	4.5%
275.2	2035.24	88.8	4.4%
275.4	1795.4	72.6	4.0%
275.5	1534.76	118.56	7.7%
275.7	2630.36	318.08	12.1%
275.8	1859.36	149.28	8.0%
276.0	1742.44	60.28	3.5%
276.2	2165.4	205.88	9.5%
276.3	589.56	45.2	7.7%
276.5	1973.68	222.84	11.3%
276.6	1696.28	426.52	25.1%
276.8	895.4	180.24	20.1%
277.0	793.44	67.4	8.5%
277.1	686.28	37.68	5.5%
277.3	530.12	55.08	10.4%
277.5	608.68	40.28	6.6%
277.6	1002.12	57.64	5.8%
277.8	1841.16	176.52	9.6%
277.9	2817.64	176.2	6.3%
278.1	1210.28	78.32	6.5%
278.3	1142.16	66.04	5.8%
278.4	1855.76	153.92	8.3%
278.6	1536.16	152.56	9.9%
278.7	1374.92	103.12	7.5%
278.9	1755.92	149.4	8.5%
279.1	1428.32	159.88	11.2%
279.2	1262.76	68.6	5.4%
279.4	1851.92	120.32	6.5%
279.5	1854.24	184.2	9.9%
279.7	607.36	40.88	6.7%
279.9	815.48	63.92	7.8%
280.0	1769.24	120.72	6.8%
280.2	2094.84	145.16	6.9%
280.3	1689.4	147.84	8.8%

280.5	2080.68	218.6	10.5%
280.7	2666.24	217.6	8.2%
280.8	2076.72	125.48	6.0%
281.0	795.28	61.2	7.7%
281.2	1066.24	109.72	10.3%
281.3	461.4	111.68	24.2%
281.5	924.12	115.84	12.5%
281.6	285.76	12.48	4.4%
281.8	929.04	51.96	5.6%
282.0	658.56	17.24	2.6%
282.1	1306.96	37.84	2.9%
282.3	857.12	47.44	5.5%
282.4	238.92	15.44	6.5%
282.6	303.4	23.32	7.7%
282.8	105.68	8	7.6%
282.9	704.16	27.76	3.9%
283.1	269.76	16.56	6.1%
283.2	1248.24	57.92	4.6%
283.4	1257.8	59.48	4.7%
283.6	787.36	48.72	6.2%
283.7	744.92	97.2	13.0%
283.9	1018.36	69.64	6.8%
284.0	1214.56	97.2	8.0%
284.2	618.96	66.68	10.8%
284.4	324.8	17.12	5.3%
284.5	1137.64	93.92	8.3%
284.7	1996.72	346.72	17.4%
284.9	2630.76	457.12	17.4%
285.0	2116.6	173.88	8.2%
285.2	928.28	123.36	13.3%
285.3	1007.04	64	6.4%
285.5	1175.52	56.24	4.8%
285.7	3855.68	301.08	7.8%
285.8	2774.96	150.16	5.4%
286.0	566.32	43.48	7.7%
286.1	1323.8	80.68	6.1%
286.3	1479.76	71.96	4.9%
286.5	2599.32	252.84	9.7%
286.6	2371	626.96	26.4%
286.8	1912.36	146.24	7.6%
286.9	1690.08	112.24	6.6%

287.1	1666.36	81.48	4.9%
287.3	1966.88	65.72	3.3%
287.4	2265.16	125.36	5.5%
287.6	2446.56	136.16	5.6%
287.8	2080.36	106.56	5.1%
287.9	2427.6	124.04	5.1%
288.1	1886.24	107.24	5.7%
288.2	3458.68	221.04	6.4%
288.4	3314.24	109.6	3.3%
288.6	2637.04	289	11.0%
288.7	2228.12	167.16	7.5%
288.9	1192.08	125.24	10.5%
289.0	1318.08	87.52	6.6%
289.2	1925.8	472.88	24.6%
289.4	3698.28	657.28	17.8%
289.5	4907.92	556.6	11.3%
289.7	3972.8	434.12	10.9%
289.8	1075.84	62.2	5.8%
290.0	3561	168.2	4.7%
290.2	2683.52	115.12	4.3%
290.3	1563.76	202.4	12.9%
290.5	90.84	9.4	10.3%

Appendix F: EVI decline in National by .16 km river segments

River segment kilometer	Tamarisk 2009 classification meters squared	Tamarisk EVI decline meters squared	% tamarisk with EVI decline
254.9	21.72	0.48	2.2%
255.1	168.36	4.32	2.6%
255.2	133.12	13.96	10.5%
255.4	182.08	11.48	6.3%
255.6	89.12	11.52	12.9%
255.7	237.96	22.76	9.6%
255.9	277.12	14.92	5.4%
256.0	288.68	13.88	4.8%
256.2	162.28	10.88	6.7%
256.4	135.76	13.24	9.8%
256.5	130.88	17.84	13.6%
256.7	52.96	12.76	24.1%
256.9	44.12	6.88	15.6%
257.0	125.28	17.68	14.1%
257.2	101.56	34.12	33.6%
257.3	201.24	58.08	28.9%
257.5	265.32	93.84	35.4%
257.7	333.08	28.72	8.6%
257.8	201.64	14.36	7.1%
258.0	332.76	32.72	9.8%
258.1	344.6	38.32	11.1%
258.3	278.36	31.92	11.5%
258.5	606.56	45.88	7.6%
258.6	386.64	55.68	14.4%
258.8	298.92	28.52	9.5%
258.9	547.6	69.16	12.6%
259.1	491.16	67.6	13.8%
259.3	674.2	75.88	11.3%
259.4	432.24	65.2	15.1%
259.6	380.32	37.92	10.0%
259.7	121.64	8.36	6.9%
259.9	314.24	22.8	7.3%
260.1	277.44	37.4	13.5%
260.2	395.56	55.52	14.0%
260.4	930.52	108.52	11.7%
260.6	768	60.4	7.9%

260.7	618.92	53.24	8.6%
260.9	661.08	26	3.9%
261.0	451.72	26.36	5.8%
261.2	613.32	17.6	2.9%
261.4	545	22.76	4.2%
261.5	459.28	53.6	11.7%
261.7	462.8	32.16	6.9%
261.8	475.12	13.6	2.9%
262.0	353.72	35	9.9%
262.2	573.32	43.44	7.6%
262.3	609	27.2	4.5%
262.5	650.64	51.76	8.0%
262.6	697.52	85.6	12.3%
262.8	572.76	21.92	3.8%
263.0	409.52	17.24	4.2%
263.1	632.4	19.08	3.0%
263.3	1528.52	58.68	3.8%
263.4	787.8	46.2	5.9%
263.6	924.64	62.92	6.8%
263.8	809.12	47.52	5.9%
263.9	935.52	67.44	7.2%
264.1	1118.72	46.88	4.2%
264.3	1129.12	70.96	6.3%
264.4	908.44	56.12	6.2%
264.6	522.68	38.76	7.4%
264.7	57.76	6.44	11.1%
264.9	46.04	6.32	13.7%
265.1	300.72	20.36	6.8%
265.2	597.28	38.48	6.4%
265.4	101.52	18.08	17.8%
265.5	113.96	4.24	3.7%
265.7	151.04	6.92	4.6%
265.9	129.64	2.28	1.8%
266.0	435.76	26.76	6.1%
266.2	658.36	9.32	1.4%
266.3	1180.04	29.88	2.5%
266.5	1807.44	71.16	3.9%
266.7	1488.8	13.96	0.9%
266.8	1104.16	13.8	1.2%
267.0	1552.96	76.04	4.9%
267.2	1735.88	71.96	4.1%

267.3	1662.08	192.72	11.6%
267.5	1164.76	122.76	10.5%
267.6	1404.8	152.64	10.9%
267.8	1296.8	78.32	6.0%
268.0	1193.48	95.52	8.0%
268.1	1314.16	79	6.0%
268.3	1486.6	102.2	6.9%
268.4	1456.6	60.56	4.2%
268.6	1038.4	81.2	7.8%
268.8	1304.16	102.88	7.9%
268.9	1342.12	159.96	11.9%
269.1	412.28	35.84	8.7%
269.2	426.8	29.6	6.9%
269.4	908.76	67.6	7.4%
269.6	1150.64	127.8	11.1%
269.7	1137.32	22.32	2.0%
269.9	1967.64	98.8	5.0%
270.0	1047.4	225.04	21.5%
270.2	1003.12	16.16	1.6%
270.4	1066.24	26.24	2.5%
270.5	1538.48	40.52	2.6%
270.7	1520.76	79.16	5.2%
270.9	1621.52	184.32	11.4%
271.0	2142.2	116.08	5.4%
271.2	1238.72	203.36	16.4%
271.3	338.72	18.6	5.5%
271.5	34.6	1.04	3.0%
271.7	750.2	96.2	12.8%
271.8	1231.84	259	21.0%
272.0	539.12	94.72	17.6%
272.1	713.36	218.92	30.7%
272.3	1328.48	71.2	5.4%
272.5	824	23.8	2.9%
272.6	1100.88	28.48	2.6%
272.8	788.52	26.96	3.4%
272.9	1559	120.92	7.8%
273.1	1528.8	263.4	17.2%
273.3	1401.56	125.68	9.0%
273.4	1349.72	36.6	2.7%
273.6	1392.96	76.8	5.5%
273.7	798.88	29.68	3.7%

273.9	657.4	36.24	5.5%
274.1	695.48	35.16	5.1%
274.2	431.84	16.64	3.9%
274.4	480.84	45.52	9.5%
274.6	431.52	38.84	9.0%
274.7	290.28	11.92	4.1%
274.9	636.24	22.76	3.6%
275.0	895.96	31.64	3.5%
275.2	2035.24	94.64	4.7%
275.4	1795.4	58.16	3.2%
275.5	1534.76	105.44	6.9%
275.7	2630.36	388.76	14.8%
275.8	1859.36	175.36	9.4%
276.0	1742.44	72.72	4.2%
276.2	2165.4	171.72	7.9%
276.3	589.56	33.52	5.7%
276.5	1973.68	234.76	11.9%
276.6	1696.28	245.76	14.5%
276.8	895.4	144.16	16.1%
277.0	793.44	45.28	5.7%
277.1	686.28	26.32	3.8%
277.3	530.12	19.56	3.7%
277.5	608.68	14.92	2.5%
277.6	1002.12	34	3.4%
277.8	1841.16	121.36	6.6%
277.9	2817.64	168.92	6.0%
278.1	1210.28	57.28	4.7%
278.3	1142.16	34.88	3.1%
278.4	1855.76	113.2	6.1%
278.6	1536.16	173.68	11.3%
278.7	1374.92	127.84	9.3%
278.9	1755.92	161.12	9.2%
279.1	1428.32	218.12	15.3%
279.2	1262.76	85.88	6.8%
279.4	1851.92	121.44	6.6%
279.5	1854.24	133.6	7.2%
279.7	607.36	17.24	2.8%
279.9	815.48	47.96	5.9%
280.0	1769.24	81.88	4.6%
280.2	2094.84	143.88	6.9%
280.3	1689.4	183.4	10.9%

280.5	2080.68	251.4	12.1%
280.7	2666.24	337.76	12.7%
280.8	2076.72	209.84	10.1%
281.0	795.28	68.24	8.6%
281.2	1066.24	121.8	11.4%
281.3	461.4	96.88	21.0%
281.5	924.12	106.6	11.5%
281.6	285.76	8.92	3.1%
281.8	929.04	38.56	4.2%
282.0	658.56	21.92	3.3%
282.1	1306.96	59.6	4.6%
282.3	857.12	63.12	7.4%
282.4	238.92	13.48	5.6%
282.6	303.4	29.2	9.6%
282.8	105.68	7.64	7.2%
282.9	704.16	47.2	6.7%
283.1	269.76	13.4	5.0%
283.2	1248.24	77.92	6.2%
283.4	1257.8	107.16	8.5%
283.6	787.36	53.48	6.8%
283.7	744.92	87.48	11.7%
283.9	1018.36	41.68	4.1%
284.0	1214.56	131.6	10.8%
284.2	618.96	74.12	12.0%
284.4	324.8	14.52	4.5%
284.5	1137.64	74.04	6.5%
284.7	1996.72	262.04	13.1%
284.9	2630.76	350.24	13.3%
285.0	2116.6	140.28	6.6%
285.2	928.28	84.2	9.1%
285.3	1007.04	47.04	4.7%
285.5	1175.52	38.64	3.3%
285.7	3855.68	350.88	9.1%
285.8	2774.96	148.2	5.3%
286.0	566.32	33.6	5.9%
286.1	1323.8	75.56	5.7%
286.3	1479.76	103.88	7.0%
286.5	2599.32	314.92	12.1%
286.6	2371	806.08	34.0%
286.8	1912.36	195.08	10.2%
286.9	1690.08	109.64	6.5%

287.1	1666.36	111.56	6.7%
287.3	1966.88	86.44	4.4%
287.4	2265.16	95.96	4.2%
287.6	2446.56	171.6	7.0%
287.8	2080.36	72.28	3.5%
287.9	2427.6	176.4	7.3%
288.1	1886.24	123.64	6.6%
288.2	3458.68	286.96	8.3%
288.4	3314.24	129	3.9%
288.6	2637.04	380.2	14.4%
288.7	2228.12	201.24	9.0%
288.9	1192.08	150.56	12.6%
289.0	1318.08	96.48	7.3%
289.2	1925.8	468.72	24.3%
289.4	3698.28	680.52	18.4%
289.5	4907.92	330.84	6.7%
289.7	3972.8	253.24	6.4%
289.8	1075.84	16.88	1.6%
290.0	3561	68.56	1.9%
290.2	2683.52	25.08	0.9%
290.3	1563.76	147.28	9.4%
290.5	90.84	2.4	2.6%

Appendix G: Band values for NDVI declined pixels

G1: Glen Canyon

Bands	Min	Max	Mean	Stdev
2009 Blue	215.00	519.00	357.01	34.25
2009 Green	236.00	1100.00	689.18	84.96
2009 Red	146.00	1474.00	667.40	108.07
2009 NIR	733.00	3133.00	2236.54	267.70
2009 NDVI	0.26	0.78	0.54	0.06
2009 EVI	0.32	1.18	0.74	0.09
2009 LAI	2.12	9.66	5.82	0.77
2013 Blue	93.00	917.00	324.99	80.03
2013 Green	99.00	2243.00	589.30	210.69
2013 Red	82.00	3022.00	707.06	285.91
2013 NIR	134.00	3666.00	1220.48	461.02
2013 NDVI	0.00	0.50	0.27	0.06
2013 EVI	0.02	0.90	0.30	0.09
2013 LAI	-0.52	7.15	1.93	0.77

G2: Kanab Reach

Bands	Min	Max	Mean	Stdev
2009 Blue	133.00	346.00	225.73	23.59
2009 Green	159.00	782.00	461.98	72.43
2009 Red	105.00	946.00	387.30	77.50
2009 NIR	533.00	2232.00	1346.59	211.96
2009 NDVI	0.20	0.82	0.55	0.07
2009 EVI	0.19	0.84	0.47	0.08
2009 LAI	0.95	6.65	3.43	0.71
2013 Blue	117.00	1082.00	385.33	91.57
2013 Green	131.00	2197.00	752.31	234.94
2013 Red	119.00	2783.00	887.38	312.16
2013 NIR	239.00	2985.00	1541.38	374.56
2013 NDVI	0.00	0.52	0.28	0.07
2013 EVI	0.06	1.24	0.37	0.07
2013 LAI	-0.19	10.20	2.55	0.64

G3: National Reach

Bands	Min	Max	Mean	Stdev
2009 Blue	169.00	378.00	255.10	25.39
2009 Green	200.00	856.00	498.16	67.54
2009 Red	174.00	933.00	453.31	77.88
2009 NIR	470.00	2005.00	1278.26	186.79
2009 NDVI	0.18	0.71	0.47	0.07
2009 EVI	0.15	0.76	0.43	0.08
2009 LAI	0.61	5.93	3.09	0.67
2013 Blue	84.00	1158.00	335.94	122.80
2013 Green	82.00	3141.00	628.54	295.96
2013 Red	73.00	2967.00	744.82	395.56
2013 NIR	98.00	3440.00	1180.85	516.78
2013 NDVI	0.00	0.46	0.24	0.07
2013 EVI	-0.48	19.04	0.27	0.10
2013 LAI	-4.89	165.71	1.66	0.86

Appendix H: Band values for EVI declined pixels

H1: Glen Canyon Reach

Bands	Min	Max	Mean	Stdev
2009 Blue	206.00	597.00	372.13	32.51
2009 Green	105.00	1192.00	688.56	89.98
2009 Red	106.00	1447.00	661.18	106.82
2009 NIR	465.00	3231.00	2178.07	279.64
2009 NDVI	0.23	0.84	0.53	0.06
2009 EVI	0.23	1.59	0.76	0.09
2009 LAI	1.31	13.24	5.99	0.82
2013 Blue	75.00	1582.00	262.00	59.21
2013 Green	47.00	3497.00	463.69	142.79
2013 Red	15.00	3866.00	523.67	201.72
2013 NIR	76.00	3666.00	1133.57	348.29
2013 NDVI	-0.11	0.89	0.37	0.12
2013 EVI	0.00	0.84	0.33	0.10
2013 LAI	-0.68	6.65	2.18	0.91

H2: Kanab Reach

Bands	Min	Max	Mean	Stdev
2009 Blue	124.00	346.00	229.75	23.93
2009 Green	171.00	782.00	480.62	67.83
2009 Red	118.00	819.00	397.63	72.64
2009NIR	536.00	2539.00	1461.99	240.85
2009 NDVI	0.18	0.80	0.57	0.07
2009 EVI	0.16	0.85	0.51	0.09
2009 LAI	0.68	6.78	3.77	0.79
2013 Blue	86.00	1082.00	315.51	129.60
2013 Green	97.00	2197.00	585.35	327.86
2013 Red	64.00	2783.00	702.45	440.70
2013 NIR	78.00	3491.00	1099.14	543.44
2013 NDVI	-0.10	0.75	0.26	0.10
2013 EVI	0.00	0.53	0.24	0.09
2013 LAI	-0.68	3.95	1.44	0.80

H3: National Reach

Bands	Min	Max	Mean	Stdev
2009 Blue	169.00	397.00	253.27	27.38
2009 Green	200.00	865.00	493.00	73.14
2009 Red	148.00	1104.00	444.01	80.80
2009 NIR	448.00	2416.00	1324.33	206.51
2009 NDVI	0.09	0.75	0.50	0.08
2009 EVI	0.13	0.83	0.45	0.08
2009 LAI	0.50	6.59	3.29	0.72
2013 Blue	79.00	1187.00	277.29	105.27
2013 Green	27.00	3141.00	487.69	255.19
2013 Red	32.00	3056.00	567.00	344.97
2013 NIR	75.00	3304.00	934.87	419.47
2013 NDVI	-0.11	0.78	0.28	0.12
2013 EVI	0.00	0.50	0.23	0.08
2013 LAI	-0.68	3.73	1.33	0.67

Appendix I: Simple Regression Variables for Tamarisk NDVI Percent Decline

I1: Simple Regression Variables for Glen Canyon NDVI Tamarisk Decline

Summarized simple regression statistics for independent variables relating to dependent percent NDVI tamarisk decline for Glen Canyon. '*******' where P < 0.001, '******' where P<0.01, '*****' where P<.05,'·' where P<0.1.

Independent variable	Adjusted R^2	Unstandardized Coefficient B	Std. Error (Unstandardized)	Standardized Coefficient Beta	P (Sig)
River Segment	-.005	-.034	.133	-.018	.801
Constant		22.7	1.78		.000
Tamarisk Area	.286	.008	.001	.538	.000***
Constant		11.9	1.61		.000
Viewshed	.012	-29.8	16.2	-.131	.068·
Constant		42.8	10.8		.000
Total Daylight	.008	80	51	.112	.117
Constant		-5.73×10^4	3.64×10^4		.118
Diffuse Daylight	.011	71	40	.127	.076·
Constant		-5.53×10^4	3.10×10^4		.076
Direct Daylight	.001	-.015	.014	-.077	.284
Constant		28.6	5.30		.000
Adult Beetle	.010	-.023	.019	-.192	.247
Constant		26.4	3.59		.000
Early Larvae	-.016	.023	.036	.108	.518
Constant		24.2	3.68		.000
Late Larvae	.060	-.334	.182	-.293	.075·
Constant		27.5	3.59		.000

I2: Simple Regression Variables for Kanab NDVI Tamarisk Decline

Summarized simple regression statistics for independent variables relating to dependent percent NDVI tamarisk decline for Kanab. '*******' where P < 0.001, '******' where P<0.01, '*****' where P<.05,'·' where P<0.1.

Independent variable	Adjusted R^2	Unstandardized Coefficient B	Std. Error (Unstandardized)	Standardized Coefficient Beta	P (Sig)
River Segment	.093	.402	.085	.312	.000***
Constant		-72.6	19.9		.000
Tamarisk Area	-.005	-.001	.004	-.015	.826
Constant		21.7	1.25		.000
Viewshed	.133	-59.7	10.4	-.371	.000***
Constant		55.3	5.93		.000
Total Daylight	.025	66	26.055	.173	.012**
Constant		-4.75×10^4	1.88×10^4		.012
Diffuse Daylight	.126	21	4	.361	.000***
Constant		-1.67×10^4	2999		.000
Direct Daylight	.118	-.048	.009	-.350	.000***
Constant		36	2.80		.000
Adult Beetle	-.013	.003	.040	.008	.942
Constant		23.2	1.69		.000
Early Larvae	-.007	-.035	.051	-.078	.490
Constant		23.9	1.82		.000
Late Larvae	-.011	-.015	.035	-.047	.678
Constant		23.5	1.69		.000

I3: Simple Regression Variables for National NDVI Tamarisk Decline

Summarized simple regression statistics for independent variables relating to dependent percent NDVI tamarisk decline for National. '***' where P < 0.001, '**' where P<0.01, '*' where P<.05,'·' where P<0.1.

Independent variable	Adjusted R^2	Unstandardized Coefficient B	Std. Error (Unstandardized)	Standardized Coefficient Beta	P (Sig)
River Segment	.295	-.573	.059	-.546	.000***
Constant		171.0	16.2		.000
Tamarisk Area	.093	-.004	.001	-.312	.000***
Constant		18.8	1.15		.000
Viewshed	.122	-96.0	17.1	-.354	.000***
Constant		66.8	9.37		.000
Total Daylight	.079	175	39	.288	.000***
Constant		-1.26×10^5	2.81×10^4		.000
Diffuse Daylight	.270	183	20	.523	.000***
Constant		-1.44×10^5	1.58×10^4		.000
Direct Daylight	.030	-.037	.013	-.184	.006**
Constant		24.8	3.84		.000
Adult Beetle	-.011	.007	.037	.021	.846
Constant		15.5	1.54		.000
Early Larvae	-.008	.031	.054	.062	.571
Constant		15.3	1.52		.000
Late Larvae	-.002	-.041	.046	-.097	.376
Constant		16.1	1.49		.000

Appendix J: Simple Regression Variables for Tamarisk EVI Percent Decline

J1: Simple Regression Variables for Glen Canyon EVI Tamarisk Decline

Summarized simple regression statistics for independent variables relating to dependent percent EVI tamarisk decline for Glen Canyon. '*******' where P < 0.001, '******' where P<0.01, '*****' where P<.05,'·' where P<0.1.

Independent variable	Adjusted R^2	Unstandardized Coefficient B	Std. Error (Unstandardized)	Standardized Coefficient Beta	P (Sig)
River Segment	.229	-1.233	.161	-.482	.000***
Constant		41.5	2.14		.000
Tamarisk Area	.357	.012	.001	.600	.000***
Constant		36.5	2.11		.000
Viewshed	.182	-135	20	-.432	.000***
Constant		144	14		.000
Total Daylight	.072	-270	67	-.277	.000***
Constant		1.94×10^5	4.85×10^4		.000
Diffuse Daylight	.265	396	47	.518	.000***
Constant		-3.10×10^5	3.68×10^4		.000
Direct Daylight	.092	-.083	.018	-.311	.000***
Constant		84	7		.000
Adult Beetle	.059	-.046	.025	-.291	.077·
Constant		52.5	4.8		.000
Early Larvae	-.019	.027	.049	.092	.584
Constant		48.8	5.0		.000
Late Larvae	.135	-.618	.238	-.398	.013*
Constant		54.4	4.7		.000

J2: Simple Regression Variables for Kanab EVI Tamarisk Decline

Summarized simple regression statistics for independent variables relating to dependent percent EVI tamarisk decline for Kanab. '***' where P < 0.001, '**' where P<0.01, '*' where P<.05,'·' where P<0.1.

Independent variable	Adjusted R^2	Unstandardized Coefficient B	Std. Error (Unstandardized)	Standardized Coefficient Beta	P (Sig)
River Segment	.034	.222	.078	.196	.005**
Constant		-43.8	18.1		.017
Tamarisk Area	-.002	-.003	.003	-.057	.411
Constant		8.91	1.10		.000
Viewshed	.009	-17	10	-.119	.086·
Constant		18	6		.002
Total Daylight	.017	-50	23	-.148	.032*
Constant		3.58×10^4	1.66×10^4		.032
Diffuse Daylight	.041	11	4	.214	.002**
Constant		-8737	2768		.002
Direct Daylight	.015	-.017	.008	-.139	.045**
Constant		13.3	2.6		.000
Adult Beetle	-.011	-.009	.026	-.041	.717
Constant		9.29	1.09		.000
Early Larvae	.036	-.064	.032	-.219	.051·
Constant		10.31	1.15		.000
Late Larvae	-.010	-.011	.023	-.056	.622
Constant		9.35	1.10		.000

J3: Simple Regression Variables for National EVI Tamarisk Decline

Summarized simple regression statistics for independent variables relating to dependent percent EVI tamarisk decline for National. '***' where P < 0.001, '**' where P<0.01, '*' where P<.05,'·' where P<0.1.

Independent variable	Adjusted R^2	Unstandardized Coefficient B	Std. Error (Unstandardized)	Standardized Coefficient Beta	P (Sig)
River Segment	.034	.222	.078	.196	.005**
Constant		-43.8	18.1		.017
Tamarisk Area	-.002	-.003	.003	-.057	.411
Constant		8.91	1.10		.000
Viewshed	.009	-17	10	-.119	.086·
Constant		18	6		.002
Total Daylight	.017	-50	23	-.148	.032*
Constant		3.58×10^4	1.66×10^4		.032
Diffuse Daylight	.041	11	4	.214	.002
Constant		-8738	2768		.002
Direct Daylight	.015	-.017	.008	-.139	.045*
Constant		13	3		.000
Adult Beetle	-.011	-.009	.026	-.041	.717
Constant		9.289	1.091		.000
Early Larvae	.036	-.064	.032	-.219	.051·
Constant		10.305	1.153		.000
Late Larvae	-.010	-.011	.023	-.056	.622
Constant		9.346	1.095		.000

Appendix K: Residual Histograms for Multivariate Regressions for Tamarisk NDVI Percent Decline

K1: Histogram for Multivariate Regression plotting Tamarisk Percent NDVI decline for Glen Canyon without beetle observation data using Equation 15.

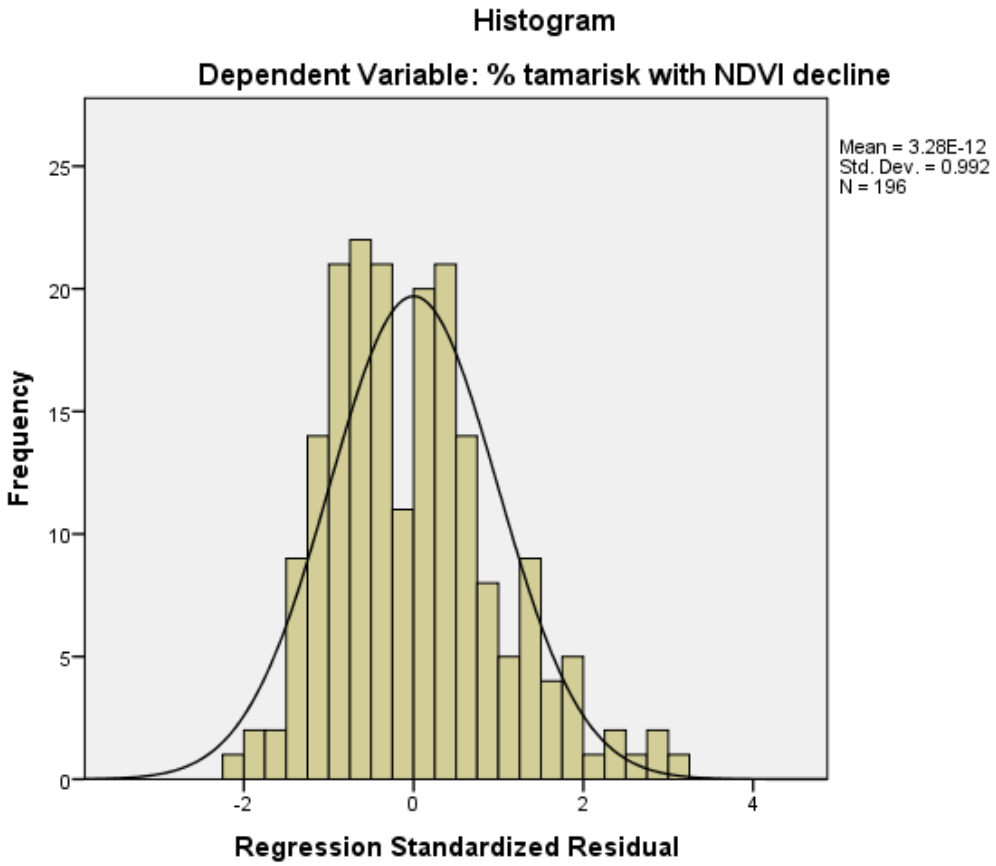

K2: Histogram for Multivariate Regression plotting Tamarisk Percent NDVI decline for Glen Canyon with beetle observation data using Equation 16.

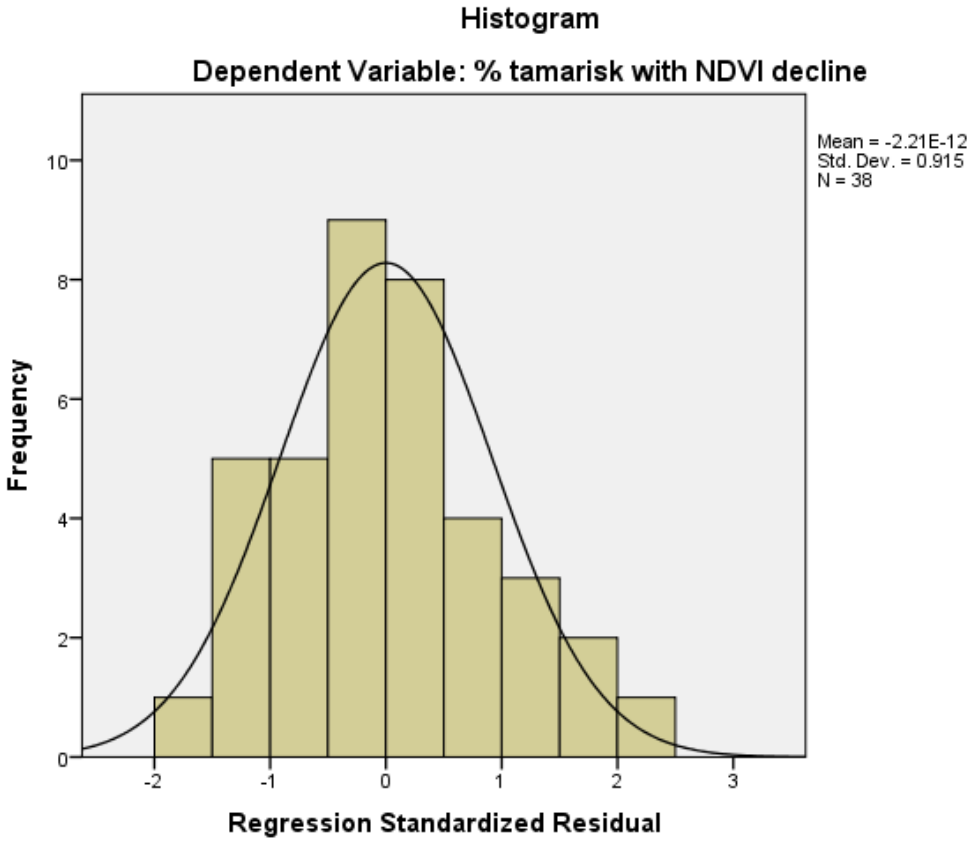

K3: Histogram for Multivariate Regression plotting Tamarisk Percent NDVI decline for Kanab without beetle observation data using Equation 19.

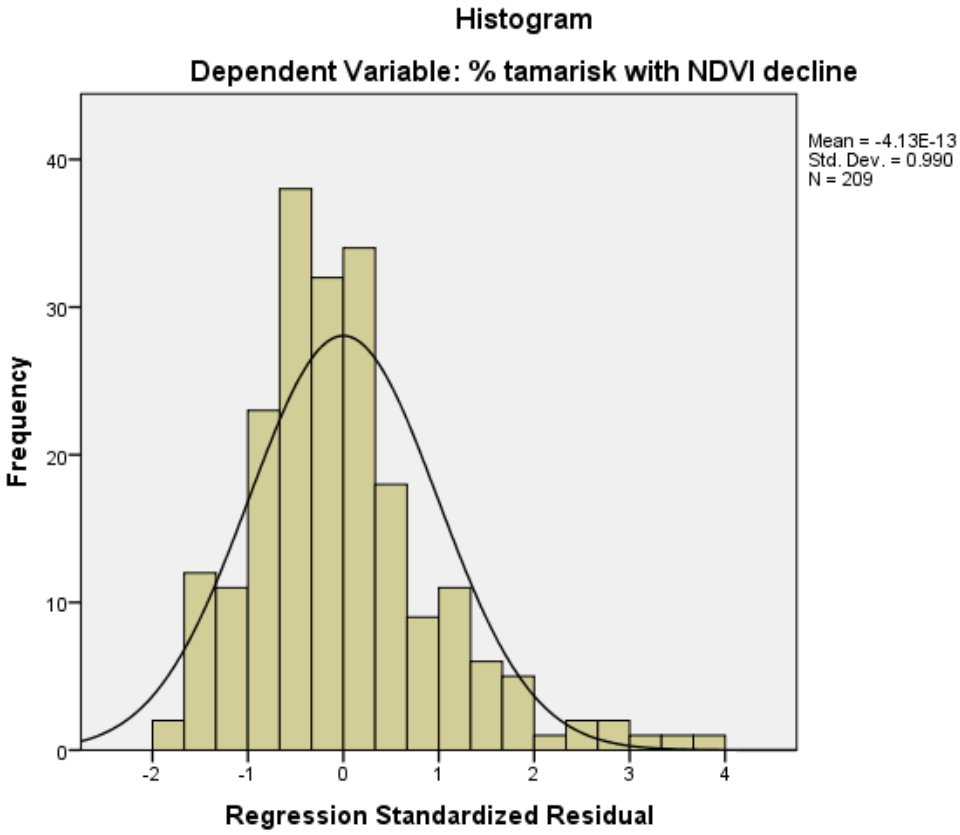

K4: Histogram for Multivariate Regression plotting Tamarisk Percent NDVI decline for Kanab with beetle observation data using Equation 20.

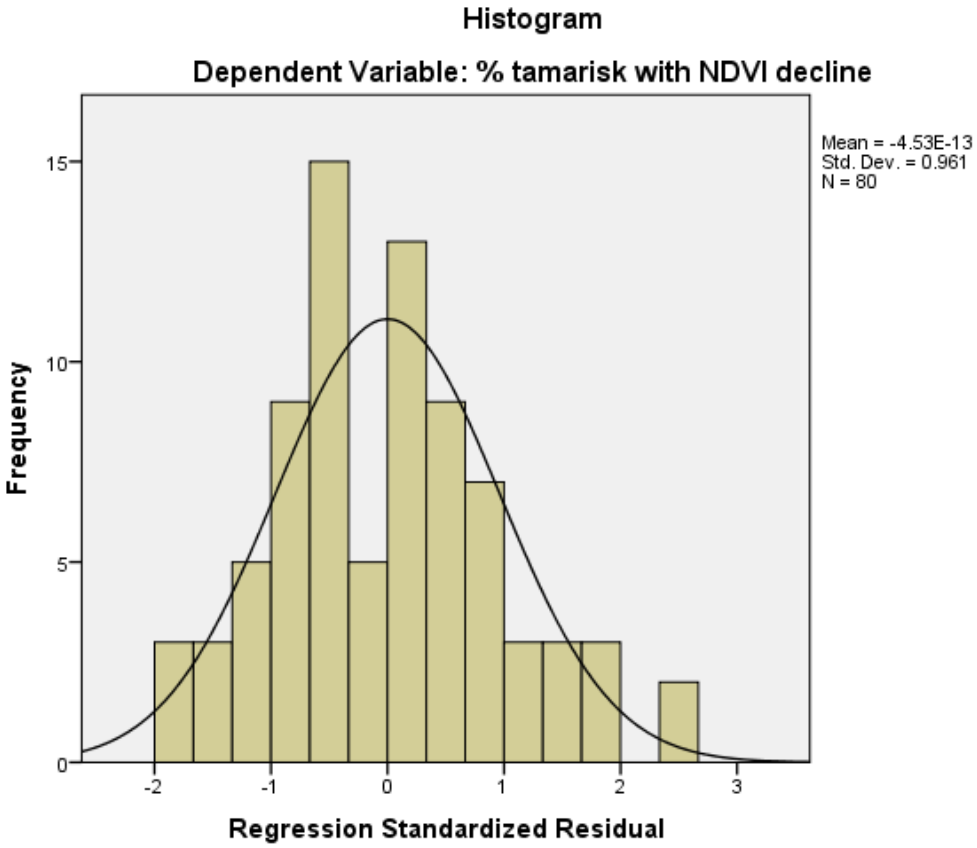

K5: Histogram for Multivariate Regression plotting Tamarisk Percent NDVI decline for National without beetle observation data using Equation 23.

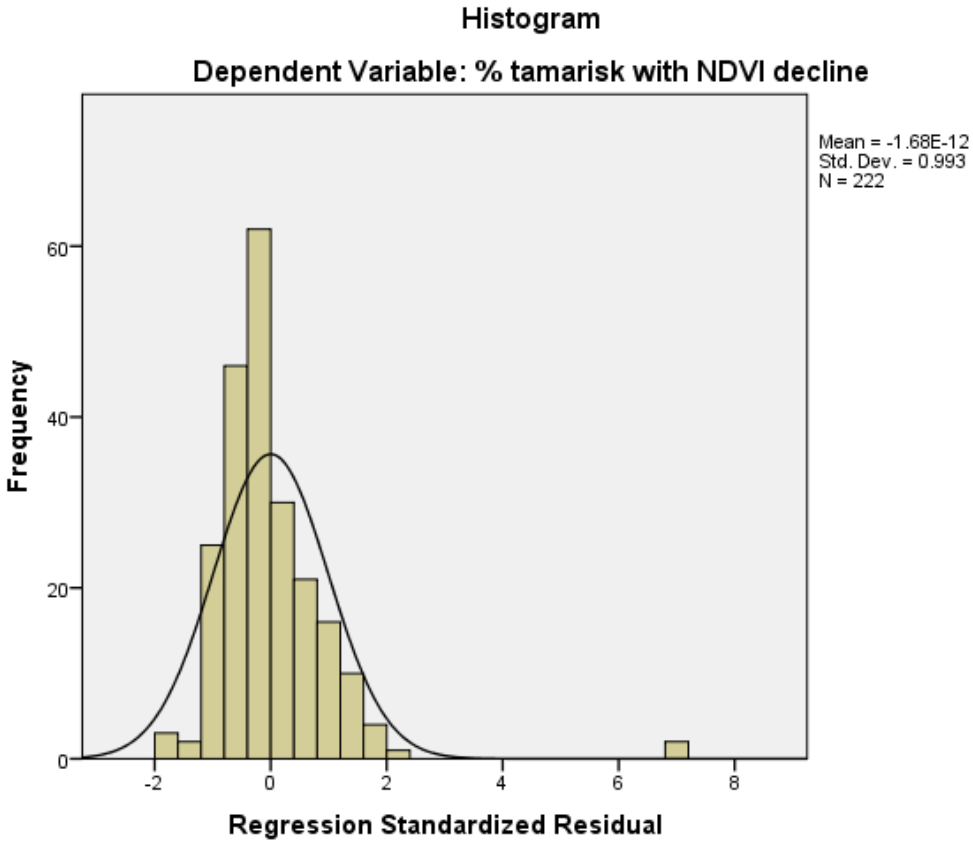

K5: Histogram for Multivariate Regression plotting Tamarisk Percent NDVI decline for National with beetle observation data using Equation 24.

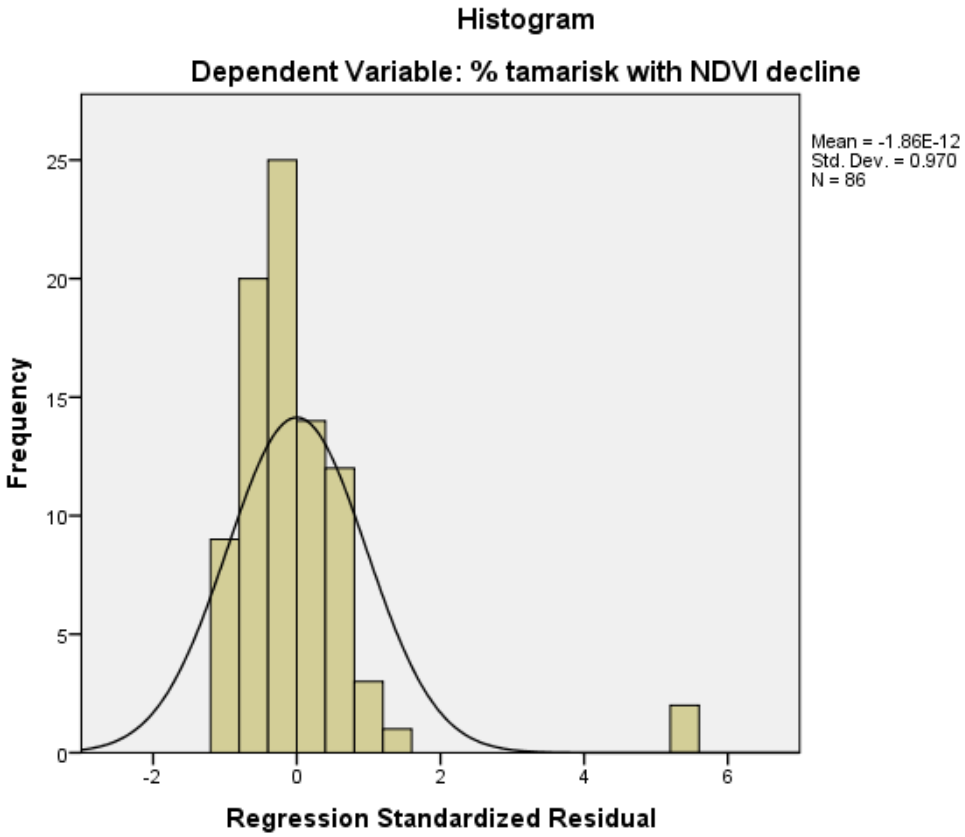

Appendix L: Residual Histograms for Multivariate Regressions for Tamarisk EVI Percent Decline

L1: Histogram for Multivariate Regression plotting Tamarisk Percent EVI decline for Glen Canyon without beetle observation data using Equation 17.

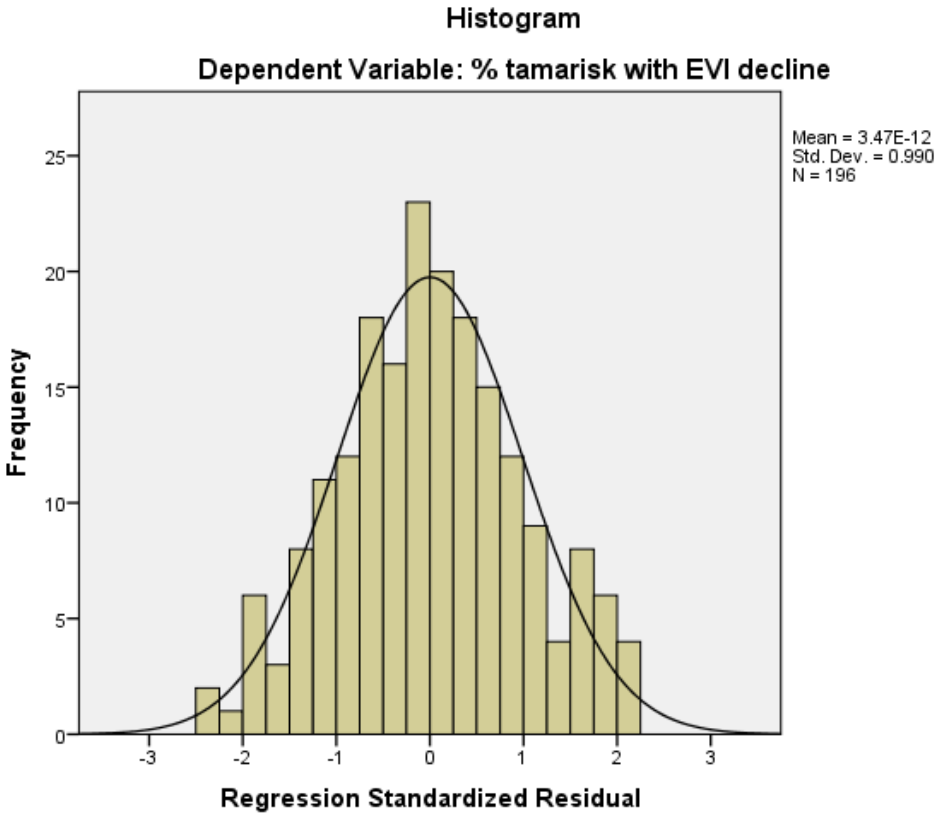

L2: Histogram for Multivariate Regression plotting Tamarisk Percent EVI decline for Glen Canyon with beetle observation data using Equation 18.

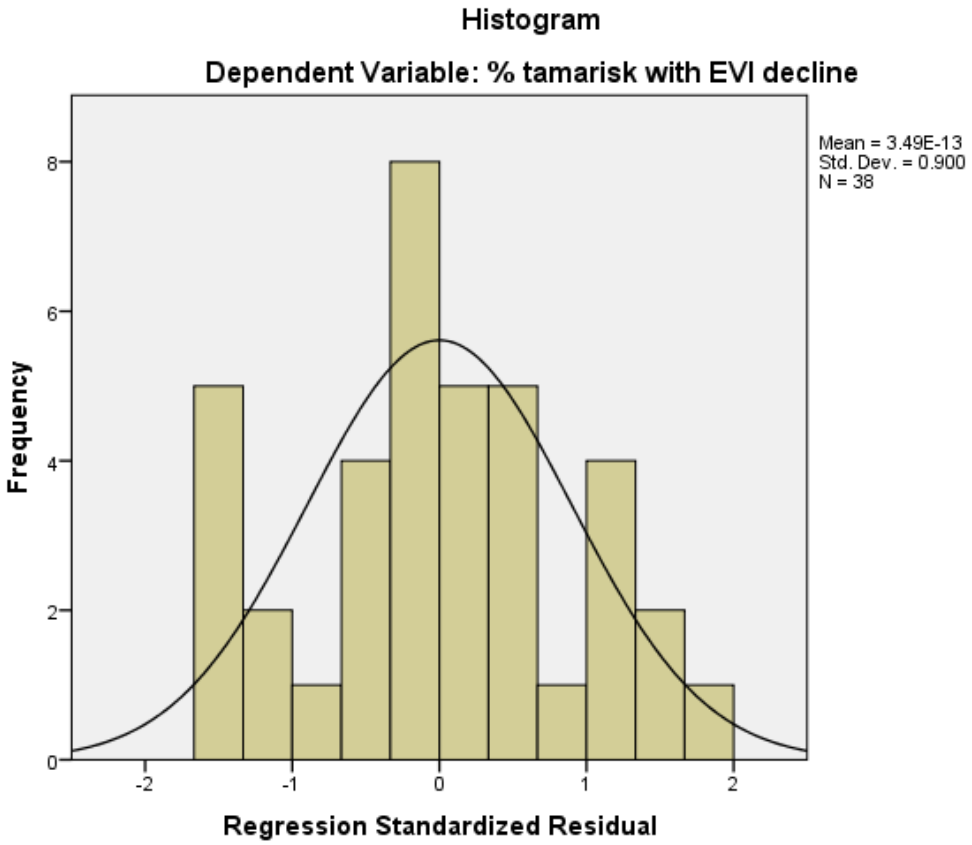

L3: Histogram for Multivariate Regression plotting Tamarisk Percent EVI decline for Kanab without beetle observation data using Equation 21.

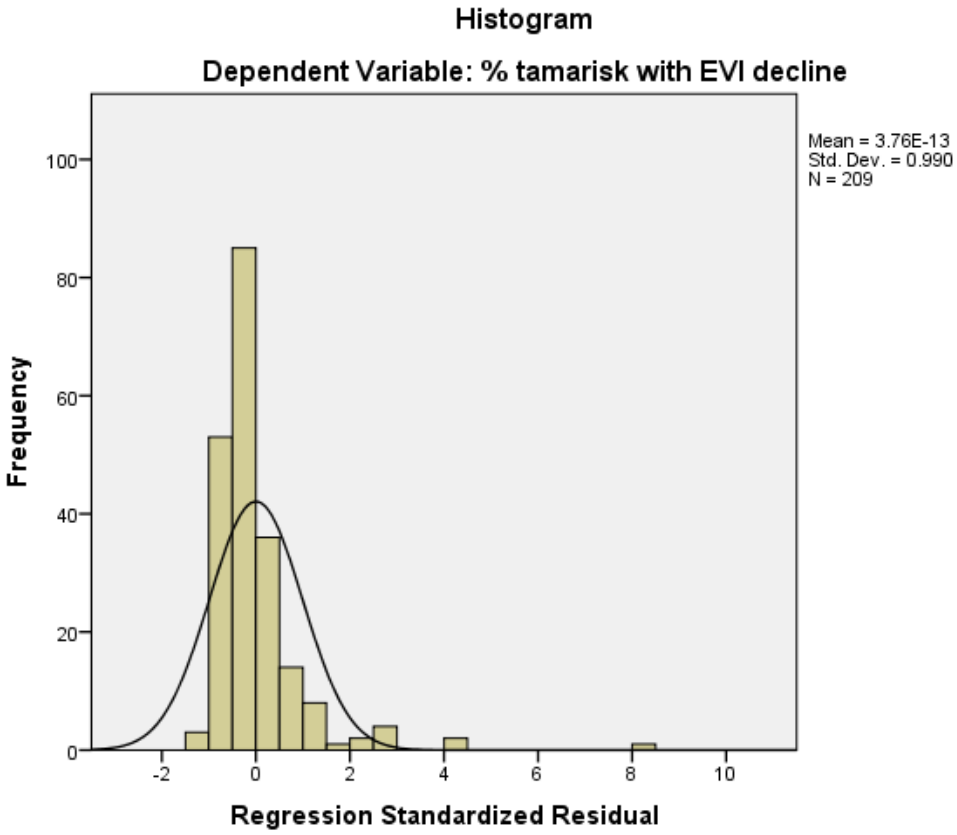

L4: Histogram for Multivariate Regression plotting Tamarisk Percent EVI decline for Kanab with beetle observation data using Equation 22.

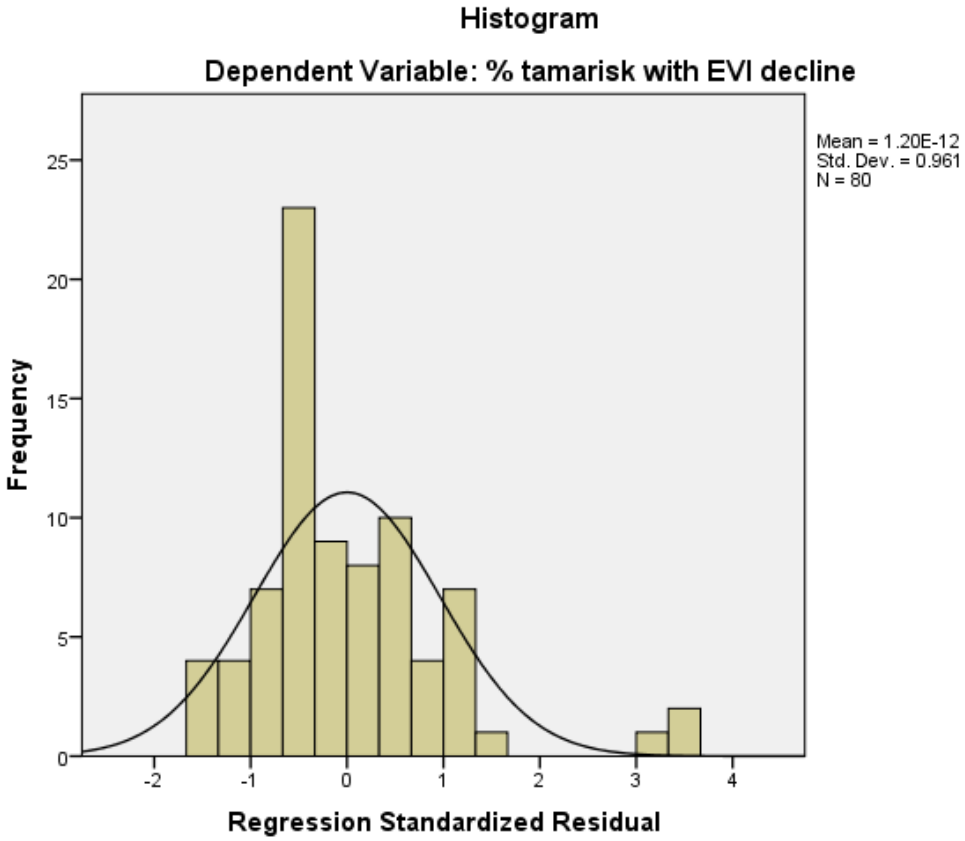

L5: Histogram for Multivariate Regression plotting Tamarisk Percent EVI decline for National without beetle observation data using Equation 25.

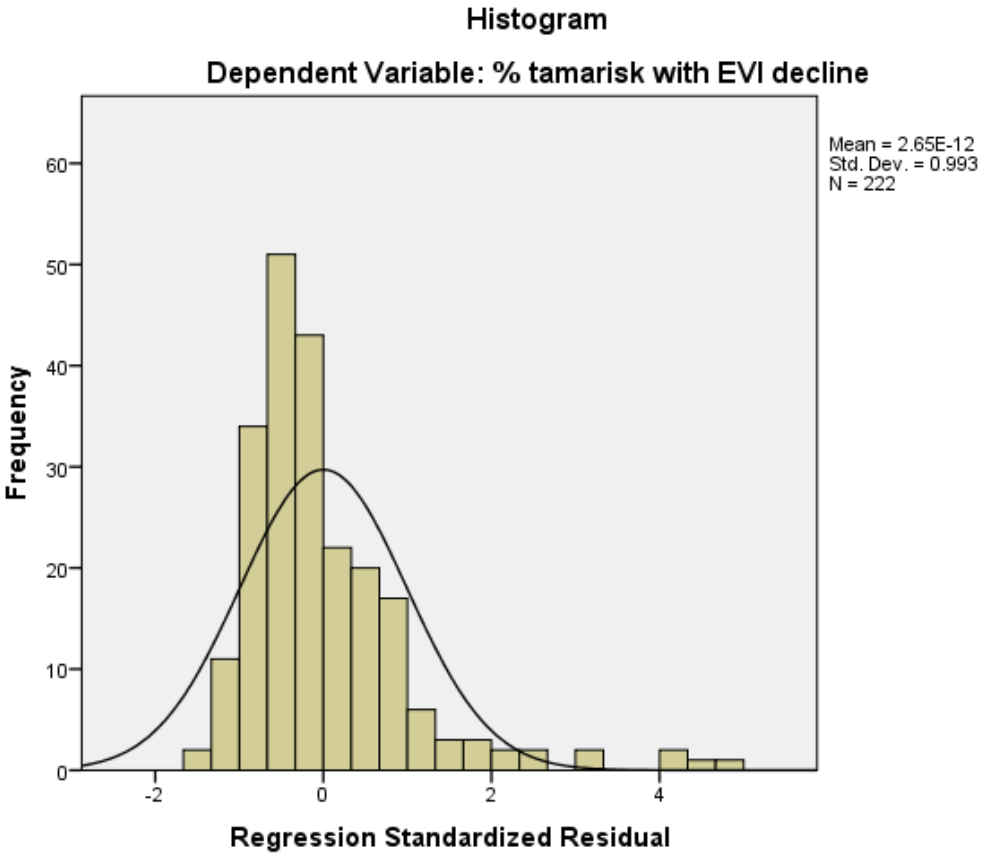

L6: Histogram for Multivariate Regression plotting Tamarisk Percent EVI decline for National with beetle observation data using Equation 26.

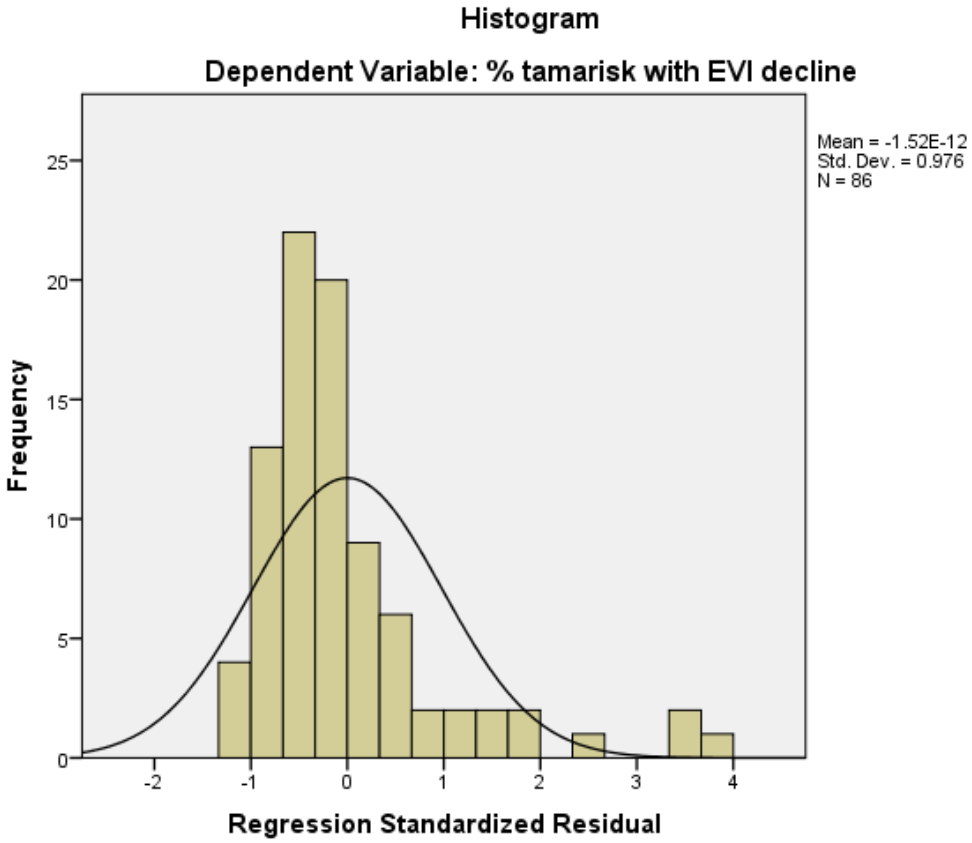

Appendix M: Residual Histograms for prediction of adult tamarisk beetle occurrence

M1: Histogram for Equation 27 using direct day length to predict adult tamarisk beetles in Grand Canyon Reach

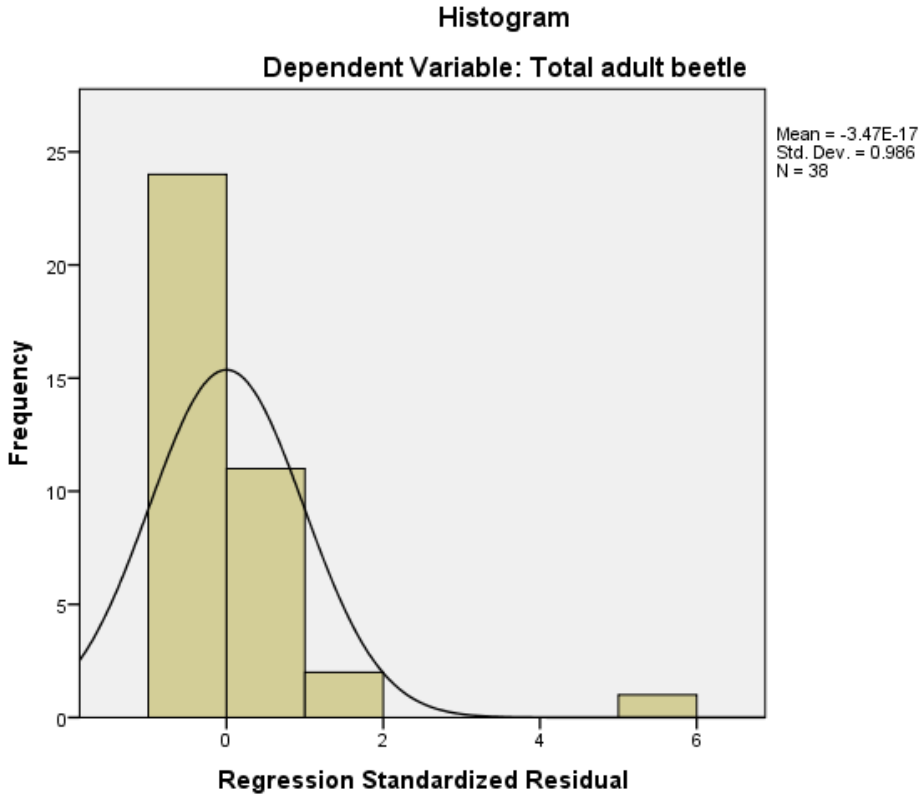

M2: Histogram for Equation 28 using direct day length to predict adult tamarisk beetles in Kanab Reach

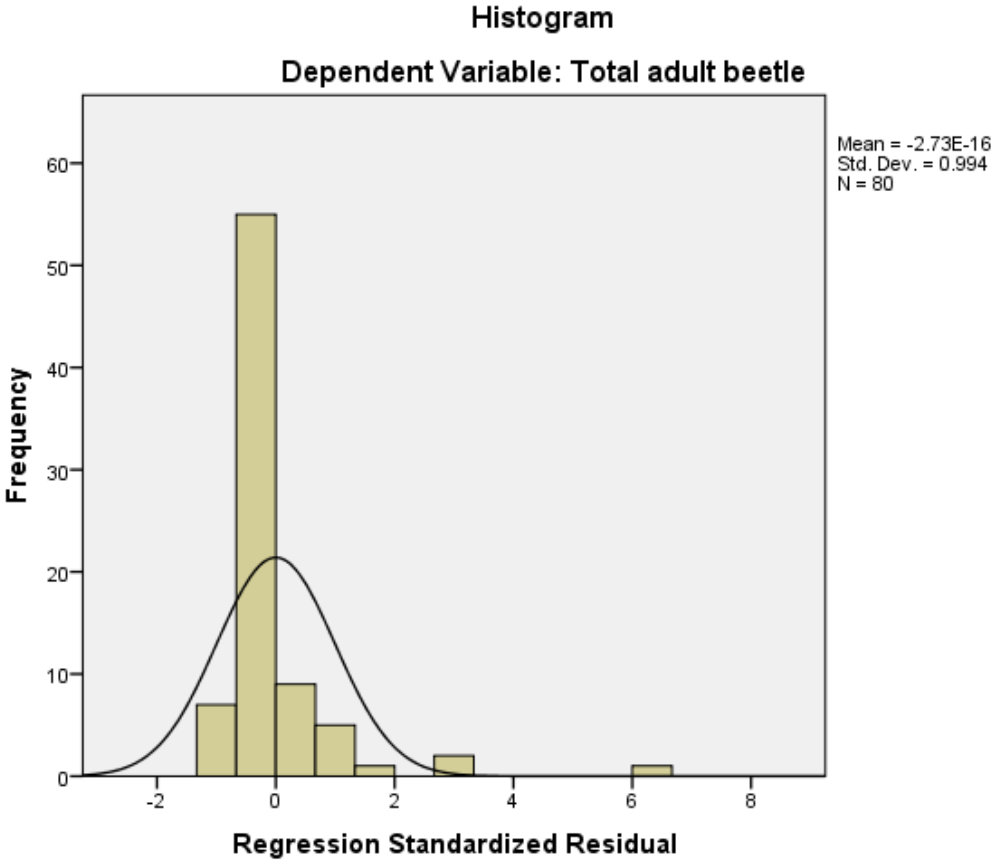

M3: Histogram for Equation 29 using total day length to predict adult tamarisk beetles in National Reach